BIOFILTRATION TREATMENT FOR IRON- AND MANGANESE-RICH GROUNDWATER AT LOW ON-SITE TEMPERATURES

A Thesis Submitted to the College of

Graduate and Postdoctoral Studies

In Partial Fulfillment of the Requirements

For the Degree of Master of Science

In the Department of Civil, Geological and Environmental Engineering

University of Saskatchewan

Saskatoon, Saskatchewan, Canada

By

SANDEEP RAJA DANGETI

PERMISSION TO USE

In presenting this thesis/dissertation in partial fulfillment of the requirements for a Postgraduate degree from the University of Saskatchewan, I agree that the Libraries of this University may make it freely available for inspection. I further agree that permission for copying of this thesis/dissertation in any manner, in whole or in part, for scholarly purposes may be granted by the professor or professors who supervised my thesis/dissertation work or, in their absence, by the Head of the Department or the Dean of the College in which my thesis work was done. It is understood that any copying or publication or use of this thesis/dissertation or parts thereof for financial gain shall not be allowed without my written permission. It is also understood that due recognition shall be given to me and to the University of Saskatchewan in any scholarly use which may be made of any material in my thesis/dissertation.

DISCLAIMER

Reference in this thesis/dissertation to any specific commercial products, process, or service by trade name, trademark, manufacturer, or otherwise, does not constitute or imply its endorsement, recommendation, or favoring by the University of Saskatchewan. The views and opinions of the author expressed herein do not state or reflect those of the University of Saskatchewan, and shall not be used for advertising or product endorsement purposes.

Requests for permission to copy or to make other uses of materials in this thesis/dissertation in whole or part should be addressed to:

Head of the Department of Civil, Geological, and Environmental Engineering
57 Campus Drive
University of Saskatchewan
Saskatoon, Saskatchewan S7N 5A9
Canada

OR

Dean
College of Graduate and Postdoctoral Studies
University of Saskatchewan
116 Thorvaldson Building, 110 Science Place
Saskatoon, Saskatchewan S7N 5C9
Canada

ABSTRACT

Manganese (Mn) is frequently detected in its reduced form, aqueous Mn(II), in groundwaters used as drinking water in Canada. Excess Mn(II) poses the potential risks of water discolouration, infrastructure corrosion, and health problems, as uncontrolled Mn(II) oxidation occurs and produces solid Mn(III/IV)-oxide precipitates in water supplies. As a solution for Mn(II) in groundwater, biofiltration technology has been considered globally to promote microbially mediated Mn(II) oxidation and produce solid Mn(III/IV) oxides that can be filtered out. However, previous studies have consistently reported that the biofiltration of cold groundwater with high Mn(II) and coexisting metal concentrations (typically Fe(II)) is challenging at low temperatures below 15 °C.

Diverse cold-adapted manganese-oxidizing bacteria (MnOB) are ubiquitous in cold groundwater. The biofiltration of cold Mn(II)-rich groundwater, which relies on the onset, acclimation and acceleration of Mn(II) removal associated with the enrichment of cold-adapted MnOB and biofilter media ripening in the field, has not been extensively understood.

The objectives of this research were therefore (1) to elucidate the onset, acclimation, and acceleration of Mn(II) oxidation (removal) from cold, natural Fe(II)- and Mn(II)-rich groundwater (4 to 8 °C) continuously fed into a two-stage pilot-scale biofiltration unit operated in the field at varying low on-site temperatures (8–14.8 °C) at the Langham Water Treatment Plant, Saskatchewan (Canada), (2) to characterize the microbial communities in the Mn and Fe biofilters and incoming groundwater, as well as in the surface coatings on field-ripened filter media, and (3) to explore the potential enhancement of biological *and* physicochemical Mn(II) oxidation in the field biofiltration unit.

Over the course of the 183-day pilot-scale biofiltration experiment in the field, the onset of Mn(II) removal from the cold groundwater commenced at 8 °C in the Mn filter after 29 days elapsed and after complete Fe(II) removal through the Fe filter. The Mn filter (1.55 m high and 0.3 m in diameter) reached steady-state functioning after 97 days, consistently exhibiting a high Mn(II)-removal efficiency of 97±0.9%. A gradual shift in redox-pH conditions in the Mn filter, to oxidation-reduction potential (ORP) values over 300 mV, favoured biological Mn(II) oxidation, the growth of viable MnOB populations, and an increase in microbial metabolic activity estimated by the adenosine triphosphate (ATP) assay. These changes reflected enhanced biological Mn(II) oxidation at the low on-site temperatures. However, the empty bed contact time (EBCT) first-order rate constants (k) for Mn(II) removal were very low, in the range of 10^{-6} and 10^{-5} min^{-1}, with a long half-life of 40 days, even though the Mn(II) removal efficiency was consistently at 97%. The

Mn(II) removal rate constant accelerated to 0.21 min^{-1} with a very short half-life of 3.31 minutes at 11±0.6 °C, immediately after three consecutive backwashes and injections of backwash sludge slurry back into the filter. The substantial increase in *k* was correlated to the vertical progress of biofilter ripening from the bottom to the top of the Mn filter, which was not limited by the low on-site temperatures. Intermediate and end-product Mn(III/IV) oxides (birnessite and pyrolusite) were detected by synchrotron-based powder X-ray diffraction, confirming the occurrence of Mn(II) oxidation based on the known Mn(II)-oxidation pathway.

High-throughput sequencing (16S rRNA genes, V4 region) of the microbial communities in the untreated incoming groundwater and filter media from the Fe and Mn filters revealed genus-level shifts in the bacterial community across the biofiltration unit. Previously known Mn(II)-oxidizing bacteria (MnOB) were minor members of the Mn-filter community. *Betaproteobacteria* including iron-oxidizing bacteria (FeOB) appeared in both the Fe and Mn filters. *Hydrogenophaga* sp., known FeOB, likely acted as a MnOB. Specifically, *Hydrogenophaga* strain CDMN isolated in this study can oxidize Mn(II) at the Mn-filter start-up temperature of 8 °C. Three new potential MnOB—*Azospirillum* sp. CDMB, *Solimonas soli* CDMK, and *Paenibacillus* sp. CDME—were also isolated from the Fe or Mn filters. A microbial consortium (51 genera including *Pseudomonas, Leptothrix, Flavobacterium,* and *Zoogloea*) was cultured from the field-aged biofilter and rapidly produced biogenic Mn oxides at 8 °C.

Synchrotron-based X-ray absorption near-edge spectroscopy (XANES) coupled with electron paramagnetic resonance (EPR) suggested that biogenic birnessite was the dominant Mn oxide in the Mn-filter media surface coatings. The co-existence of amorphous and crystallized Mn-oxide surface morphologies on the Mn-filter media, observed using scanning electron microscopy with energy dispersive X-ray spectroscopy (SEM/EDX), suggested concomitant biological and autocatalytic (physicochemical) Mn(II) oxidation in the Mn filter.

This study suggested that enhancing both biological and physicochemical Mn(II) oxidation is critical for the onset, acclimation and acceleration of Mn(II) removal during the biofiltration of cold groundwater. This study provides crucial insights for improving biofiltration performance in cold climates, representing a potential breakthrough for rapid biofiltration start-up, the biological acclimation of cold-adapted MnOB, and accelerated Mn(II) removal kinetics associated with the microbially mediated autocatalysis of Mn(II) oxidation at low temperatures.

ACKNOWLEDGEMENTS

In the first place, I would like to take this opportunity to thank my academic supervisors Dr. Wonjae Chang and Dr. Joyce M. McBeth for giving me an opportunity to work on this Masters thesis project, their time and support, their mentorship, and their guidance through graduate studies.

I am very grateful for my committee members, Dr. Terry Fonstad and Dr. Grant Ferguson, and my external reviewer, Dr. Jaafar Soltan, whose inputs and expertise are priceless.

I am very thankful to Dr. Babak Roshani for his technical expertise and Delco Water for giving me opportunity to conduct my Masters research on biofiltration technology. Thank you to Jay Dynes for his proficiency and guidance in the use of the IDEAS beamline at the Canadian Light Source.

I would also like to thank the Natural Sciences and Engineering Research Council of Canada (NSERC), Mitacs Accelerate Cluster, and Delco Water for providing the principal funding for this study. Special thanks to the College of Graduate Studies and Research and College of Engineering at the University of Saskatchewan for further financial support through scholarships and fellowships.

Thanks to my lab mates and colleagues for their support and encouragement. Also to Canadian Light Source for allowing me to use the life sciences lab and to Helen Yin for her time and support in Environmental Engineering lab.

Special thanks to my family and my best friends, Jihun, Jarvis, Sunny, Asad, Anureet, and Nick for being my side and supporting me in every possible way. And finally, I would like to thank this world for inspiring me, keeping me motivated, and making me a better person.

DEDICATION

To my academic supervisors and my family

TABLE OF CONTENTS

LIST OF TABLES

LIST OF FIGURES

ABBREVIATIONS & SYMBOLS

Å	Angstrom
AMOVA	Analysis of molecular variance
ANOVA	Analysis of variance
AOB	Ammonia-oxidizing bacteria
ATP	Adenosine triphosphate
BWS	Backwash sludge
CFU	Colony forming units
CLS	Canadian Light Source
CMCF-BM	Canadian Macromolecular Crystallography Facility bending magnet beamline
DNA	Deoxyribonucleic acid
DO	Dissolved oxygen
DWS	Drinking water standard
EBCT	Empty bed contact time
EDS	Energy dispersive spectroscopy
eH’	Effective number of species
ENA	European Nucleotide Archive
EPA	Environmental protection agency
EPR	Electron paramagnetic resonance
Fe	Iron
Fe-An	Fe filter anthracite
Fe-BW	Fe filter backwash
FeOB	Iron-oxidizing bacteria
Fe-Sa	Fe filter sand
GW	Groundwater
H’	Shannon index
ICP-OES	Inductively coupled plasma optical emission spectroscopy

ICP-MS	Inductively coupled plasma mass spectroscopy
J’	Pielou’s evenness
k	First-order rate constant
LBB I	Leucoberbelin blue I
LCF	Linear combination fitting
LWTP	Langham water treatment plant
MAC	Maximum acceptable concentrations
Mn	Manganese
Mn-An	Mn filter anthracite
Mn-BW	Mn filter backwash
MnOB	Manganese-oxidizing bacteria
Mn-Sa	Mn filter sand
MPN	Most probable number
NH_3-N	Ammonia as nitrogen
NOB	Nitrite-oxidizing bacteria
NOM	Natural organic matter
OD	Optical density
ORP	Oxidation-reduction potential
OTU	Operational taxonomic units
PCA	Principal component analysis
PCoA	Principal coordinate analysis
PXRD	Powdered X-ray diffraction
RDP	Ribosomal database project
rRNA	Ribosomal ribonucleic acid
SEM	Scanning electron microscopy
XANES	X-ray near-edge spectroscopy
XRF	X-ray fluorescence

1. GENERAL INTRODUCTION

1.1. Rationales and objectives of the research

Groundwater is a crucial water resource in Canada. Nearly 75% of Saskatchewan's communities, including First Nations communities, rely on groundwater for their drinking water sources (Water Security Agency, 2012). However, it has been reported that approximately 50% of groundwater treatment plants in Saskatchewan deal with groundwater rich with naturally occurring metals, typically including manganese (Mn) at a high level over 0.05 mg/L (Island, 2016). Manganese in groundwater is present mainly in its reduced form, Mn(II), in the aqueous phase. Uncontrolled oxidation of aqueous Mn(II) to solid Mn(III/IV) oxides causes substantial black discolouration of water and scaling damage to water supply infrastructure. Frequent consumption of water that is high in Mn may pose potential health risks associated with intellectual impairment in school-age children (Bouchard et al., 2011). Excess Mn(II) in groundwater must be treated for drinking water production. Commonly, dissolved Fe(II) is also naturally abundant when groundwater is rich in Mn(II). In such cases, Fe(II) concentrations often exceed the drinking water standard (0.3 mg/L). Fe(II) must be treated, typically prior to Mn(II) treatment, because Fe(II) oxidation is thermodynamically more favorable than Mn(II) oxidation. Fe(II) is rapidly oxidized via aeration, and Fe precipitates are easily removed using filtration. However, Mn(II) removal is challenging, especially for cold groundwater (4 to 8 °C) continuously flowing into a water treatment plant in cold climates. This study focuses on Mn(II) removal through a two-stage, on-site, flow-through biofiltration unit that continuously receives natural Fe(II)- and Mn(II)-rich groundwater at on-site low temperatures at the Langham water treatment plant (LWTP) in Saskatoon, Saskatchewan, Canada.

In Saskatchewan, conventional manganese greensand filtration technology for Mn removal has been generally adopted in many local regions. Manganese greensand filtration requires chemical oxidizing agents such as potassium permanganate and chlorine for Mn(II) oxidation. Mn-

oxide precipitates produced by Mn(II) oxidation are physically removed through filters and settling tanks (Island, 2016). Biofiltration technology for Mn(II) removal promotes microbially mediated Mn(II) oxidation by enhancing Mn(II)-oxidizing bacteria (MnOB) (Gage et al., 2001). The biofiltration treatment uses minimal chemicals (e.g., nutrients), and does not require strong oxidizing agents. In biofiltration, MnOB play a crucial role in initiating Mn(II) oxidation under aerobic conditions and producing biogenic Mn-oxides (Burger et al., 2008b). The formation of biogenic Mn-oxides is important in the formation of Mn-oxide coatings on aging filter media, potentially contributing to autocatalytic Mn(II) oxidation (physicochemical oxidation) (Bruins et al., 2015a). In other words, enhancing MnOB is a prerequisite for the start-up, biological acclimation, and successful maintenance of Mn(II) oxidation during biofiltration.

However, biological Mn(II) removal from cold groundwater is very challenging due to depressed mesophilic microbial activity under low temperature regimes below 15 °C in cold climates. At such low temperatures, the start-up period for Mn(II) oxidation is typically prolonged (e.g., 6 to 8 months or even to years), which increases the operation and maintenance costs of the biofiltration technology (Cai et al., 2014, Tekerlekopoulou et al., 2013, Li et al., 2013). Cold-adapted MnOB communities and the formation of biogenic Mn-oxides could be advantageous for groundwater biofiltration in cold climates. However, few studies have sought to describe cold-adapted MnOB community compositions enriched in field biofiltration units that continuously receive cold groundwater using high-throughput sequencing analysis, or the characteristics of Mn(III/IV)-oxide-rich surface coatings of field-ripened filter media. The overarching goal of the present research is to expand our knowledge of biofiltration for cold Fe(II)- and Mn(II)-rich groundwater and the underlying Mn(II) removal mechanisms associated with biological and physicochemical Mn(II) oxidation triggered by cold-adapted MnOB. The specific objectives of this research are to:

1. Describe the onset, acclimation and potential acceleration of Mn(II) removal during the operation of the two-stage on-site pilot-scale biofiltration system;
2. Demonstrate biological and physicochemical biofiltration parameters and kinetics of Mn(II) removal under the on-site conditions;
3. Characterize microbial communities of the groundwater and filter media using high-throughput sequencing analyses and culture-dependent analyses;

4. Characterize Mn-oxides in aged filter media obtained from the on-site biofiltration unit, using multiple instrumentation analyses;
5. Explore potential synergistic treatment strategies that combine biological and physico-chemical Mn-oxidation for cold groundwater treatment.

1.2. Significance of the research

In general, MnOB are polyphyletic in nature (meaning these microbes have origins from more than one common evolutionary ancestor), making it difficult to accurately identify the bacteria involved in Mn(II) oxidation in the environment (Dick et al., 2006). At the same time, MnOB are ubiquitous and have been identified in various natural and engineered environments. In this study, microbial community compositions throughout the biofiltration system for cold groundwater rich in Fe and Mn were characterized extensively using high-throughput sequencing and culture-independent analyses. Mn-oxides in the field-aged filter media are thoroughly characterized using synchrotron-based X-ray near edge spectroscopy (XANES), synchrotron-based powdered X-ray diffraction (PXRD), X-ray Fluorescence (XRF), scanning electron microscopy (SEM) with energy dispersive X-ray spectrometry (EDS), and electron paramagnetic resonance (EPR). Previous studies provide only a limited understanding of how indigenous, cold-adapted microbial communities are linked to the field aging of filter media and groundwater chemistry throughout cold-temperature biofilters. In this study, microbial data, groundwater chemistry, and field media characteristics are integrated to uniquely suggest the synergistic link between biological and physiochemical Mn(II) oxidation at temperatures below 15 °C. This study contributes to expanding our knowledge of enhancing Mn(II) oxidation in cold groundwater through biofiltration technology.

Furthermore, this study successfully cultured a cold-adapted microbial consortium derived from the field-aged biofilter that can rapidly oxidize Mn(II) and produce biogenic Mn(III/IV) oxides at 8 °C. In particular, this study discovered that *Hydrogenophaga* sp. are capable of oxidizing Mn(II) at 8 °C. To the best of our knowledge, this is reported for the first time in this thesis. The findings of this research are very important for improving biofiltration technology through the early formation of biogenic Mn-oxides. Ultimately, this study provides insight into the potential development of cost-effective, energy-efficient, and environmentally friendly biofiltration systems for environmentally challenging conditions.

1.3. Thesis organization

This thesis is a manuscript-style thesis and consists of five chapters, as follows:

- Chapter 1 is a general introduction to present the rationales and objectives of the research and the structure of this thesis.
- Chapter 2 is a literature review that presents background information and identifies key knowledge gaps in the area of Mn(II)-biofiltration technology. This chapter covers problems linked to manganese in water supplies in Canada, conventional physicochemical water treatment, and biofiltration treatment principles.
- Chapter 3 demonstrates the commencement, acclimation, and acceleration of Mn(II) removal in the pilot-scale field biofiltration unit, focusing on groundwater chemistry, operational parameters, and the kinetics of Mn(II) removal in response to the vertical aging of the biofilter columns. In this chapter, a cold-adapted Mn(II)-oxidizing microbial consortium derived from the filter media during the steady-state functioning of the biofiltration system is reported along with characterization of biogenic Mn-oxides formed. Finally, this chapter suggests a potential biofiltration strategy for cold groundwater.
- Chapter 4 is an in-depth characterization study of microbial community compositions in the biofiltration system that uses various instrumentation analyses. This chapter explores the prevailing mechanisms for Mn(II) oxidation. Changes in bacterial community compositions are examined in the context of the chemical data and filter media characteristics, including Mn oxidation states, the surface morphology of filter media coatings, and field aging (biogenic and abiotic aging).
- Chapter 5 summarizes the major contributions, conclusions, and limitations of the research. Recommendations for further research are also stated.

2. BACKGROUND REVIEW AND KNOWLEDGE GAPS

2.1. Manganese in water supplies

Manganese is a commonly occurring element found in soil and water and is the second most abundant transition metal on earth, after iron (Turekian and Wedepohl, 1961). Manganese in Canadian groundwater occurs naturally as a result of groundwater contact with Mn-containing rocks and soils in sub-surface environments. Aqueous Mn concentrations in groundwater vary and depend on various natural environmental factors, such as the abundance of Mn present in the regional geology and groundwater chemistry. Redox conditions associated with groundwater chemistry may favour the dissolution of manganese in its reduced state, Mn(II) (Stokes, 1988). In Canada, Mn(II) is most commonly detected in groundwater, but can also be found in surface waters (e.g., in the Elbow and Bow rivers in Calgary) (Island, 2016).

Groundwater is a major water resource for 30% of Canadians (Environment and Climate Change Canada, 2013). The development of Saskatchewan's groundwater resources will contribute to meeting current and future water requirements in both the public and private sectors. However, Health Canada has identified manganese, which is often detected in Canadian and Saskatchewan groundwater in the form of dissolved Mn(II), as an element of concern at concentrations exceeding 0.05 mg/L, the national and provincial drinking water standards (DWS) (Island, 2016). Mn(II) in aquifers is not easily removed at a treatment facility. In water distribution infrastructure, it can be oxidized by residual disinfectants, bacteria, or household oxidants such as bleach, and precipitate as dark Mn-oxides (Cerrato et al. 2010). Precipitated Mn-oxides cause black discoloration in water and can cause scaling in pipes and fixtures. Scaling in distribution systems can occur at Mn(II) concentration as low as 0.02 mg/L (Sly et al., 1989, Bean, 1974, Griffin, 1960). The Environmental Protection Agency (EPA) and Health Canada have therefore set an aesthetic objective of 0.05 mg/L for Mn(II) in drinking water (Kohl and Medlar, 2006). However, a target of 0.01–0.02 mg/L is considered more appropriate to minimize the risk of water discoloration and pipe scaling. The potential risks of intellectual impairment in children associated

with frequent consumption of drinking water containing Mn at high concentrations has been reported (Kondakis et al., 1989, Bouchard et al., 2011).

Considering the possible aesthetic effects associated with Mn(II) at low concentrations, Sly et al. (1989) recommended that the Mn(II) drinking water guideline issued by the EPA should be lowered from 0.05 to 0.01 mg/L. Currently, Health Canada is reviewing the latest available information on the effects of Mn(II) concentrations in drinking water and is proposing to reduce the aesthetic objective to 0.02 mg/L and introduce a maximum acceptable concentration (MAC) of 0.1 mg/L (Island, 2016). However, aqueous Mn(II) is not easily removed by aeration in neutral pH conditions, and appropriate treatments for Mn(II) removal are therefore required. Cost-effective treatment technology for the removal of Mn(II) and other contaminants from water resources has been increasingly demanded in the water treatment industry in Saskatchewan. Therefore, considering future water consumption rates and water infrastructure costs, the development of a cost-effective treatment technology for Mn(II) removal is needed.

2.2. Water treatment technologies for manganese removal

2.2.1. Physical and chemical treatment

In neutral pH conditions, aqueous Mn(II) is not readily oxidized to form Mn-oxides that can be subsequently removed (Stumm and Morgan, 1996). Therefore, specialized treatment methods are needed if water resources contain Mn(II) in concentrations higher than the DWS. The commonly used methods for treating Mn(II) at water treatment plants include: chemical oxidation using oxidizing agents followed by physical separation, chemical oxidation by filter media coated with Mn-oxides, dissolved air flotation, and membrane filtration (Granger et al., 2014).

Chemical oxidation followed by physical separation involves the use of oxidizing agents such as chlorine (Cl_2), potassium permanganate ($KMnO_4$), or ozone (O_3) to oxidize Mn(II) to Mn (III/IV) oxide precipitates. The precipitated Mn-oxides are subsequently separated from the aqueous phase using settling tanks and/or filters. The purpose of applying chemical oxidants such as permanganate, or the application of free chlorine to the filter beds, is to stimulate the natural greensand effect (NGE). The NGE refers to Mn(II) in the aqueous phase becoming immobilized by oxidation on the surfaces of filter media (Knocke et al., 1991). Filter media coated with Mn oxides (e.g., green sand) adsorb soluble Mn(II) onto its surfaces and oxidize Mn(II) to Mn(IV) due

to the autocatalytic nature of Mn oxides (Kohl and Dixon, 2012). Dissolved air flotation and membrane filtration are additional treatments that can support chemical oxidation and increase the treatment efficiency (Kohl and Medlar, 2006).

A possible drawback of using Mn-oxide-coated filter media to remove Mn(II) from water is surface deactivation as the media are coated with precipitates, necessitating surface regeneration, which requires strong oxidants such as Cl_2 or $KMnO_4$. This treatment option is commonly employed, but can be expensive in the long run. Using Cl_2 as an oxidizing agent can cause the formation of chlorinated disinfection by-products (DBPs) when Cl_2 reacts with natural organic matter (NOM) in the water, such as humic acids (Singer, 1999). These reactions can produce chlorinated compounds that often have known or suspected adverse health effects (Singer, 1999). Employing other conventional treatments for the removal of aqueous Mn(II) is not economical due to the high operational and maintenance costs. To overcome the drawbacks associated with conventional treatment methods, biofiltration technology is currently considered a promising alternative Mn(II)-removal technology in the water treatment industry.

2.2.2. Biofiltration technology

A standard biofiltration setup consists of a closed column containing filter media (e.g., particles of anthracite and silica sand) that support the growth of indigenous microbial populations that contribute to the removal of heavy metals and organic contaminants from the aqueous phase (Chaudhary et al., 2003). The combination of contaminant removal mechanisms involved in the biofiltration process include microbial degradation, adsorption, absorption, and auto-catalysis. The biofilter media provide surface areas to promote the growth of indigenous microbial communities seeded in to it, which are enriched to remove specific contaminants using their metabolic activity. The type of filter media, start-up period, hydraulic loading rates, empty bed contact time (EBCT) and backwashing are some important design and operational parameters that need to be considered for biofiltration.

Manganese biofiltration is gaining importance across the globe and is widely implemented in Europe and North America to treat Mn(II)-rich groundwater. Mn biofiltration is an eco-friendly, chemical-free and cost-effective water treatment technology that can overcome the economical, operational and health-related drawbacks of conventional treatment methods. Mn(II) removal in

biofilters has been shown to be very effective and consistent at influent Mn(II) concentrations over 1 mg/L (Li et al., 2005, Pacini et al., 2005, Štembal et al., 2005).

Under anoxic and circumneutral conditions, Mn(II) is very stable and is not readily oxidized by the limited available oxygen. The Mn Pourbaix diagram (Fig. 2.1) indicates that the oxidation of aqueous Mn requires specific geochemical conditions: a redox potential (ORP) over +300 mV, a pH of 7.5–8, and dissolved oxygen (DO) concentration of 3–5 mg/L. Under these conditions, Mn(II) removal in biofilters is reported to be initiated by the biological oxidation activity of Mn-oxidizing bacteria (MnOB) (Burger et al., 2008b). During biofiltration, indigenous MnOB from the groundwater accumulate and are enriched on the filter media. They metabolically oxidize soluble Mn(II) to form Mn(III/IV)-oxide precipitates. The oxidized Mn(III/IV)-precipitate solids are then separated from the filtrate by the biofilter materials, sand and gravel.

The effectiveness of bacterially-mediated Mn biofiltration is dependent on the redox potential (Eh), DO concentrations, and pH of the groundwater. MnOB activity for Mn(II) oxidation is optimal at pH >6.3, DO >5 mg/L, and ORP/Eh >+300 mV (Burger et al., 2008b, Pacini et al., 2005, Li et al., 2005, Štembal et al., 2005). Under these conditions, MnOB can actively oxidize Mn(II) into precipitates as Mn(III/IV) oxides (Fig. 2.1). In addition to biological Mn(II) oxidation, physico-chemical Mn(II) oxidation may also be promoted by the presence of biogenic Mn(III/IV) oxide precipitates on filter media (Bruins et al., 2015a). Therefore, biological oxidation by MnOB and autocatalytic physico-chemical oxidation, which both form removable Mn-oxides, are the key mechanisms governing Mn(II) removal in biofilters.

The performance of Mn biofilters are largely influenced by the design and operational parameters, which mainly include the start-up period, empty bed contact time (EBCT), and backwashing rate (Tekerlekopoulou et al., 2013). The start-up period in Mn biofilters refers to the time required for effluent Mn(II) concentrations to be stable and below the DWS, and unaffected by changes in influent Mn(II) concentrations. Mn biofilters are reported to show a start-up period of 2 to 8 months depending on geochemical conditions and filter design (Tekerlekopoulou et al., 2013). Seeding backwash water with an active microbial community before reintroducing it to biofilter, as well as replacing virgin media with biologically-aged filter media, have been shown to reduce the start-up period (Mouchet, 1992, Vandenabeele et al., 1992).

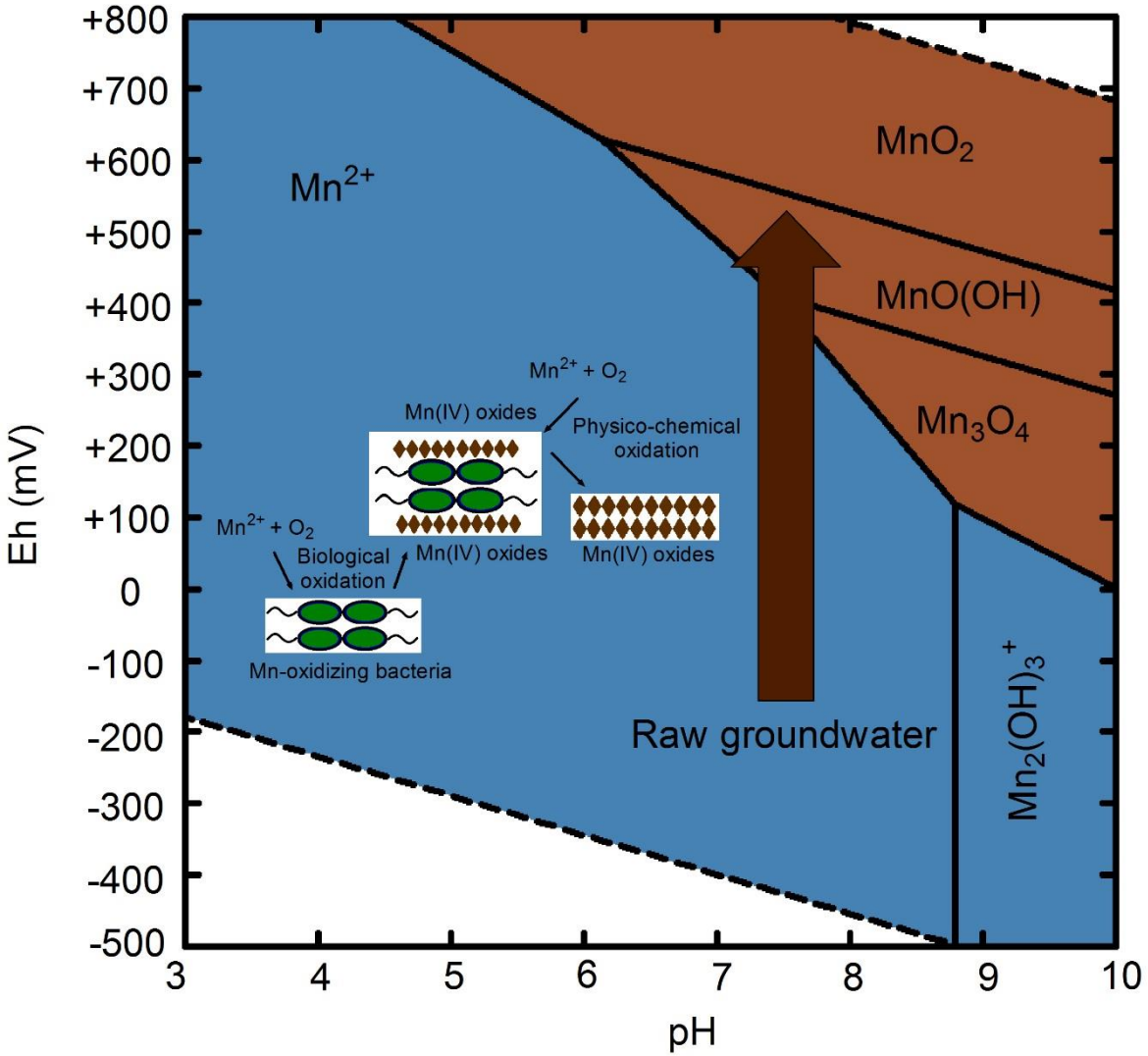

Fig. 2.1 **Conceptual approach for Mn(II) oxidation mediated by MnOB and associated geochemical response.**

The EBCT refers to the time period required for the influent water stream to flow through the media and is considered an important factor for effective biofiltration. An EBCT of 15 minutes for biofilters that were aged for 8 months has been shown to remove >90% of influent Mn(II) (Katsoyiannis and Zouboulis, 2004). Backwashing is essential for improving biofilter performance. It cleans the biofilter by reversing the direction of flow to remove the insoluble Mn-oxides trapped in the filter. Backwashing considerations include the frequency, water type, flow rate and backwash water disposal. Table 2.1 lists removal efficiencies for biofiltration designs adopted for Mn(II) removal and the groundwater geochemical conditions for the studies where these designs were reported.

2.3. Manganese-oxidizing bacteria

Mn(II)-oxidizing bacteria are ubiquitous in nature and found in various environments such as the deep sea, rivers, lake sediments, groundwater, fjords, soils, and water distribution facilities (Tebo et al., 2005). The MnOB play integral roles in the biogeochemical cycles of manganese, iron, nitrogen, carbon, sulfur, and several other nutrients and trace metals (Tebo et al., 2005). MnOB are diverse, and including species in the phyla *Firmicutes*, *Actinobacteria* and *Alpha-*, *Beta-* and *Gamma-proteobacteria* (Tebo et al., 2005). Webb et al. (2005) reported that the Mn(II)-to-Mn(IV) oxidation reaction by *Bacillus sp.* SG-1, a model MnOB organism, proceeds via Mn(III) intermediates. Multicopper oxidase genes (MCOs) found in MnOB (*Bacillus* sp. SG-1, *Pseudomonas putida* MnB1 and GB-1, and *Leptothrix discophora* SS1) have been reported for their involvement in Mn(II) oxidation. Bacterially-mediated Mn(II) oxidation by *Bacillus sp.* SG-1 is a sequence of two enzymatic reactions or one-electron transfer reactions mediated by MnxG (MCO) enzyme. The presence of Mn(III) intermediates and mechanism of the two-step catalysis by the MCO suggest that Mn(II) oxidation involves a MCO system that can catalyze the two-electron oxidation of Mn(II) (Tebo et al., 2005).

The ability of MnOB to oxidize Mn(II) is strongly dependent on nutrient and carbon source availability. Growth media with limited organic carbon sources, e.g., succinate or pyruvate, has been shown to increase the growth of MnOB over nutrient-rich media (Tani et al., 2003). Additionally, growth media enriched with Mn(II) has also been found to enhance the growth of MnOB, more than for other heterotrophic bacterial species (Francis et al., 2001, Tani et al., 2003), suggesting that MnOB receive some competitive advantage for growth because of Mn(II)

oxidation. At pH 7.5–7.8, higher Mn(II) oxidation rates by MnOB have been observed (Boogerd and de Vrind, 1987, Vandenabeele et al., 1992), which supports the theory based on empirical observations in groundwater treatment plants that MnOB oxidize Mn(II) best at pH conditions greater than 7.4 (Mouchet, 1992).

A study from Gouzinis et al. (1998) reported that the presence of MnOB in biofilters can increase Mn(II) removal from 25% (based solely on chemical oxidation) to almost 100%, with combined physical, chemical and biological oxidation. Burger et al. (2008b) reported that bench-scale biofilters achieved a 90% removal efficiency when inoculated with indigenous microflora. In the same study, Mn(II) removal was not achievable in the absence of MnOB. These lines of evidence suggest that MnOB are crucial for initiating Mn(II) oxidation in biofilters and to allow filter ripening (i.e. maturation of filter bed where optimal conditions are developed for manganese removal in the filter).

Scientific literature about microbial compositions in Mn biofilters reveals that no single type of bacterium is responsible for Mn(II) oxidation. Instead, microbial consortia are responsible (Li et al., 2013, Yang et al., 2014, Thapa Chhetri et al., 2013). Through culture-independent analysis, known MnOB relatives belonging to *Leptothrix*, *Pseudomonas*, *Siderocystis*, *Hyphomicrobium*, *Flavobacterium*, *Variovorax*, *Arthrobacter*, *Ralstonia*, and *Planctomyces* genera were identified in Mn biofilters previously (Thapa Chhetri et al., 2013, Cai et al., 2014, Yang et al., 2014, Burger et al., 2008a, Li et al., 2013). The diversity of MnOB populations in Mn-biofilter communities, isolated and identified in pure cultures, suggests bacterially-mediated Mn(II) oxidation is a common process in many environments. Several studies have cultured MnOB from biofilters (Beukes and Schmidt, 2012, Burger et al., 2008a, Abu Hasan et al., 2015). Isolates of *Bacillus* sp., *Pseudomonas* sp., *Micrococcus* sp. (Abu Hasan et al., 2015), *Leptothrix* sp. (Burger et al., 2008a), and *Acinetobacteria* sp. (Beukes and Schmidt, 2012) are a few of the MnOB found in Mn biofilters.

In Mn biofilters, biogenic birnessite formed on filter media by microbial consortia can have a high adsorptive capacity for Mn(II) (Learman et al., 2011). Lattice structures of biogenic birnessite have been reported for their outstanding ability to adsorb Mn(II) and subsequently promote its physico-chemical oxidation by auto-catalysis (Post, 1999). Therefore, the formation of biogenic birnessite promotes and accelerates further Mn(II) removal in biofilters through physico-chemical Mn(II) oxidation.

Table 2.1 Biofiltration designs for Mn(II) removal from groundwater (Granger, 2013)

Design	Mn concentration (mg/L)	pH	ORP (mV)	Temperature (^{O}C)	Mn removal (%)	Scale	References
Aeration, biofiltration and sand filtration	1.0-1.8	6.8-7.4	361-423	15-24	88-92	Pilot - scale	Pacini et al. (2005)
Aeration and biofiltration	0.4	7.2	340	N/A	>88	Pilot-scale	Katsoyiannis and Zouboulis (2004)
Biofiltration	0.7-1.0	7.2-7.5	N/A	N/A	100	Pilot-scale	Mouchet (1992)
Aeration and biofiltration	1-6	6-7	346-473	N/A	>90%	Pilot-scale	Abu Hasan et al. (2014)
Biofiltration	0.9-1.4	6.5-7.5	295-368	N/A	100	Full-scale	Burger et al. (2008a)
Aeration and biofiltration	0.52	7.5	N/A	3-4	>80%	Pilot-scale	Cai et al. (2014)
Biofiltration	0.8	7.5-7.8	N/A	18–22	>90%	Pilot-scale	Cai et al. (2015)

Low temperatures can negatively influence biofilter performance. With MnOB activity significantly decreased below 15 °C (Berbenni et al., 2000, Francis et al., 2001, Tebo and Emerson, 1985, Tipping, 1984), the growth of cold-adapted MnOB populations is critical for the acceleration of Mn removal under these challenging conditions. Understanding microbial diversity and community compositions in Mn biofilters and characterizing the Mn-oxides formed at low temperatures can expand our knowledge of microbially-mediated Mn(II) oxidation for the treatment of cold groundwater using biofiltration technology.

2.4. Manganese biofiltration in Canada

In Canada, the commonly applied methods to treat Mn(II)-rich groundwater are chemical oxidation followed by sand filtration, adsorption/oxidation, separation using Mn-oxide coated filter media, and reverse osmosis. All these treatment methods require either strong oxidants (e.g., O_3, Cl_2, ClO_2, or $KMnO_4$), adsorbents (e.g., manganese green sand), or membranes. As a result, the application of these technologies in practice can be costly.

In Canada, water treatment companies are becoming interested in using biofiltration technology to treat Mn(II) in water resources. For the first time in 1992, ONDEO Degremont Ltd. successfully conducted pilot-scale and full-scale biofilter operations to treat iron (Fe(II)) and Mn(II) from local groundwater wells in Woodstock, NB (Gage et al., 2001). This study reported that biofiltration technology is economically cheaper than conventional treatments. The total installation cost for a full-scale biofiltration plant was about 60% less than for a physical/chemical plant (about $800,000 compared to $1,460,0000). According to the Industry Canada (2008) report, UV treatment and biological treatment are increasingly preferred in the water treatment industry. According to the same report (Industry Canada, 2008), the survey conducted by EBI Inc. showed that biological treatment is one of the most preferred technologies for the water industry in Canada.

Currently a Research and Development team at Delco Water, a Saskatoon-based water treatment company, is developing a new biofiltration system specifically for Fe(II) and Mn(II) removal from local groundwater supplies. The ultimate goal of this R&D project is to accelerate biofilteration functionalization for Fe and Mn removal in the water sources, and then scale up the biofiltration for integration into the existing water treatment plants. As a part of this project, a pilot-scale biological filtration unit has recently been designed, constructed and operated by Delco Water at the Langham water treatment plant (LWTP) in Saskatchewan, Canada.

With total initial concentrations of 2.81±0.02 mg/L for Fe(II) and 0.88±0.01 mg/L for Mn(II) in the influent groundwater, the pilot-scale biofilters at LWTP achieved removal efficiencies of 99% for Fe(II) and 60% for Mn(II). Plastic media, sand, and gravel were used as filter media in this pilot-scale biofilteration. However, Mn(II) concentration in the biofilter effluent did not meet the DWS of 0.05 mg/L, even after the pilot-scale biofilter operated for 6 months (Fig. 2.2). At that stage of the project, the long start-up period for Mn(II) removal particularly at the low temperatures specific to the local groundwater source (4 to 8 °C) was observed. The long start-up periods at that stage of the project was a major concern to Delco Water. Low groundwater temperatures in biofiltration systems hinder microbial metabolic activity, causing slower rates of biological Mn oxidation. It is necessary to address this challenge in order to improve the functioning and efficiency of biofiltration technology under low-temperature regimes.

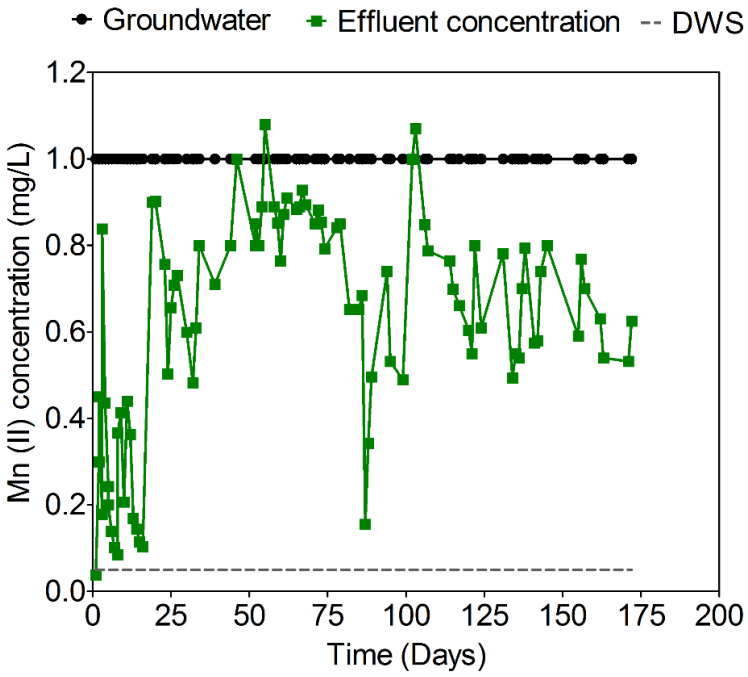

Fig. 2.2 Monitoring of Mn(II) concentrations in the groundwater influent and effluent of the pilot-scale biofiltration unit with newly filled with virgin filter media at the Langham water treatment plant, showing the long acclimation period for Mn(II) removal (over 100 days), during which Mn(II) removal from the groundwater fluctuated greatly at low temperatures (4 to 8 °C).

2.5. Problems with biofilter functionalization for manganese removal

Biofiltration technology has been widely adopted in Europe and North America to remove Mn(II) from water sources. However, some problems associated with the functionalization of Mn biofiltration for full-scale operations need to addressed.

Firstly, the long start-up periods observed in Mn biofilteration. A start-up period of several months is required for biofilters to achieve steady-state functioning and meet DWS with virgin filter media. Especially under low- temperature regimes, start-up periods can be further prolonged leading to greater associated costs and reduced treatment capacity (Tekerlekopoulou et al., 2013).

Secondly, Mn(II) removal in biofilters is also dependent on the existing geochemical conditions in the local groundwater source. Inefficient Mn biofiltration may be caused by the groundwater chemistry, (*i.e.,* low pH (<7) and/or high ammonia (NH_3-N) concentrations (>2.5 mg/L)) (Gouzinis et al., 1998).

Long start-up periods in Mn biofiltration at low temperatures are a major concern and the primary challenge to address in this study. It is known that Mn(II) removal in biofilters is initiated by bacterial oxidation and MnOB are critical for biofilter performance (Burger et al., 2008b). Bacterial metabolic activity is temperature-dependent and varies from site to site (Berbenni et al., 2000, Gulay et al., 2016). Low on-site temperatures can hinder MnOB activity, which may result in long start-up periods or the need for an energy-intensive water treatment facility, and may ultimately increase the cost of biofiltration operations (Cai et al., 2014, Tekerlekopoulou et al., 2013). This is a concern particularly in the vast northern cold-climates of Canada, China, some European countries, and the U.S. (Alaska) (Cai et al., 2014, Berbenni et al., 2000, Bourgine et al., 1994, Susanne et al., 2017).

Previous biofiltration studies conducted for groundwater at low temperatures (3–15 ºC) have reported a wide range of start-up periods on the order of 2 to 8 months (Bourgine et al., 1994, Cai et al., 2014, de Vet et al., 2009, Li et al., 2005, Li et al., 2013). Previous studies also reported that biological Mn(II) oxidation activity significantly decreases below 15 ºC (Berbenni et al., 2000, Francis et al., 2001, Tebo and Emerson, 1985, Tipping, 1984). However, other studies demonstrated the ubiquity of indigenous MnOB that are adapted to cold habitats in Antarctica lakes (Krishnan et al., 2009), which might suggest a reliable resource for Mn biofiltration initiation. The functionality of these cold-adapted MnOB specific in low-temperature Mn(II) biofiltration has been reported for a few biofiltration studies at low temperatures (Cai et al., 2014,

Li et al., 2013). These studies reported the occurrence of relatives of known MnOB genera (*Pseudomonas, Crenothrix, Leptothrix,* and *Hyphomicrobium*) in the successfully operated low-temperature Mn biofilters. However, their functionality and importance in Mn(II) removal specially at low temperatures is not described (Table 2.2). Therefore, additional research is needed to investigate the role of MnOB adapted and enriched in biofilters operating at low temperatures, which may be critical for successful biofiltration. Examining factors that can improve the conditions for biological Mn(II) oxidation is critical for designing, planning, and managing biofiltration, especially when it is implemented in cold climates.

Ripened biofiltration unit filter media, with Mn-oxide coating plays a significant role in enhancing physico-chemical/auto-catalytic Mn(II) oxidation (Sahabi et al., 2009). Mn-oxide surface coatings on filter media tend to adsorb and further oxidize soluble Mn(II), which is an autocatalytic oxidation reaction. Katsoyiannis and Zouboulis (2004), Cerrato et al. (2011), and Voegelin et al. (2014) reported that Mn(II) was oxidized to form Mn(III/IV)-oxide precipitates in the biofilters, likely promoting autocatalytic oxidation. Bourgine et al. (1994) and Bruins et al. (2015a) reported the formation of Mn(III/IV) oxides in a successfully operated, low-temperature manganese removal filter. Bruins et al. (2015a) reported the presence of birnessite, a Mn-oxide with valence +3.5 to +3.9, in the filter media coatings and backwash sludge of a pilot-scale Mn removal filter operated at 10.5-12.5 °C. In this study, Bruins et al. (2015a) reported the birnessite formation in the filter column was most likely initiated via biological activity. With the progress of filter ripening and development of the surface coating, birnessite formation was predominantly controlled by physico-chemical mechanisms (Table 2.2). Therefore, the autocatalytic property of Mn-oxide surface layers may accelerate Mn(II) oxidation under low-temperature regimes (Learman et al., 2011). However, additional research is still required. Specifically, the types of Mn-oxides formed on the filter media surfaces in low-temperature biofilters has not been adequately studied, nor has the synergy between biological and physico-chemical Mn(II) oxidation. Understanding the formation of Mn-oxides on virgin filter media, and expanding our knowledge of key operational and design parameters, are required to overcome the challenges of treating Mn(II) in cold-region groundwater.

Table 2.2 Literature review on characterization of microbial communities and filter media in a low temperature Mn biofiltration systems.

Design	Contaminants	Temperature (°C)	Analytical tools employed	Key information	Known AOB, FeOB and MnOB genera	Reference
Pilot-scale	Fe, Mn, and NH_4^+	11	SEM [a]	Presence of Mn(IV)-oxide identified	NA	Bourgine et al. (1994)
Bench-scale	Fe, Mn, and NH_4^+	10.5-12.5	SEM, EPR, and Raman spectroscopy [a]	Presence of birnessite on the aged filter media confirmed. Formation of birnessite was most likely initiated via biological activity. With the progress of filter ripening and development of the coating, birnessite formation became predominantly by physico-chemical mechanisms	NA	Bruins et al. (2015a)
Field-scale	Fe, Mn, and NH_4^+	8	Clone sequencing and T-RFLP [b]	The spatial distribution of microbial populations along the depth of the biofilter demonstrated the stratification of the removal of iron, manganese and ammonia	*Nitrospira*, *Prostecobacter*, *Pseudomonas*, *Gallionella*, *Leptothrix*, and *Hyphomicrobium*	Li et al. (2013)

Design	Contaminant	Temperature (°C)	Analytical tools employed	Key information	Known AOB, FeOB and MnOB genera	Reference
Pilot-scale	Fe, Mn, and NH_3-N	3-4	454 pyroseque-ncing [b]	This study has demonstrated that Fe, Mn, and NH_4^+ functional oxidizing bacteria that can be acclimated to low-temperature water conditions	*Candidatus Nitrotoga*, *Crenothrix*, *Hyphomicrobium*, *Leptothrix*, *Nitrosomonas*, *Nitrospira*, and *Nitrosospira*	Cai et al. (2014)

a: analytical tools employed characterization of filter media

b: analytical tools employed characterization of microbial community

3. BIOFILTRATION FIELD STUDY FOR COLD Fe(II)- AND Mn(II)- RICH GROUNDWATER: ACCELERATED Mn(II) REMOVAL KINETICS AND COLD-ADAPTED Mn(II)-OXIDIZING MICROBIAL POPULATIONS

Accepted in Water Quality Research

This chapter is written in joint authorship with Wonjae Chang (supervisor), Joyce M. McBeth (co-supervisor), Babak Roshani (Delco Water), and Brian Rindall (Delco Water). The study is part of an NSERC Engage project and MITACS Accelerate Research in collaboration with Delco Water led by Dr. Wonjae Chang (Principal Investigator). Babak Roshani and Brian Rindall designed and operated a pilot-scale biofiltration unit at Langham Water Treatment Plant. Sandeepraja Dangeti designed and conducted all the lab experiments. PXRD data was collected by Sandeepraja Dangeti and Joyce McBeth. SEM analysis performed at Saskatchewan Research Council. EPR data was collected by Dr. Ramaswami Sammynaiken. Jonathan Vyskocil prepared and executed the sequencing data pipeline in mothur. Data analysis and interpretation, and manuscript preparation was conducted by Sandeepraja Dangeti under the supervision of Wonjae Chang, Joyce McBeth, and Babak Roshani. The tables, figures, and references cited herein have been reformatted to fit the thesis style.

3.1. Abstract

Removal of Mn(II) from Fe(II)- and Mn(II)-rich groundwater in cold regions is challenging, due to slow Mn(II) removal kinetics below 15 °C. This study demonstrated the onset, acclimation and acceleration of Mn(II) removal in a two-stage pilot-scale biofilter (Fe and Mn filters) at varying low on-site temperatures (8–14.8 °C). Mn(II) removal commenced at 8 °C in the Mn filter after Fe(II) removal. A shift in redox-pH conditions favored biological Mn(II) removal and Mn(II)-oxidizing bacteria increased. The Mn filter reached steady-state functioning after 97 days, exhibiting high removal efficiencies (97±0.9%). Yet, first-order rate constants (*k*) for Mn(II) removal were low (10^{-6}–10^{-5} min^{-1}; $t_{1/2}$=~40 d). After consecutive backwashes and a filter inoculation with backwashed sludge, *k* remarkably accelerated to 0.21 min^{-1} ($t_{1/2}$=3.31 min at 11±0.6 °C). The cold-adapted microbial consortium (51 genera), including *Pseudomonas, Leptothrix*, *Flavobacterium*, and *Zoogloea*, cultured from the field-aged biofilter rapidly produced biogenic Mn-oxides at 8 °C, which was confirmed by the electron paramagnetic resonance spectroscopy. Birnessite and pyrolusite detected by synchrotron-based powder X-ray diffraction, and a repetitive birnessite-like surface morphology on the ripened filter materials, were consistent with autocatalytic oxidation. Shifting in *k* indicated the vertical progress of biofilter ripening, which was not limited by low temperature.

Keywords: Biofiltration; Biological Mn(II) oxidation; Groundwater; Accelerated Mn(II) removal; Mn(II)-oxidizing bacteria; Birnessite

3.2. Introduction

Dissolved manganese in groundwater exists in its reduced form, Mn(II). Excess soluble Mn(II) is a common element of concern in water supplies. Under redox conditions favorable for Mn(II) oxidation, Mn(II) is converted to solid, dark brown Mn (III/IV) oxides, which results in black discoloration and lowers the aesthetic quality of drinking water. The deposition of Mn(III/IV) oxides causes scaling and corrosion in water supply infrastructure (Pacini et al., 2005).

Biofiltration technology has been widely considered for the treatment of Mn-rich groundwater. Biofiltration promotes microbially mediated Mn(II) oxidation that converts soluble Mn(II) to insoluble Mn(III/IV)-oxide precipitates, which are easily filtered out by filter media in

biofiltration systems. However, microbial activity is temperature-dependent. Low temperatures greatly hinder the activity of mesophilic Mn(II)-oxidizing bacteria (MnOB), resulting in long start-up periods and the need for energy-intensive biofiltration (Tekerlekopoulou et al., 2013). This is a concern particularly in vast northern cold-climate regions (e.g., Canada, Alaska, and northern China and Europe) (Štembal et al., 2005, Cai et al., 2014, Susanne et al., 2017). Previous studies report that Mn(II) removal promoted by MnOB activity and/or Mn-oxide surface coatings on filter materials significantly decreases below 15 °C (Berbenni et al., 2000, Cooley and Knocke, 2016). The Mn(II) oxidation activity of *Leptothrix discophora* (MnOB) incubated at 8 °C, for example, was suppressed to 50–80% of its oxidation activity at room temperature (Boogerd and de Vrind, 1987).

However, at the same time, MnOB are ubiquitous in natural and engineered environments such as the deep sea, rivers, lake sediments, fjords, and water pipes (Tebo et al., 2005). Indigenous MnOB tolerant to low temperatures may be abundant or even prevail in cold habitats (Krishnan et al., 2009). Enriching growth of MnOB adapted to low temperatures may be crucial for the onset of Mn(II) oxidation and the generation of biogenic Mn-oxides. Those biogenic Mn-oxides may then trigger autocatalytic Mn(II) oxidation during biofiltration (Bruins et al., 2015a, Burger et al., 2008b), which may positively influence the kinetics of Mn(II) removal in cold environments. Yet, cold-adapted MnOB capable of rapidly generating Mn-oxides at low temperatures have not been extensively reported in previous field studies. In addition, the onset, acclimation, and acceleration of Mn(II) removal under low temperature regimes has not been extensively described in biofiltration studies conducted at field sites.

In this study, a flow-through pilot-scale biofiltration unit containing virgin filter media (anthracite, sand, and gravel) was installed for a field experiment for the treatment of cold Fe(II)- and Mn(II)-rich groundwater. Aqueous Fe(II) is often naturally abundant when groundwater is rich in Mn(II). Iron oxidation is very thermodynamically favorable and occurs rapidly in the presence of oxygen. However, the Mn(II) oxidation kinetics are very slow or negligible in the absence of biotic and/or abiotic catalysts (Mouchet, 1992). This study focuses on Mn(II) removal through a two-stage biofiltration unit at a water treatment plant in the town of Langham (Saskatchewan, Canada), which has an annual mean temperature of ~2 °C. The temperature of the influent groundwater that continuously flowed into the biofiltration unit ranged from 4 to 8 °C, and the effluent temperature of the Mn filter ranged from 8 to 14.8 °C throughout the study. The objective

of this study was to demonstrate how Mn(II) oxidation activity commenced, acclimated and accelerated in the biofiltration unit under the low on-site temperature regime. This study also addresses how Mn(II) removal kinetics is related to filter ripening. A cold-adapted MnOB consortium derived from the sufficiently aged Mn filter was investigated.

3.3. Materials and methods

3.3.1. Natural groundwater

The groundwater source in this field experiment was the Floral Formation of the Dalmeny aquifer in Saskatchewan (SK) (Fortin et al., 1991), accessed via a groundwater well at the Langham Water Treatment Plant (52.36 N 106.95 W). Water chemistry data and operational parameter data for the influent groundwater used in this study are presented in Table 3.1.

3.3.2. Pilot-scale biofiltration system

Fig. 3.1 illustrates the schematic diagram for the biofiltration unit. The biofiltration unit was designed to remove Fe(II) in the first filter (Fe filter) and Mn(II) in the second filter (Mn filter). From top to bottom, the two filter columns contained four layers of filter media: granular anthracite, fine sand, coarse sand, and gravel. An aeration tank with an air compressor was installed between the Fe and Mn filters to aerate the groundwater. The biofiltration experiment was conducted over 6 months from July 2014 to January 2015, to include both a summer and a winter season. The operational parameters for the biofiltration unit are summarized in Table 3.1. Detailed information about the biofiltration operation is available in Supplementary Material.

3.3.3. On-site monitoring and chemical analyses

During biofiltration, water chemistry data were collected on-site for the effluents of the two biofilters: Fe(II) and Mn(II) concentrations, temperature, pH, oxidation-reduction potential (ORP), and dissolved oxygen (DO). Colorimetric analyses were used to measure Fe(II) and Mn(II) concentrations (Hach Methods 8146 and 8149, respectively). Two sets of three probes were installed at the outlet of each biofilter (Hach-PD2P1, Hach-RD1P5, and Hach-5540D0C) to monitor pH, ORP, DO, and temperature. The formation of Mn-oxides on the filter media in the biofiltration unit was assessed on-site using the leucoberbelin blue I (LBB I) colorimetric assay

(Sigma-Aldrich Canada). For water samples collected from the Mn filter, off-site analyses were performed using inductively coupled plasma optical emission spectroscopy (ICP-OES) to precisely measure Fe(II) and Mn(II) concentrations in the groundwater before and after the biofiltration treatment. Detailed information about effluent sampling (triplicate) and data analyses, including statistical analyses, is presented in Supplementary Material.

Table 3.1 Operational parameters for the pilot-scale biofiltration unit and water chemistry data for the influent and effluent groundwater.

Operational parameters		
Flow velocity	3.21 m/h	
Number of backwashes	9	
Filter depth (cm)		
Head space	44	
Anthracite	50	
Fine and coarse sand	41	
Gravel	20	
Groundwater chemistry		
	Influent	Mn filter effluent
Temperature (°C)[a]	4–8	8–14.8
pH[a]	7.1	7.2–7.8
ORP (mV)[a]	-45	300 to 500
Total Fe (mg/L)[b, c]	2.81±0.02	0.002±0.001
Total Mn (mg/L)[b, c]	0.88±0.01[d]	<0.001
NH_3-N (mg/L)[b, c]	0.53	0.13
NO_3^--N (mg/L)[b, c]	0.009	0.49

a: Measured using the sensors on-site
b: Sampled at 110 days
c: ICP-OES analyses/colorimetric method
d: 0.88±0.01 mg/L in groundwater influent; and 0.84 mg/L in Fe filter effluent

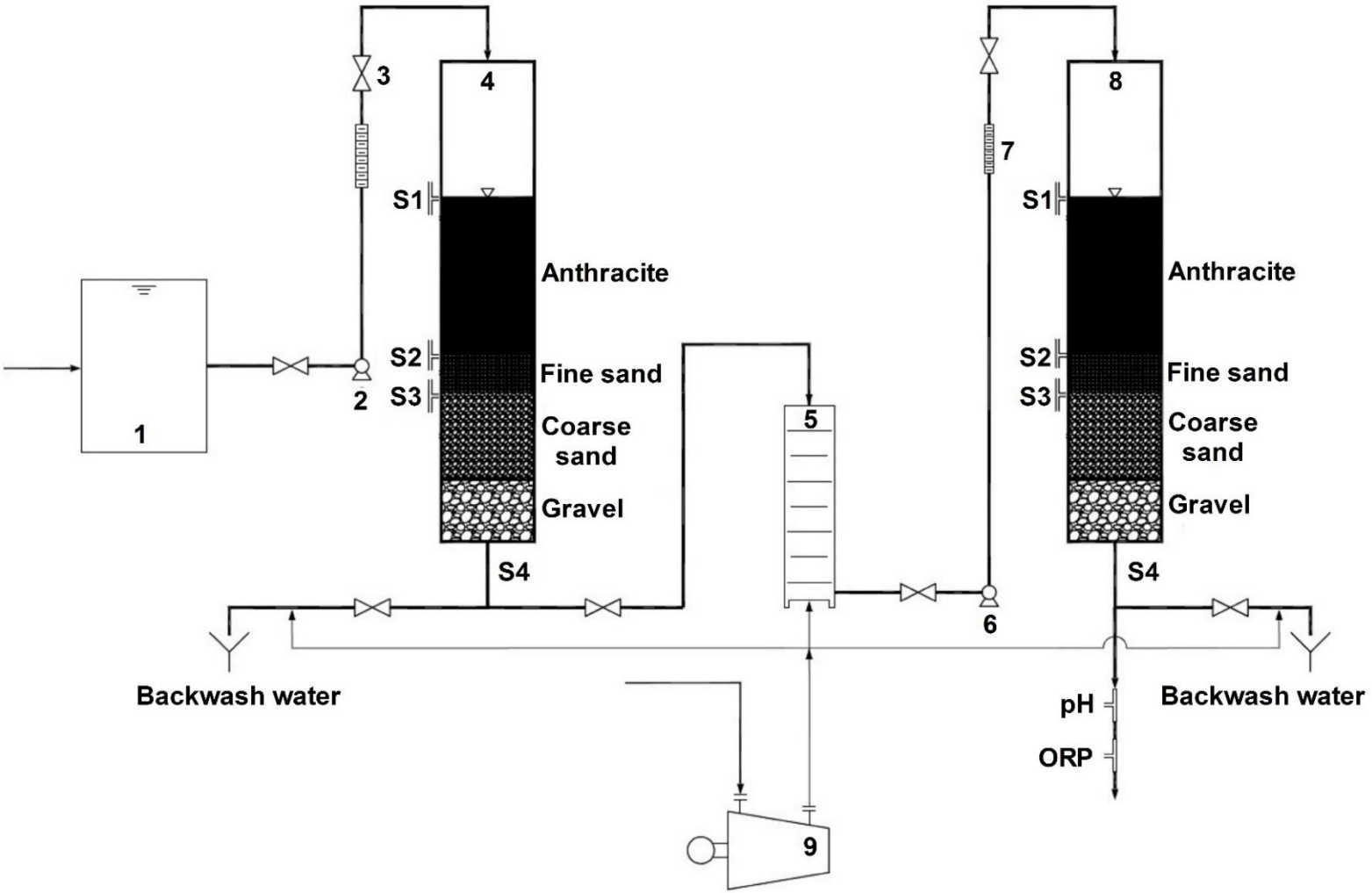

Fig. 3.1 Schematic representation of the two-stage pilot-scale biofiltration unit (1: Reservoir, 2: Pump, 3: Flow meter, 4: Inlet of Fe filter, 5: Aeration tank, 6: Pump, 7: Flow meter, 8: Inlet of Mn filter, 9: Compressor, and S1, S2, S3, S4: Sampling ports).

3.3.4. Viability, metabolic activity, and cold-adapted MnOB consortium culturing

The number of viable MnOB, the most probable number (MPN), and adenosine triphosphate (ATP) concentrations were determined using similar methods to those media in previous studies (Tebo et al., 2007). Cold-adapted MnOB consortia were cultured at 8 °C using backwash water collected on Day 110 from the Mn filter. Further information for the culture-dependent analyses above is presented in Supplementary Material.

Genomic DNA was extracted from the cultured consortium using PowerWater® DNA Isolation Kits (MoBio Laboratories). Extracted DNA was sent to RTLGenomics (Lubbock, Texas) for high-throughput amplicon sequencing using the Illumina-MiSeq platform. Raw sequence reads were processed using the mothur software package, version v.1.32.0, following the standard operating procedure for MiSeq analyses (Schloss et al., 2009). Paired 16S rRNA gene amplicon reads from the enriched MnOB consortium was deposited in the European Nucleotide Archive (ENA) under project number PRJEB15479, and accession numbers ERS1360945 and ERS1360944.

3.3.5. Mn-oxide characterization

To characterize the surface morphology and elemental composition of the solid precipitates and filter materials, analyses were conducted using scanning electron microscopy with energy dispersive X-ray spectrometry (SEM/EDS; Hitachi S3000-N SEM with a Quartz PCI XOne SSD X-ray analyzer). An electron paramagnetic resonance (EPR) spectroscopy analysis was performed for the precipitates obtained from the culturable MnOB consortium (Supplemental Material). Synchrotron-based powder X-ray diffraction (PXRD) analyses were conducted using the Canadian Macromolecular Crystallography Facility's bending magnet beamline (CMCF-BM, 08B1-1) at the Canadian Light Source (CLS). Detailed information about the data processing is available in Supplementary Material.

3.3.6. Kinetic analyses for Mn(II) removal

Mn(II) removal kinetics are expressed using the following first-order kinetic model that considers empty bed contact time (EBCT), as described in previous studies (Yang et al., 2015, Zeng et al., 2015, Cheng et al., 2016, Katsoyiannis and Zouboulis, 2004).

$$\frac{d[Mn(II)]_t}{dt} = -k[Mn(II)]_t \quad \text{..... (3.1)}$$

In the equation above (3.1); k is the first-order rate constant (min^{-1}) for the overall removal of Mn(II), which may include biological and/or physico-chemical removal; $[Mn]_t$ is the concentration of Mn(II) at the EBCT; and EBCT is the amount of time an influent to be treated is in contact with the filter media in a vertical filter column. The EBCT is calculated as follows:

$$EBCT = \frac{Volume\ (L)}{Flow\ rate\ (\frac{L}{min})} \quad \text{.....} \quad \text{(3.2)}$$

The Mn(II) concentrations in samples collected from the four sampling ports of the Mn filter were measured for the kinetic analysis calculations. Temporal changes in the vertical distribution of Mn(II) concentrations were assessed using the four sampling ports installed vertically along the biofiltration unit at varying depths. Contour maps for Mn(II) concentrations in the Mn filter were generated using Surfer 13 (Golden software).

3.4. Results and discussion

3.4.1. Start-up and steady-state functioning of the biofilter

Dissolved Fe(II) concentrations in the groundwater decreased dramatically through the Fe filter (Fig. 3.2A). Fe(II) concentrations in the effluent stream of the Fe filter were consistently below the drinking water standard (DWS) for Fe(II) of 0.3 mg/L. Dissolved Fe(II) was removed from the groundwater prior to Mn biofiltration consistently over the course of the field experiment (183 days).

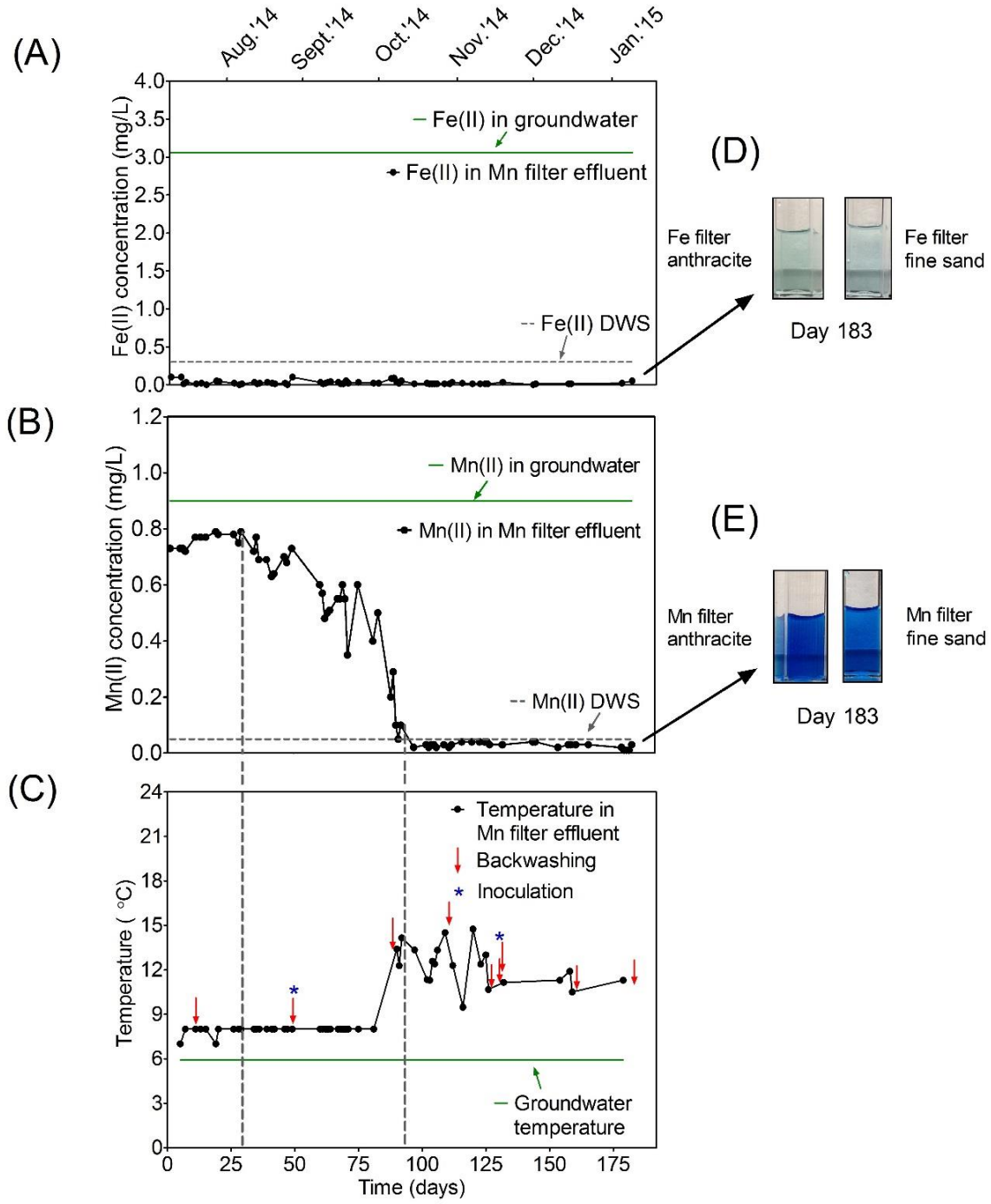

Fig. 3.2 Profiles of (A) Fe(II), (B) Mn(II) concentrations, and (C) temperatures measured from the effluent stream of the Mn filter. DWS refers to the Canadian drinking water standards of 0.3 and 0.05 mg/L for Fe(II) and Mn(II), respectively. (D, E) Leucoberbelin blue I (LBB I) assay indicated Mn (III/IV) oxides desorbed from anthracite and sand collected from the Fe and Mn filters.

Fig. 3.2B presents changes in the Mn(II) concentrations in the Mn filter effluent over time. Fig. 3.2C shows the effluent temperatures monitored at the outlet of the Mn filter. Mn(II) concentrations in the Mn filter effluent were relatively stable over the first month (Days 0–29) at ~0.8 mg/L, which was only ~0.1 mg/L less than the Mn(II) concentration in the influent groundwater (0.88±0.01 mg/L). However, between Days 29 and 34, Mn(II) concentrations began to decrease in the Mn filter effluent (Fig. 3.2B). Meanwhile, the effluent temperatures were stable at 8 °C for the first 81 days of the biofiltration experiment, indicating that Mn(II) removal commenced in 29–34 days at the on-site temperature of 8 °C. Two additional months were required to reach steady-state functioning of the Mn filter at 97 days, at which point the Mn(II) removal efficiency was high and stable (97±0.9%). The mean effluent temperature during the steady-state functioning period was 12±0.6 °C.

Mn(II) concentrations in the Mn filter effluent collected at the site were 0.03±0.01 mg/L during the steady-state functioning period. The ICP-OES analyses for the effluent collected on Day 110 confirmed that total Mn(II) concentrations in the effluent were below the DWS of 0.05 mg/L (Table 3.1). The difference in the datasets for mean total Mn(II) concentrations in the groundwater before and after biofiltration was statistically significant, with $p < 0.0001$ (t-test, Table 3.1). The LBB I assay (Fig. 3.2E) provided an on-site indication of Mn-oxide formation on the anthracite and sand collected from the Mn filter on Day 183 (at the end of the experiment). Mn(II) oxidation in the Fe filter was negligible, as indicated by the LBB I assay for the filter media collected from the Fe filter (Fig. 3.2D). Total Mn concentrations in the Fe filter effluent (Day 110) were as high as 0.84 mg/L. This is most likely due to the lower redox potential in the Fe filter (e.g., < 200 mV), which allows Fe(II) oxidation but not Mn(II) oxidation (Mouchet, 1992). NH_3-N concentrations were as low as 0.53 mg/L in the groundwater influent, and nitrifying activity would most likely not prevail in the Fe filter at that low NH_3-N concentration.

After Mn(II) removal began at 8 °C and shortly before the start of steady-state functioning in the Mn biofilter, the effluent temperature increased from 8 to 13 °C due to indoor heating in the water treatment facility in October (Fig. 3.2C). There was no direct heat supply to the biofiltration units. After October, effluent temperatures fluctuated between 9.5 and 14.8 °C until early December (after the steady-state condition was reached), and then stabilized at 11±0.6 °C for the rest of the winter period (until January), during which the Mn(II) removal efficiency of the Mn

filter was still stable at 97% and was not influenced by the temperature fluctuations (Fig. 3.2B and 3.2C).

3.4.2. Shift in oxidation-reduction potential

The ORP in the Mn filter gradually increased as the Mn(II) concentrations decreased in the Mn filter effluent stream (Fig. 3.3A). This correlation was statistically significant based on a Spearman correlation analysis (correlation coefficient: -0.84, $p < 0.0001$). Once the ORP in the Mn filter reached 300 and 313 mV around Days 29 and 34, Mn(II) removal commenced as described above (Fig. 3.3A). A steep increase in the ORP from ca. 300 to ca. 430 mV was observed shortly after a filter backwash with a subsequent inoculation of the Mn biofilter with the backwashed sludge. At that point, the ORP remained over 400 mV and became relatively stable between 400 and 500 mV. Once the steady-state functioning of the Mn filter was established, the ORP was less sensitive to both temperature fluctuations and backwashing frequency (Fig. 3.2C and 3.3A).

Using the ORP and corresponding pH data measured from the influent groundwater and Mn filter effluent, a Pourbaix diagrams (Mn-H_2O system) was constructed (Fig. 3.3B). The Eh (or ORP) and pH conditions of the Mn filter notably shifted from reducing to oxidizing conditions over the course of biofiltration. As the Mn filter acclimated, Eh-pH conditions in the Mn filter gradually shifted to conditions suited for biological Mn(II) oxidation, similarly to the results reported by Mouchet (1992) and Pacini et al. (2005). Once the steady-state functioning of the Mn filter was reached (after 97 days), all Eh-pH data points fell within the field of *biological* Mn(II) removal. The shift in the redox conditions and pH in the Mn filter suggested the enhancement of biological Mn(II) oxidation.

The Fe(II), NH_3-N, DO concentrations, and pH were not within their limiting ranges for biological Mn(II) oxidation (Table 3.1). The DO content in the Mn filter was consistent at 9±1.7 mg/L. An increase in NO_3-N concentrations from 0.009 to 0.49 mg/L was observed during biofiltration. However, nitrification did not appear to inhibit Mn(II) oxidation in the Mn filter, presumably due to the low initial concentrations of NH_3-N (< 1.0 mg/L).

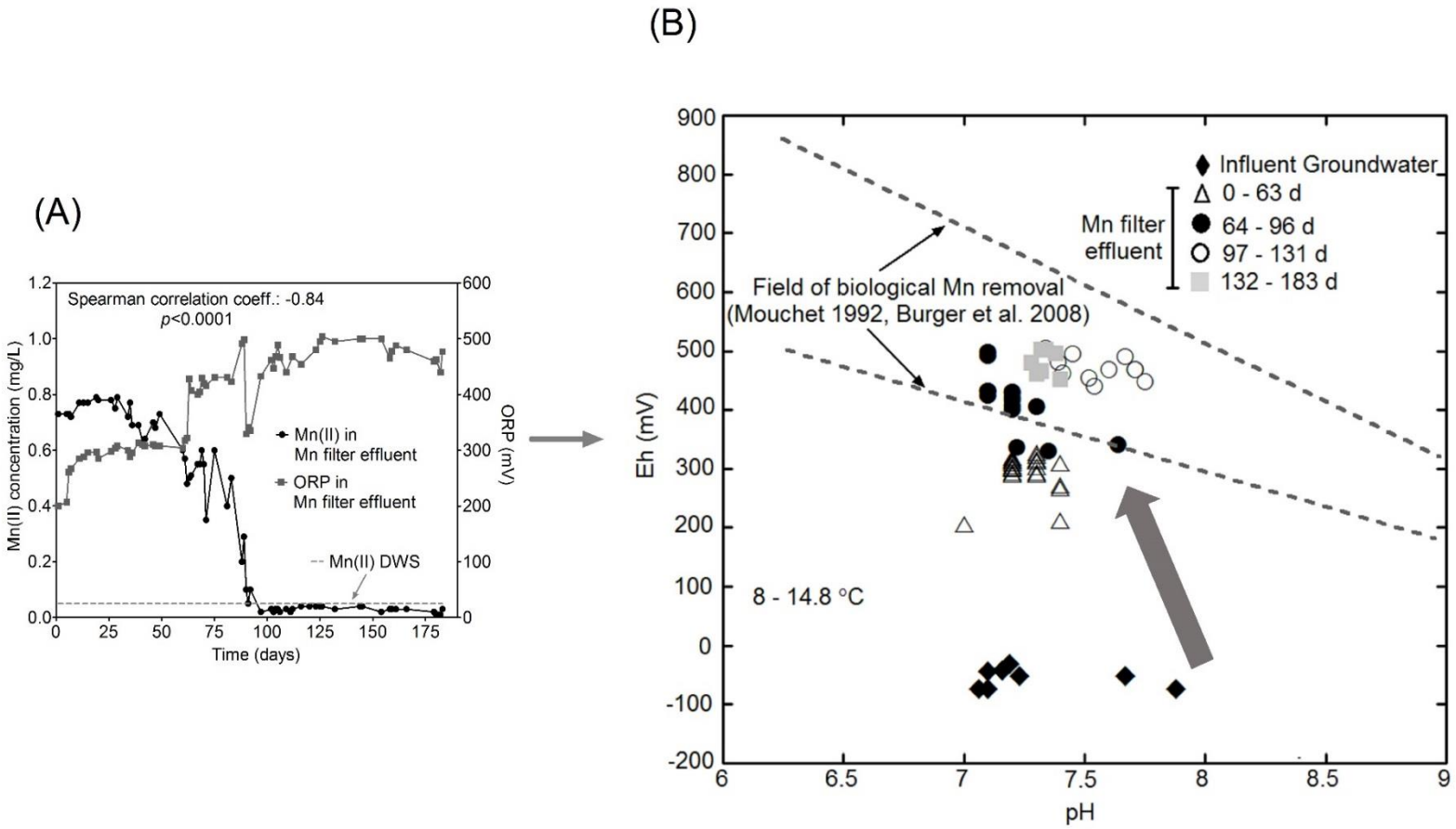

Fig. 3.3 (A) The correlation between changes in Mn(II) concentrations and ORP. (B) The Eh-pH diagram indicates a shift in Eh and pH conditions in favor of biological Mn(II) oxidation.

3.4.3. Viability and metabolic activity of microbial populations

The viable populations of culturable aerobic MnOB in the effluent and backwash water of the Mn filter (collected on Day 110, early in the period of steady-state functioning) were significantly greater than in the untreated groundwater (also sampled on day 110), based on the plate-count enumerations of MnOB at the start-up temperature of 8 °C (Fig. 3.4A; one-way ANOVA, $p < 0.0001$). Similarly, the MPN data for Day-106 samples showed that a greater number of culturable heterotrophs were present in the Mn filter effluent (93 MPN/mL) than in the influent groundwater (2 MPN/mL) and the Fe filter effluent (59 MPN/mL). The ATP concentrations measured after the experiment in the groundwater, storage reservoir, Fe filter effluent, and Mn filter effluent indicated that ATP was notably elevated in the Mn filter effluent, indicating that microbial metabolic activity continued throughout the period of steady-state functioning (Fig. 3.4B).

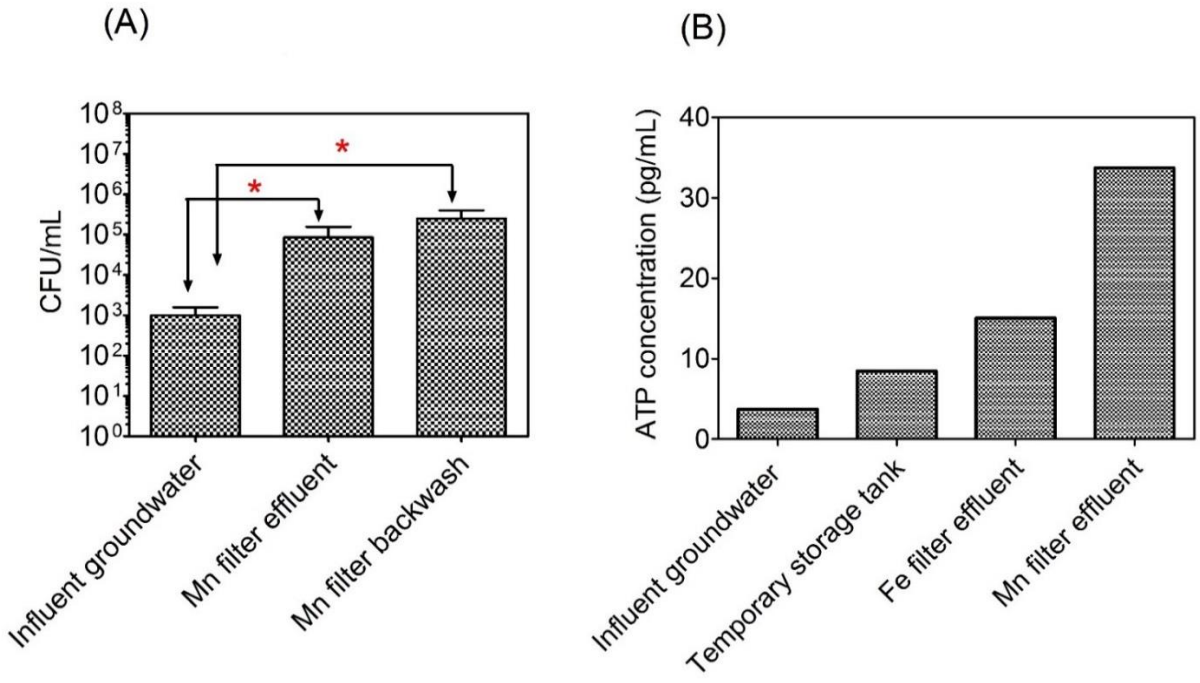

Fig. 3.4 (A) Viable Mn(II)-oxidizing bacteria in the Mn filter effluent on Day 110, enumerated at 8 °C. (B) ATP concentration.

3.4.4. Cold-adapted MnOB consortium

The culturing experiment using backwash water collected on Day 110 was conducted to identify a culturable MnOB consortium adapted to the start-up temperature (8 °C), and to visually observe biogenic M- oxide formation. The backwash water, used as inoculum, was collected when the ORP of the Mn filter exceeded 400 mV (Fig. 3.3B). The MnOB consortium enriched from the backwash water was able to rapidly produce biogenic Mn-oxides within five days at 8 °C (Fig. 3.5). The EDS analysis detected Mn in the precipitates (Fig. 3.5D). The SEM images showed poorly crystalized precipitates with amorphous morphology, which is characteristic of biogenic Mn-oxides (Fig. 3.9). The Mn-bearing solid precipitates exhibited a ΔH of 394 gauss, centered at a g-factor of 2.0, confirming the biogenic origin of the Mn-oxides (Fig. 3.5E). Conversely, the ΔH and g-factor of chemically synthesized birnessite mineral (standard) were 2816 gauss and 2.0, respectively, indicating an abiotic origin for the Mn-oxides (Fig. 3.10). The rapid formation of biogenic Mn-oxides at 8 °C reflected that the Mn filter had biologically acclimated to the low on-site temperatures. Even for filter media that were pre-coated with Mn-oxides in other Mn(II)-removal studies, temperatures below 15 °C (especially below 10 °C) still significantly decreased the Mn(II) removal efficiencies (Cooley and Knocke, 2016, Jia et al., 2015).

The Illumina-MiSeq 16S rRNA gene sequencing analysis for the microbial consortium identified known MnOB genera, *Pseudomonas*, *Leptothrix*, *Flavobacterium*, and *Zoogloea* (highlighted in bold font in Fig. 3.5C). Approximately 60% of the microbial consortium sequence reads were relatives of known MnOB. Of these, *Pseudomonas*, *Leptothrix*, and *Flavobacterium* have been frequently reported in Mn biofiltration studies (Cai et al., 2015, Tekerlekopoulou et al., 2013). However, the microbial consortium includes other diverse populations (over 46 genera), including *Rhodocista* (11.3%), *Phaselicystis* (7.3%), *Bdellovibrio* (5.1%), and *Hydrogenophaga* (<2.5%).

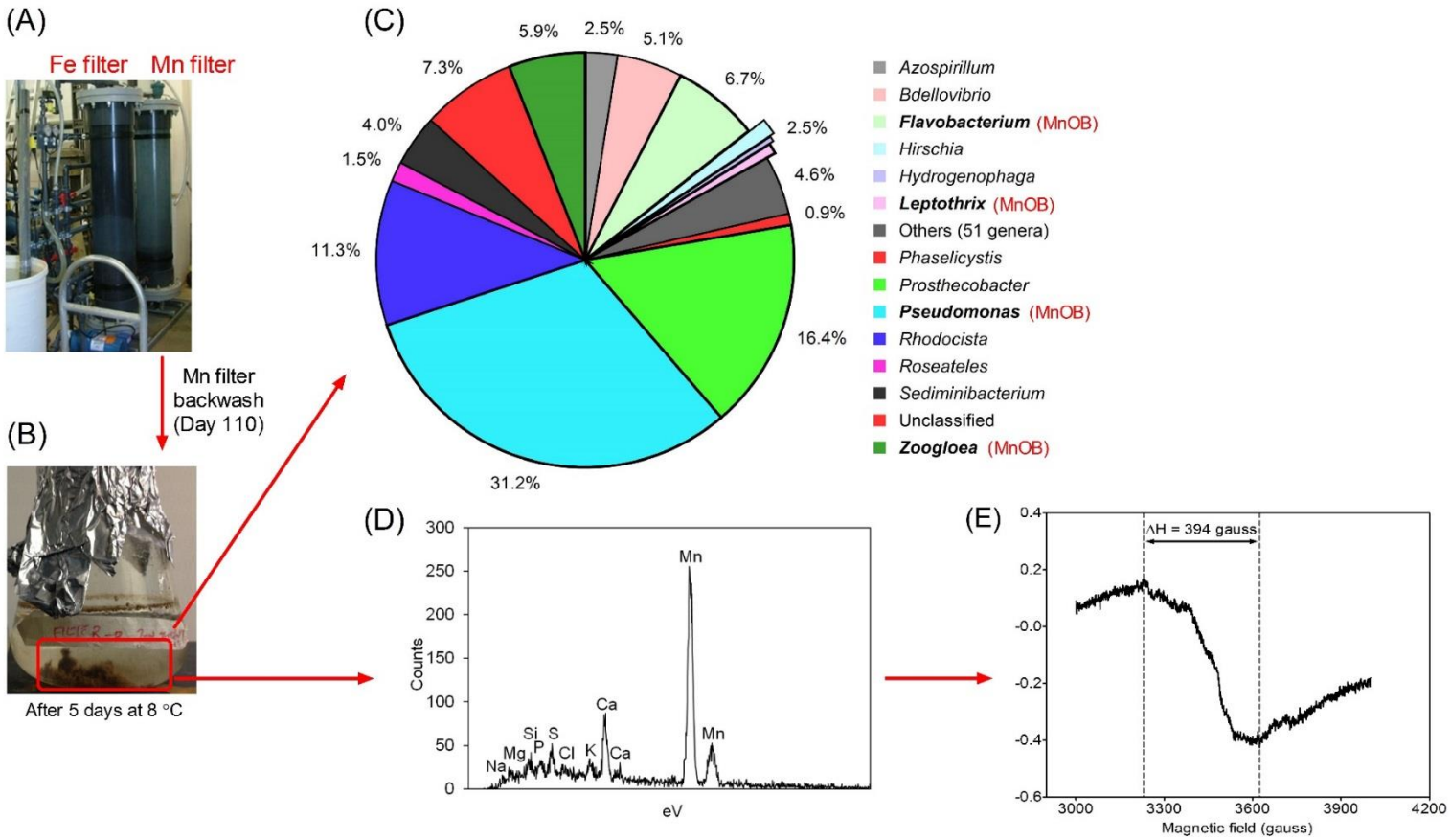

Fig. 3.5 **(A) The field biofiltration unit. (B) The formation of precipitates in the backwash water after 5 days in a culturing flask, beginning immediately after the backwash water was collected from the Mn filter on Day 110 (steady-state functioning period). (C) Genera presented as a percentage of high-throughput amplicon sequence reads from the microbial consortium enriched at 8 °C. Known MnOB genera are presented in bold. (D) The energy dispersive spectroscopy (EDS) analysis for the detection of Mn-rich precipitates. (E) The EPR analyses for solid precipitates formed in the culturing flasks of the MnOB consortium, containing biogenic Mn-oxides (ΔH=394 gauss).**

3.4.5. Accelerated Mn(II) removal and filter media ripening

After the multiple backwashes and inoculation of the Mn filter with biologically-aged backwash sludge collected at high ORP values (+400 mV)—representing the strong activity of acclimated MnOB and rapid biogenic Mn-oxide formation—a drastic increase in the first-order rate constant (*k*) for Mn(II) removal was observed, an increase of up to five orders of magnitude (Fig. 3.6D). The *k* values were as low as 10^{-6} to 10^{-5} min^{-1} between Day 97 (the beginning of steady-state functioning) and Day 127. The *k* value rose steeply to 0.21 min^{-1} immediately after the multiple backwashes and backwash sludge inoculation on Days 127 to 132 (Fig. 3.6D). The corresponding half-life ($t_{1/2}$) for Mn(II) removal was substantially decreased from ~40 days on Day 92 (before the acceleration) to 3.31 min on Day 159 (after the acceleration).

The acceleration of Mn(II) removal kinetics in the Mn filter was observed in the middle of steady-state functioning, at a time when high Mn(II) removal efficiencies had already been observed (Fig. 3.6D). This finding indicates that tracking Mn(II) removal efficiency does not adequately take into account the ripening of the filter media. Fig. 3.7 shows that *k* values were as low as 0.007 to 0.068 min^{-1} between Days 132 and 148, even though the Mn filter exhibited the 97% removal efficiency due to the ripened bottom layers. Low *k* values reflected the incomplete ripening of the filter media. The drastically accelerating Mn(II) removal kinetics correlated to the progressive vertical ripening of the Mn filter media. The filter ripening progressed from the bottom (gravel), to the middle (sand), and to the top (anthracite), likely due to accumulating precipitates, biomass and/or sludge solids at the bottom (Fig. 3.7). The different types of filter media did not significantly affect biofilter ripening. As the *k* value for Mn(II) removal reached 0.21 min^{-1} with a short half-life of 3.31 min, Mn(II) from the influent groundwater was depleted rapidly as it passed through the topmost layers of the Mn filter (as specifically shown at 159 days in Fig. 3.7). At this stage, the Mn filter was considered nearly fully ripened based on the maturation of Mn(II) removal kinetics.

The findings presented herein are important from a field perspective. Tracking changes in the EBCT-based rate constant for Mn(II) removal is a simple approach to indicating filter ripening that is sufficiently advanced to trigger meaningful Mn(II) removal under low temperature regimes, and to determining the effective ripening period required for a biofilter. During the period of accelerated Mn(II) removal, the Mn filter effluent temperatures were very stable at 11±0.6 °C (Fig.

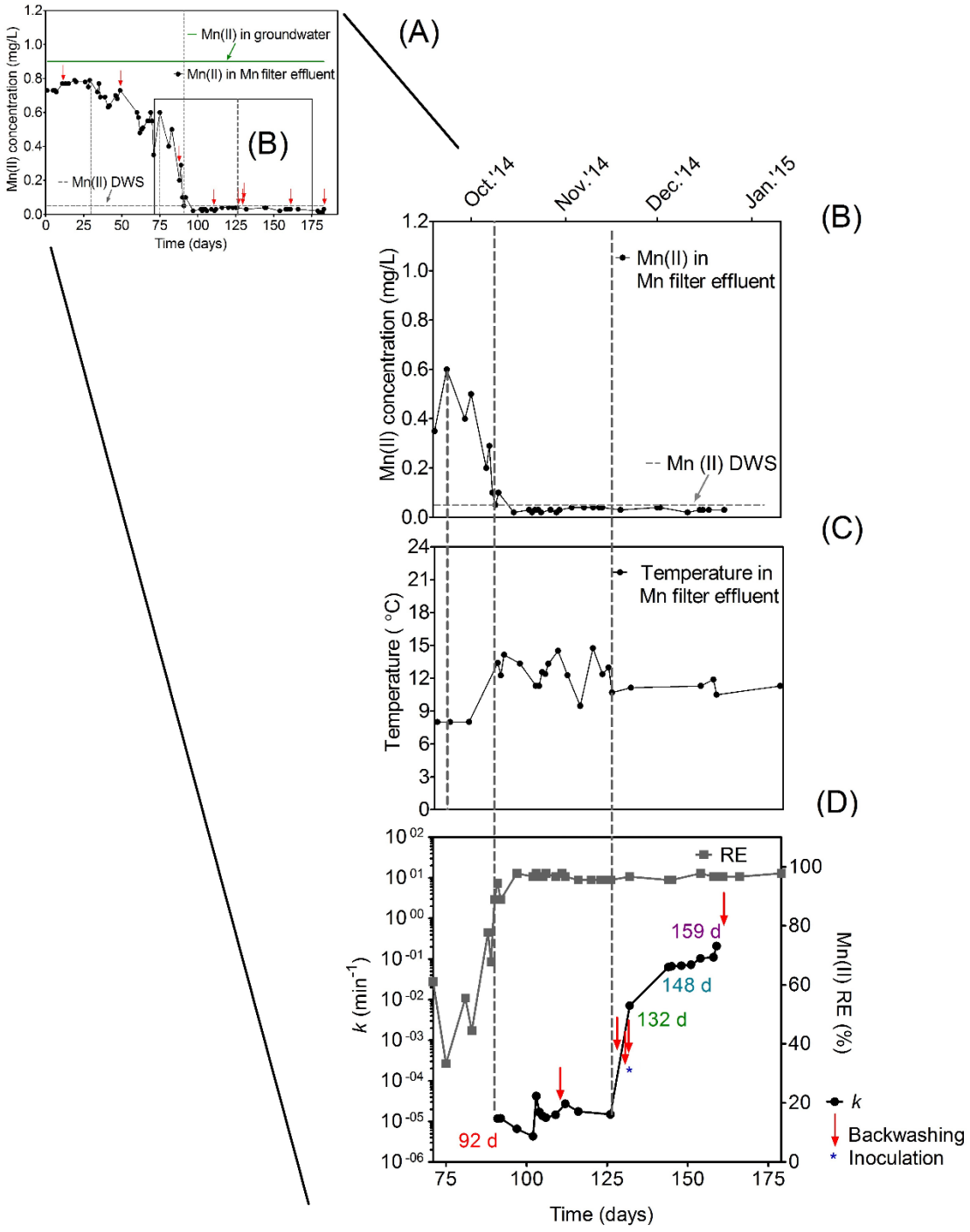

Fig. 3.6 (A) Mn(II) concentration profile, (B) Mn(II) concentration profile focused on the period of steady-state functioning, (C) the corresponding temperature profile for the Mn filter effluent, and (D) changes in the Mn(II) removal efficiency (RE) and the first-order rate constant (*k*) for Mn(II) removal.

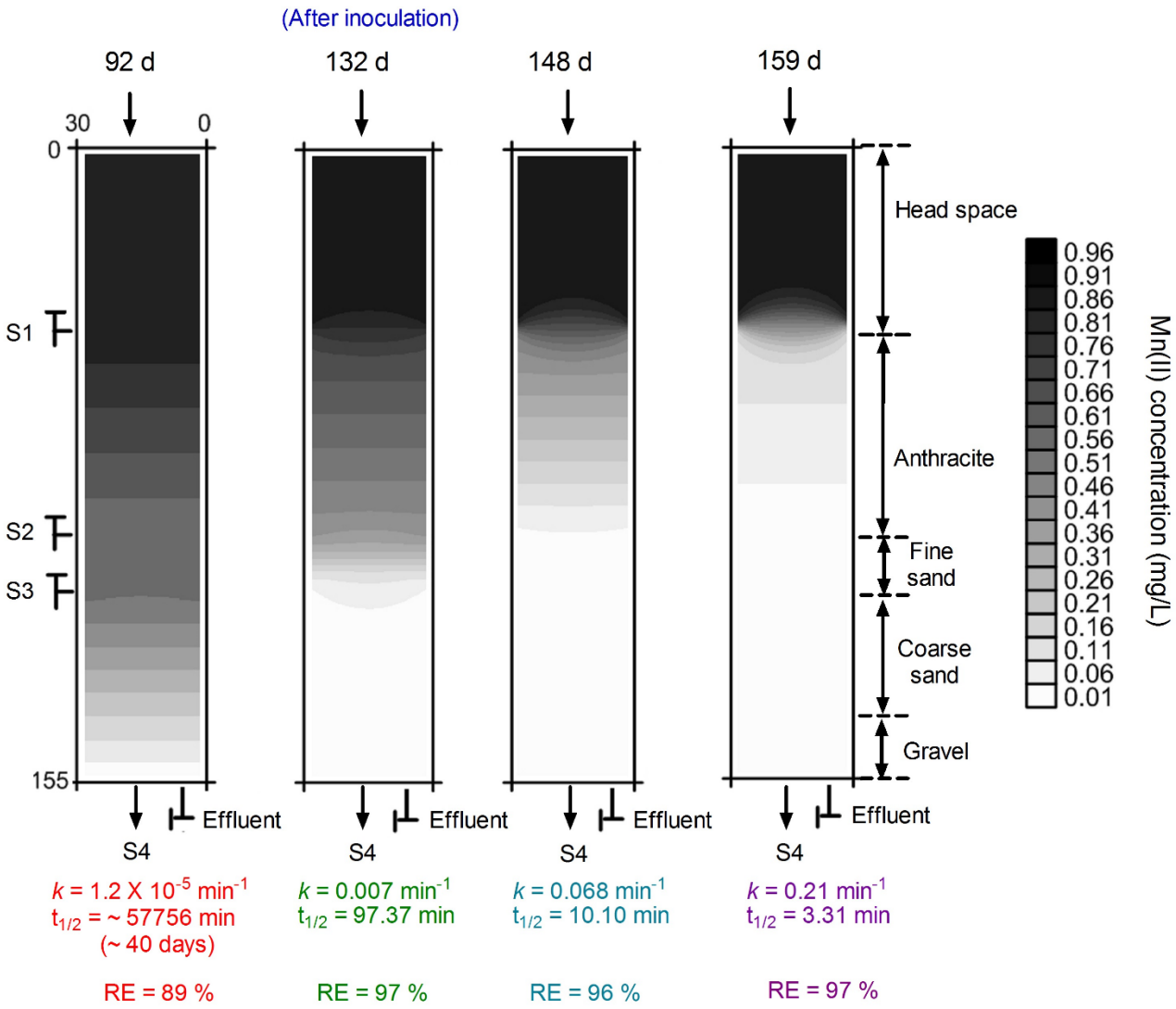

Fig. 3.7 Temporal changes in the vertical profiles of Mn(II) concentrations along the depth of the Mn filter over time, indicating the ripening of the filter media.

3.6C and 3.6D). The water temperature of 11 °C did not limit the acceleration of Mn(II) removal. The first-order rate constant of 0.21 min^{-1} obtained after filter ripening in this study is comparable to rate constants for Mn(II) removal reported in previous Mn-biofiltration studies conducted at a wide range of temperatures. Some of those studies were conducted at warmer temperatures and with pre-aged Mn filter materials (Table 3.2). The 4-month aging period in this study was shorter than those in previous studies (Table 3.2).

3.4.6. Birnessite and pyrolusite formation and surface morphology

Birnessite (K-rich MnO_2; Mn(IV) oxide) and pyrolusite (β-MnO_2; Mn(IV) oxide) were detected in the anthracite collected on Day 183 (end of the experiment), confirming that the Mn filter was fully ripened with Mn-oxides with the highest Mn oxidation states (Fig. 3.8C) based on the Mn oxidation pathway. The Mn oxidation states exhibited by birnessite and pyrolusite were +3.5 to +3.9, and +4, respectively. Hausmannite (Mn_3O_4; Mn(III) oxide) with Mn oxidation state +2.7 (Bruins et al., 2015b) was detected in centrifuged backwash water collected on Day 110 (early steady-state functioning period).

The ripened anthracite collected from the Mn filter on Day 183 was coated mainly by Mn-rich substances with a repetitive coral-like morphology (Fig. 3.8B). This surface morphology is similar to that of birnessite formed by autocatalytic Mn(II) oxidation based on visual comparisons of SEM images (Bruins et al. 2015a; Jiang et al. 2010). However, variations in the surface morphologies of Mn-rich coatings on the ripened filter media were easily observable on Day 183 (Fig. 3.8A and 3.8B). The SEM images of some surfaces of the ripened anthracite indicated a birnessite-like surface morphology that contains fewer coral-like patterns and appears to be fluffier (Fig. 3.8A). This morphology has been observed for biogenic Mn-oxide coatings previously (Bruins et al., 2015a, Jiang et al., 2010). Considering the multiple lines of evidence of enhanced biological Mn(II) oxidation, we conclude that varying birnessite-like surface-coating morphologies reflected microbially-mediated autocatalytic signatures of Mn(II) oxidation. Birnessite acts as an autocatalyst for physico-chemical Mn(II) oxidation (Bruins et al., 2015b). The detection of birnessite (crystalized) in the ripened filter media may be connected to the accelerated Mn(II) removal kinetics observed in this biofiltration study.

Table 3.2 Comparison of rate constants (k) from this study and various other Mn biofilter designs.

Temperature (°C)	*k* (min^{-1})	Flow velocity ($m\ h^{-1}$)	Experiment type	Scale	Initial filter media status	Aging characteristics	Reference
-	0.17[c]	7	Field	Full-scale	Aged	8-month pre-aging	Katsoyiannis and Zouboulis (2004)
11.2–14.6	0.50[d]	10–22	Field	Pilot-scale	Aged	8-month pre-aging	Štembal et al. (2005)
18–22[a]	0.14–0.16[c]	-	Lab	Lab scale	Virgin	MnOB pre-inoculation	Cai et al. (2015)
-	0.53[c]	7–19	Lab	Pilot-scale	Virgin	Aged using synthetic Mn(II)- and As(III)-contaminated water	Yang et al. (2015)
30[a]	0.023[c]	0.033–0.039	Field	Pilot-scale	Virgin	5-month aging	Zeng et al. (2015)
8[a]	0.69[c]	-	Field	Pilot-scale	Manganese sand	18-month pre-aging	Cheng et al. (2016)
4–8[a] 8–14.8[b]	0.21[c]	3.21	Field	Pilot-scale	Virgin	4-month aging: ORP: >+400 mV, Abundant MnOB Mn-oxide formation	This study

a: Influent water temperature

b: Effluent temperature

c: First-order rate constant

d: Treatability factor using mass-transfer-limited kinetics

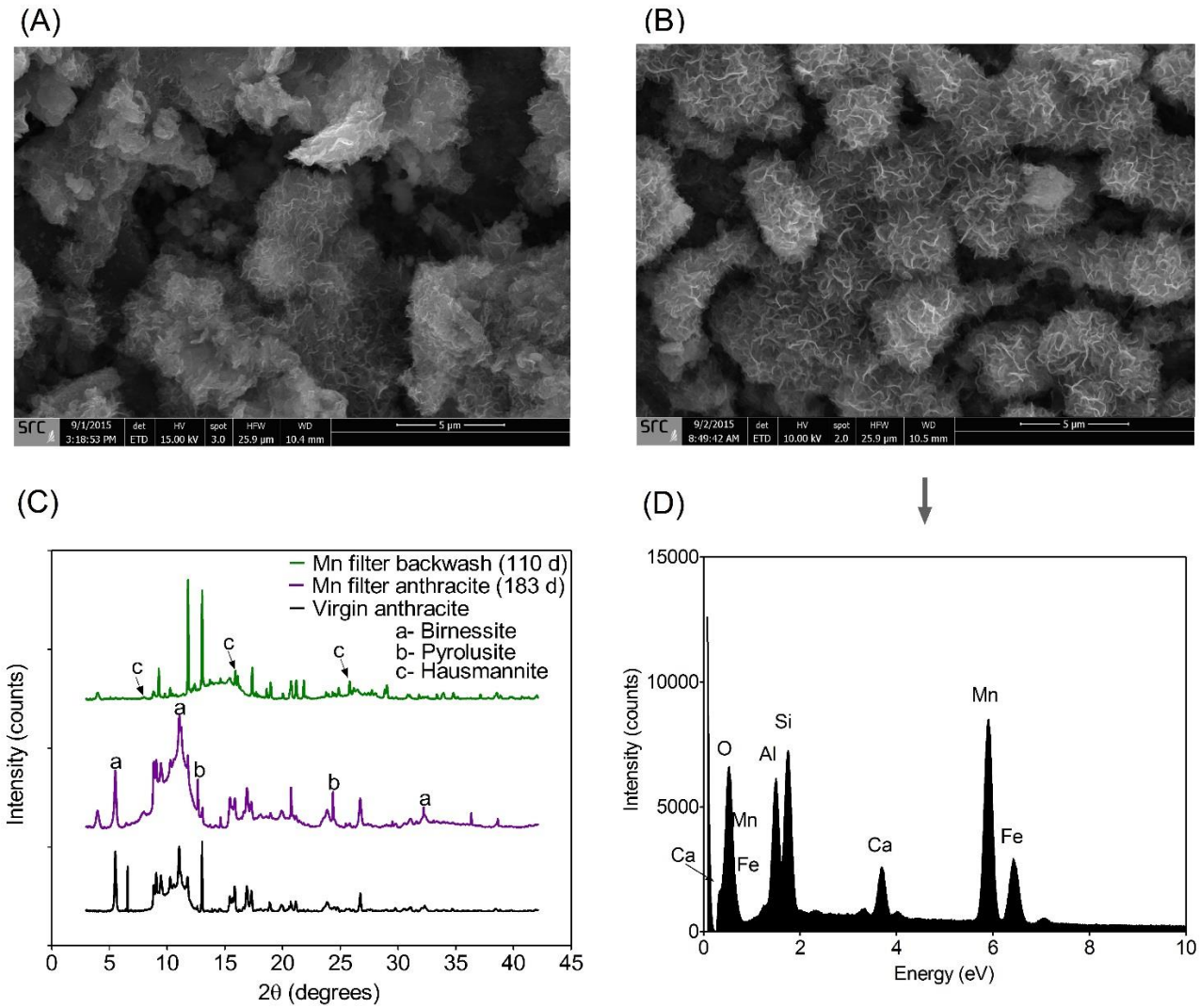

Fig. 3.8 SEM images of (A) slightly ripened and (B) well ripened surfaces within the same anthracite sample collected on Day 183, (C) synchrotron-based PXRD data, and (D) EDS analyses for detecting elemental metals on the well ripened anthracite.

3.5. Conclusions

In the Mn filter, Biological Mn(II) oxidation was significantly enhanced, based on the multiple lines of evidences including shift in ORP and elevated microbial metabolic activity. In the early stage of Mn(II) biofiltration at 8–14.8 °C, however, the Mn filter exhibited lower *k* values ranging from 10^{-6} to 10^{-5} min^{-1} at the variable on-site temperatures. Immediately after multiple backwashes and the inoculation of the biofilter with biologically-acclimated backwash sludge, *k* values markedly increased to 0.21 min^{-1} at 11±0.6 °C, which is comparable to *k* values obtained at higher temperatures in previous studies. The drastically accelerating *k* for Mn(II) removal was correlated to the vertical progression of filter media ripening through the Mn filter. The PXRD analyses detected birnessite and pyrolusite with high Mn oxidation states ranging from +3.5 to +4 in the ripened filter media. The varying surface morphologies of the ripened filter materials exhibited combined biological and autocatalytic signatures. The MnOB microbial consortium capable of rapidly producing biogenic Mn-oxides at the start-up temperature of 8 °C was obtained from the biologically-aged backwash water. These findings have important implications for improving biofiltration in cold regions, and represent a potential breakthrough for accelerating Mn(II) oxidation kinetics in cold groundwater.

3.6. Acknowledgements

We acknowledge technical and financial support provided by Delco Water Inc. This research was also funded by the Natural Sciences and Engineering Research Council of Canada (NSERC; EGP 468673-14 and RGPIN-2014-05902). The synchrotron-based PXRD analyses described in this study were performed at the Canadian Light Source (CLS), which is supported by NSERC, the National Research Council Canada, the Canadian Institutes of Health Research, the Province of Saskatchewan, Western Economic Diversification Canada, and the University of Saskatchewan. We thank Dr. Michel Fodje, Dr. Viorica Bondici, and Samira Sumaila for technical support during the PXRD analyses, and the CLS for granting access to their analytical equipment in the Life Sciences Laboratory. We also thank Dr. Ramaswami Sammynaiken for collecting the EPR data at the Saskatchewan Structural Sciences Centre at the University of Saskatchewan.

3.7. Supplementary material

3.7.1. Biofiltration system and operation

A pump, flow meter, and universal controller (SC-200, Hach) were installed for each of the two filters in the biofiltration unit. The biofilters were operated at a flow velocity of 3.21 m/h. Both filters were configured for downward flow during treatment and upward flow during regular backwashing for maintenance. Four sampling ports (S1 to S4 in Fig. 3. 1) were installed vertically along the biofiltration columns to collect water samples from the biofilters. The biofilters were backwashed using a combination of air scouring (5.8 L/min) and backwashing with raw groundwater at a flow velocity of 24.4 m/h to generate a 25–30% bed expansion. The backwash time for each filter was 2 min. Each biofilter was backwashed nine times over the course of the trial (indicated in Fig. 3.2C). For two of these backwashes (at 49 and 130 days), the Mn filter was inoculated with ~15 L of backwash sludge.

3.7.2. Effluent sampling, data analyses and Pourbaix diagram construction

Effluent water samples were collected in triplicate from sampling port S4 and preserved by spiking them at the site with 2% (w/v) nitric acid. Ammonia-N (NH_3-N), and nitrate-N (NO_3^--N) in the water samples were measured by colorimetric method using Aquakem 200 Discrete Analyzer at SRC. A statistical t-test analysis using GraphPad Prism 5 (GraphPad Software) was performed to verify the statistical significance of the difference in Mn(II) concentrations before and after biofiltration. The Pourbaix diagram (Eh-pH plot) for the Mn-H_2O system specific to the cold groundwater in this study was constructed using geochemical modeling software PhreeqcI (U.S. Geological Survey) and the Geochemist's Work Bench (Aqueous Solutions LLC).

3.7.3. Viability, metabolic activity, and cold-adapted MnOB consortium culturing

The viable MnOB from the untreated and treated groundwater samples, as well as from the backwash water collected from the Mn filter, were enumerated. The microbial enumeration was conducted using sterile Mn(II)-amended R2A agar (Sigma-Aldrich) and J medium agar plates (Tebo et al., 2007) with minor modifications. Inoculated plates were incubated at 8 °C in replicates

of four. Viable populations sizes enumerated by the R2A and modified J medium plate-counting analyses were expressed as colony-forming units per milliliter of water (CFU/mL). A statistical analysis (one-way ANOVA) was performed for the plate-count dataset (GraphPad Prism 5).

The most probable number (MPN) method was also used to estimate the abundance of heterotrophic bacterial populations in the untreated and treated groundwater, using the IDEXX SimPlate® (IDEXX Laboratories) according to the manufacturer's instructions. Concentrations of adenosine triphosphate (ATP), which is involved in energy transfer for microbial metabolism (Granger et al., 2014), were measured in the influent and effluent groundwater from the biofilters using LuminUltra's ATP measurement test kit (Lumitester^{TM} C-110, Hach).

For the MnOB consortium, the V4 region of the 16S rRNA gene was sequenced using the universal prokaryotic (archaeal and bacterial) primers 515F (5'-GTGCCAGCMGCCGCGGTAA-3') and 806R (5'-GGACTACHVGGGTWTCTAAT-3') (Caporaso et al., 2012). Raw sequence reads were processed using the mothur software package (v.1.32.0) based on the standard operating procedure for MiSeq analyses (Schloss et al., 2009). The trimmed sequences were aligned against the SILVA bacterial and archaeal database for small-subunit rRNA gene reference alignments (v.119) and classified using the RDP database.

3.7.4. J medium composition

The J medium agar plates were prepared using the following recipe (Tebo et al., 2007): 1.5 mM NH_4Cl, 20 mM HEPES buffer (~pH 7.4), 2 mM $KHCO_3$, 73 μM KH_2PO_4, 10 mM sodium succinate ($C_4H_4Na_2O_4$), 4 μM $Fe_2(SO_4)_3$, 100 μM $MnSO_4$, 15 g noble agar (Anachemia), and 0.2% (v/v) each of vitamin and trace element mixes (prepared as per ATCC MD-TMS and MD-VS, www.atcc.org; based on Wolfe's mineral and vitamin solutions) in 466 mL of Langham groundwater and 500 mL of deionized water. The media were autoclaved and poured in to sterile perti plates.

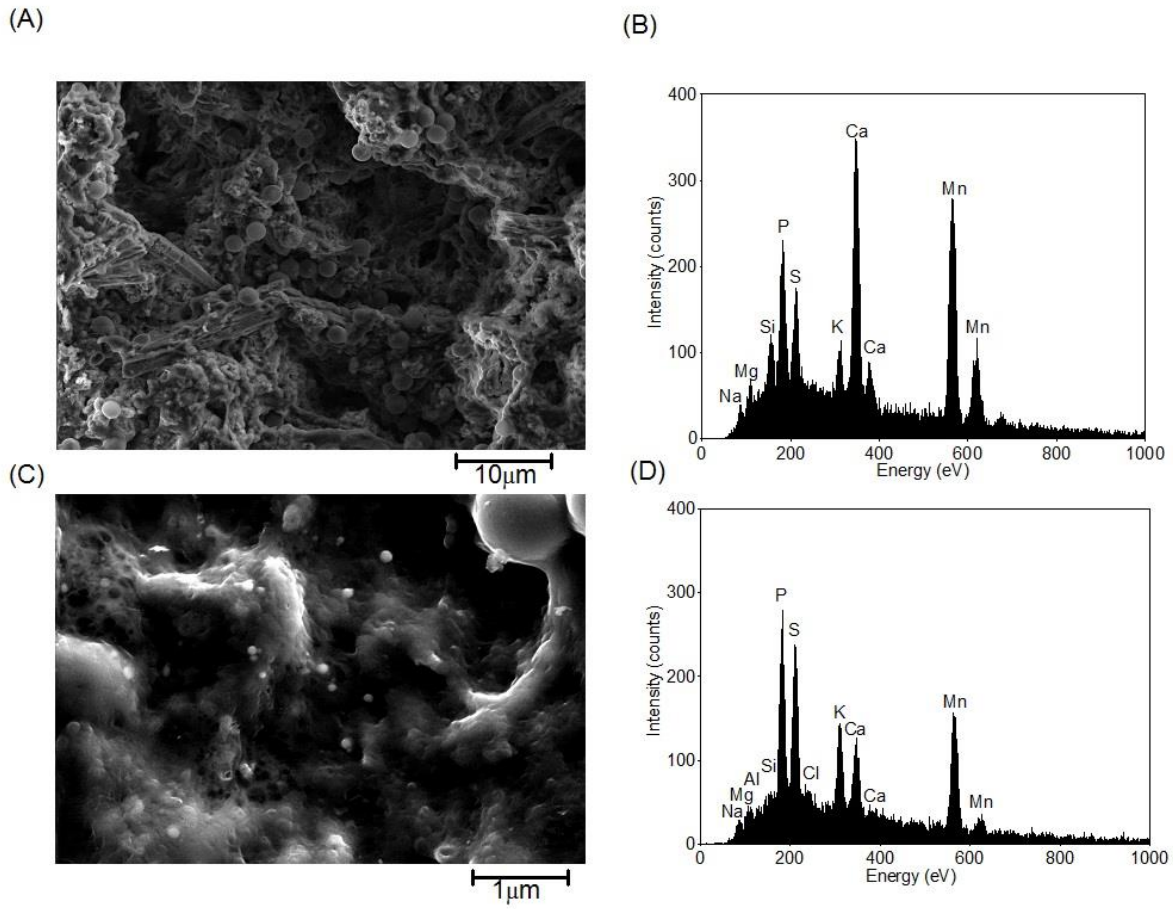

Fig. 3.9 (A)&(C): The SEM images indicating the amorphous nature of the solid precipitates collected from the MnOB consortium derived from the backwash water (Day 110). (B)&(D): the results of the EDS analyses for detecting elemental metals in the precipitates.

3.7.5. Electron paramagnetic resonance (EPR) spectroscopy

An electron paramagnetic resonance (EPR) spectroscopy analysis was performed for the solid precipitates obtained from the culturable MnOB populations enriched from the Mn filter backwash water. These precipitates were centrifuged and air dried for the EPR analysis. Chemically-synthesized birnessite mineral was used as a reference standard (Hardie et al., 2007). The EPR analysis was performed at 295 K (room temperature) using an X-band Bruker EMX EPR spectrometer operating at 9.8 GHz. The spectra were imported for analysis into Xenon data-

processing software (version 1.1b60, Bruker Organization). The EPR signal line width (ΔH in gauss) was determined from peak to peak (distance between the highest and lowest points of the first-order EPR signal wave) (Bruins et al., 2015a).

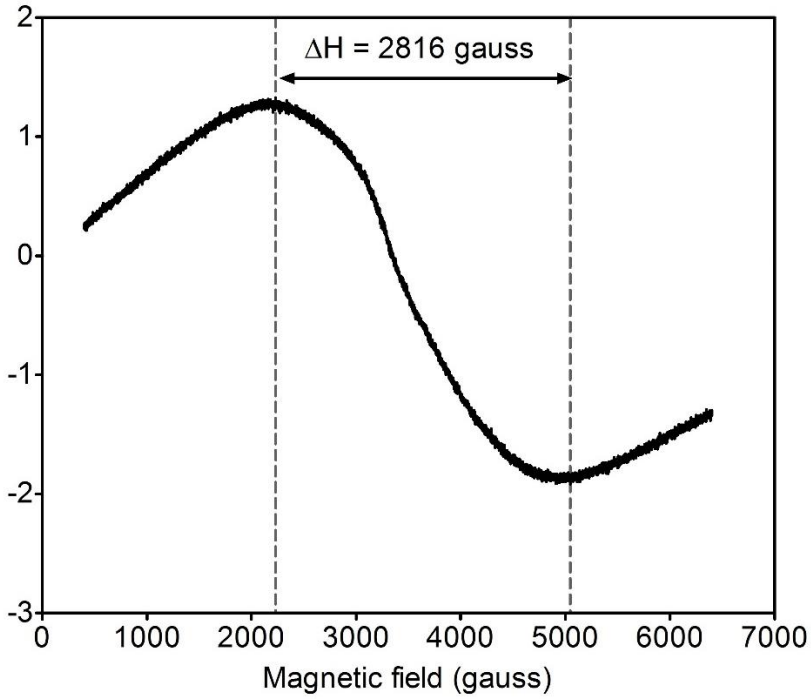

Fig. 3.10 The EPR analyses for the birnessite mineral standard (ΔH=2816 gauss).

3.7.6. Synchrotron-based powder X-ray diffraction (PXRD)

The beamline is equipped with a Rayonix MX300HE CCD X-ray detector and a silicon (111) double crystal monochromator (Fodje et al., 2014). Three types of samples were prepared in duplicate for the PXRD analyses: virgin anthracite, ripened anthracite from the Mn filter (183 days), and pellets from centrifuged backwash water samples from the Mn filter (110 days). The samples were dried in a desiccator, ground to a fine powder, and loaded into 1.5 cm long, 0.81 mm/0.032 inch polyimide capillary tubes (Cole-Parmer) sealed at both ends with cyanoacrylate adhesive (Loctite 454 Prism Instant Adhesive Gel). The PXRD patterns were collected at a capillary-to-detector distance of 200 mm and an incident beam energy of 18 keV (λ = 0.68878 Å) at ambient conditions. The sample-to-detector distance, tilt, and detector alignment were calibrated using a lanthanum hexaboride (LaB_6) standard (NIST SRM 660a LaB_6). A pattern from an empty

polyimide capillary tube was also collected at the same conditions as the samples, then subtracted from the sample data during integration. The 2-D PXRD patterns were processed using General Structure Analysis System (GSAS) II software (Toby and Von Dreele, 2013), and were radially integrated to produce intensity versus 2θ plots, with a 2θ resolution of 0.005°. Phase analyses were performed to identify Mn-oxide phases using X'Pert HighScore Plus software (v.3.0e) with a built-in Inorganic Crystal Structure Database, Powdered Diffraction File 2/4 (Degen et al., 2014).

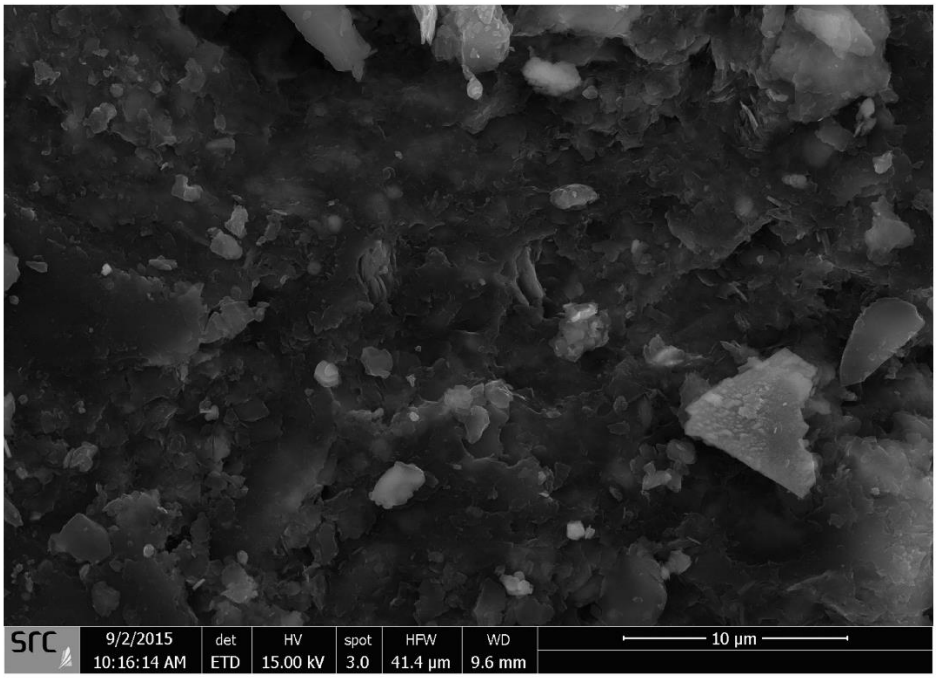

Fig. 3.11 SEM images of virgin anthracite.

4. MICROBIAL COMMUNITIES AND BIOGENIC Mn-OXIDES IN A SUCCESSFULLY-OPERATED BIOFILTRATION UNIT FOR COLD Fe(II)- AND Mn(II)-RICH GROUNDWATER

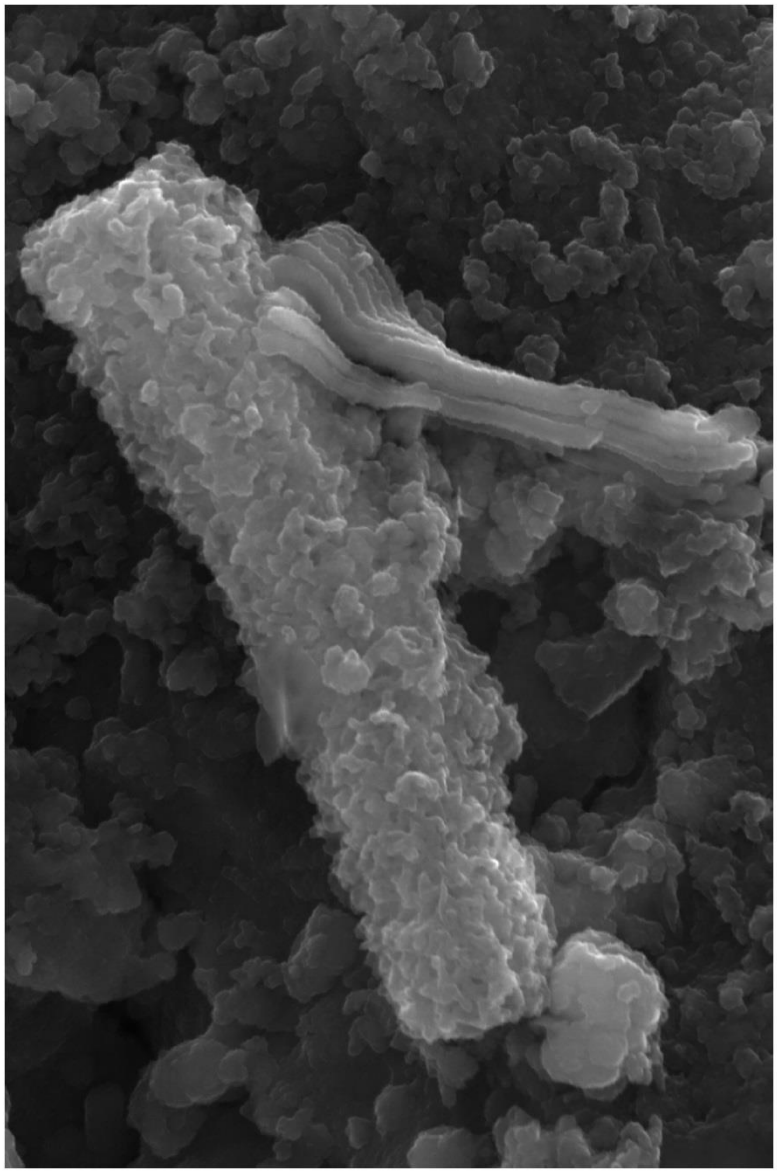

This chapter is written in joint authorship with Wonjae Chang (supervisor), Joyce M. McBeth (co-supervisor), Jonathan Vyskocil, Babak Roshani (Delco Water), and Brian Rindall (Delco Water). The work presented in this study was funded by the Delco Water Division of Delco Automation Inc., an NSERC Engage grant, a MITACS Accelerate grant, a Discovery Grant, and the Canada Foundation for Innovation (CFI) fund of Dr. Wonjae Chang (Principal Investigator). Babak Roshani and Brian Rindall designed and operated the pilot-scale biofiltration unit at Langham Water Treatment Plant. Sandeepraja Dangeti, Joyce M. McBeth, and Wonjae Chang designed the downstream laboratory experiments and analyses using the groundwater collected in the field. Sandeepraja Dangeti conducted all the lab experiments. XANES data was collected by Sandeepraja Dangeti and Joyce McBeth and analysis was performed by Sandeepraja Dangeti. SEM/EDS and XRF analyses are performed at the SRC. EPR data was collected by Dr. Ramaswami Sammynaiken at Saskatchewan Structural Sciences Centre (University of Saskatchewan). Jonathan Vyskocil prepared and executed the sequencing data pipeline in mothur. Data analysis and interpretation, and manuscript preparation was conducted by Sandeepraja Dangeti under the supervision of Wonjae Chang, Joyce McBeth, and Babak Roshani. The tables, figures, and references cited herein have been reformatted to fit the thesis style.

4.1. Abstract

This field study investigated the microbial communities in a two-stage, pilot-scale, flow-through biofiltration unit that successfully removed Fe(II) and Mn(II) from cold groundwater (4–8 °C). We have examined the relationships between the microbial data to groundwater chemistry and characteristics of the field-aged biofilter media. Illumina MiSeq sequencing of 16S rRNA gene amplicons obtained from the influent groundwater and biofilters (solids, effluents, and backwash water) revealed genus-level shifts in the bacterial community across the biofiltration unit from the influent groundwater, to the Fe filter, to the Mn filter. This community shift reflects the functional enhancement of biological Fe(II) and Mn(II) oxidation. Relatives of known Fe(II)-oxidizing bacteria (FeOB) in class *Betaproteobacteria* dominated the Fe filter. Previously-known Mn(II)-oxidizing bacteria (MnOB) were minor members of the Mn-filter community. *Betaproteobacteria* (including FeOB) appeared in both the Fe and Mn filters. *Hydrogenophaga* sp. (a known FeOB) likely acted as a MnOB; specifically, *Hydrogenophaga* strain CDMN isolated in this study can oxidize Mn(II) at 8 °C. *Alphaproteobacteria* were major (40±10%) part of the community in the Mn filter, however, none of these *Alphaproteobacteria* classified as known MnOB. Three new potential MnOB—*Azospirillum* sp. CDMB, *Solimonas soli* CDMK, and *Paenibacillus* sp. CDME—were isolated from the Fe or Mn filters. Synchrotron-based X-ray near-edge spectroscopy (XANES) coupled with electron paramagnetic resonance (EPR) revealed that biogenic birnessite was the dominant Mn-oxide. The co-existence of amorphous and crystallized surface morphologies of Mn-oxide on the Mn-filter media suggests the potential occurrence of both biological and autocatalytic Mn(II) oxidation in the biofilter.

4.2. Importance

Understanding the microbial community in *in situ* engineered biofilters is important for advancing biofiltration technology, which relies heavily on indigenous bacteria. Yet, microbial communities in operational biofiltration systems in the field, especially under environmentally-challenging conditions such as low temperature groundwater in cold climates, have not been extensively investigated. We explore how functional microbial communities changed in an on-site biofiltration unit for the treatment of cold Fe(II)- and Mn(II)-rich groundwater, and link the microbial data to groundwater chemistry and filter aging. The results show shifts in the microbial

communities reflecting the functional enrichment of useful microorganisms that form Fe- and Mn-oxides. This study reports new putative Mn(II)-oxidizing bacteria including *Hydrogenophaga* sp. which is likely responsible for Fe(II) and Mn(II) oxidization in this low temperature system (8 °C). This study also reveals the biogenic formation of birnessite in the successfully-operated biofilter, a reliable indication of microbially-mediated Mn(II) oxidation.

4.3. Introduction

Uncontrolled oxidation of dissolved Mn(II) in groundwater resources for drinking water production is a common concern (Cerrato et al., 2010). Solid dark brown Mn(III/IV) oxides formed by Mn(II) oxidation cause black discoloration of water and scaling in water distribution facilities, lowering the aesthetic quality of drinking water and damaging water supply infrastructure. High Mn content in water can also elevate the risk of neurobehavioral disorders in children (Bouchard et al., 2011). Dissolved Fe(II) and Mn(II) often coexist in groundwater. Fe(II) oxidation is thermodynamically more favorable than Mn(II) oxidation, and thus Fe(II) is generally rapidly removed from groundwater prior to Mn(II) treatment (Mouchet, 1992).

Biofiltration is an attractive water treatment technology, mainly because it does not require the use of strong oxidants (e.g., chlorine). Microbially-mediated Fe(II) and Mn(II) oxidation promotes removal of excess Fe(II) and Mn(II) from groundwater flowing into fixed-bed biofiltration columns filled with filter media (e.g., anthracite and sand). Mn(II) oxidation is kinetically negligible in the absence of abiotic catalysts and biocatalysts (Katsoyiannis and Zouboulis, 2004). The roles of Mn(II)-oxidizing bacteria (MnOB) are thus crucial for the start-up, acclimation, and successful maintenance of Mn(II) removal in biofiltration, especially under environmentally-challenging conditions such as low temperature groundwater regimes in Canada, Alaska, northern Europe and Asia, and Antarctica. In comparison to regions in the southeastern/southwestern USA where the groundwater temperatures are in range of 19.5 to 25 °C, Canadian groundwater temperatures are generally in the range of 4 to 8 °C (Health Canada, 1995, Hackbarth, 1978). In general, Mn(II) oxidation is significantly hindered below 15 °C, causing long start-up periods and slow Mn(II) removal during biofiltration (Berbenni et al., 2000, Tekerlekopoulou et al., 2013). Therefore, enriching MnOB that are tolerant to low temperatures is critical for successfully operating biofiltration for groundwater treatment in cold climates.

In addition to biological Mn(II) oxidation, physico-chemical Mn(II) oxidation may occur on Mn(III/IV)-oxide surface coatings (formed by Mn(II) oxidation) on filter media. In other laboratory studies, amorphous biogenic Mn-oxides formed by MnOB likely exhibited high surface areas for immobilizing Mn(II) and acted as strong oxidants that subsequently further enhance Mn(II) oxidation (autocatalysis) (Sahabi et al., 2009, Learman et al., 2011, Post, 1999). Bruins et al. (2015b) reported that abiotic Mn-oxides formed by physico-chemical oxidation predominate over biogenic Mn-oxide formation on filter media surfaces in a ripened rapid sand filter (RSF). However, RSF systems, which require chemical-oxidizing agents, are different from biofiltration treatment systems. Enriching useful MnOB microbial populations (biocatalysts) that are adapted to cold groundwater temperatures are crucial for achieving successful treatment of Mn(II)-rich groundwater under low-temperature regimes.

This study investigates microbial communities in a two-stage pilot-scale biofilter installed for the treatment of cold Fe(II)- and Mn(II)-rich groundwater with influent temperatures ranging from 4 to 8 °C. The microbial data were then examined in the context of changes in treated groundwater effluent chemistry (concentrations of Fe(II), Mn(II), NH_3-N, and NO_3^--N) and the characteristics of Mn-oxides associated with biofilter aging (oxidation states, Mn mineral identification, and biogenic/abiotic oxide origins). High-throughput amplicon sequencing (Illumina MiSeq) of the V4 region of 16S rRNA genes in the biofilters and groundwater, as well as culture-dependent approaches, were used to identify putative MnOB. Mn-oxides that form on the filter media (solids) were extensively characterized and identified using multiple instrumental analyses, including synchrotron-based X-ray near-edge spectroscopy (XANES), X-ray fluorescence (XRF), scanning electron microscopy (SEM) with energy dispersive X-ray spectrometry *(*EDS*),* and electron paramagnetic resonance (EPR).

This study reveals the functional enrichment of cold-tolerant microbial communities, including microbial populations acting as FeOB and MnOB in the biofilters. It also shows that biogenic birnessite (Mn-oxide) that formed on the field-aged Mn-biofilter media can be a reliable indicator of successfully engineered biofiltration that relies on biological and potentially autocatalytic Mn(II) oxidation at low on-site temperatures.

4.4. Materials and methods

4.4.1. Groundwater

The source of the groundwater used in this study was the Floral Formation of the Dalmeny Aquifer and was collected from a well at a water treatment plant (WTP) in the Town of Langham (52°21'32.9"N 106°57'02.6"W), 35 km northwest of the City of Saskatoon in Saskatchewan (SK), Canada. Aqueous Fe(II) and Mn(II) are naturally abundant in this groundwater at concentrations of 2.81±0.02 and 0.88±0.01 mg/L, respectively, which exceed the provincial drinking water standards (DWS) for Fe (0.3 mg/L) and Mn (0.05 mg/L). The temperature of the incoming groundwater at the Langham WTP is generally stable and varies between 4 and 8 °C. The oxidation-reduction potential (ORP) of the untreated groundwater varies between -32 and -75 mV, and the pH is 7.90±0.02 (Chapter 3; (Dangeti et al., 2017)).

4.4.2. Biofiltration performance

Fig. 4.1 presents a schematic diagram of the biofiltration unit, which consists of separate Fe and Mn filter columns (1.55 m high and 0.3 m in diameter). The fixed-bed filters are comprised of four filter-media layers: granular anthracite, fine sand, coarse sand, and gravel. To maintain aerobic conditions, an aerator was installed to re-oxygenate the water before it entered the Mn filter.

The pilot-scale biofiltration unit was operated continuously at Langham WTP for 183 days (Chapter 3; (Dangeti et al., 2017)). Briefly, Fe(II) concentrations in the Fe-filter effluent stream rapidly decreased below the DWS of Fe (0.3 mg/L) within five days of operation. The Fe(II) oxidation continued for the duration of the biofiltration experiment. The onset of Mn(II) removal began at around 30 days. A high Mn(II) removal percentage of 97% (bringing the Mn(II) concentrations to below the DWS of 0.05 mg/L) was maintained after 97 days, at which point the mean temperature of the Mn-filter effluent was 12.0±0.6 °C. The ORP of the Mn-filter effluent shifted to over +300 mV, within the favourable range for biological Mn(II) oxidation.

To confirm the changes in the groundwater chemistry for water samples collected from the groundwater, Fe and Mn filter effluents (sampled on Day 106 of operation), inductively coupled plasma optical emission spectroscopy (ICP-OES) and inductively coupled plasma mass spectrometry (ICP-MS) analyses were performed at the Saskatchewan Research Council (SRC).

Ammonia-N (NH_3-N) and nitrate-N (NO_3^--N) in the water samples were measured using a colorimetric method with a Aquakem 200 Discrete Analyzer at the SRC. The detection limits for Fe, Mn, ammonia (NH_3-N), and nitrate (NO_3^--N) analyses using ICP-MS/OES or colorimetry were 0.0005 mg/L, 0.0005 mg/L, 0.01 mg/L, and 0.009 mg/L, respectively.

4.4.3. Sampling and sample nomenclature

A total of 19 samples, including water, backwash sludge and filter media samples, were aseptically collected from the biofiltration unit on Days 110 (for water and backwash sludge samples) and 183 (for inner filter solids) and were shipped in an ice box to the Environmental Engineering Laboratory at the University of Saskatchewan. The shipped samples were immediately processed (by filtration or centrifugation) at the lab. For DNA extractions, each water samples was filtrated through Nalgene® 0.2 µm polyethersulfone (PES) membrane. The 50 mL aliquots of backwash sludge samples were centrifuged at 4000 g for 10 minutes and the supernatant was discarded. The processed samples and the filter media samples were then stored at -20 or -85 °C until further sample prepration.

The sample nomenclature, presented in Fig. 4.1, is associated with the sampling locations or sample types. The influent groundwater and initial backwash sludge from the Fe filter are denoted as GW and BWS, respectively. The anthracite and sand samples collected from the Fe and Mn filters are designated as Fe-An and Mn-An, and Fe-Sa and Mn-Sa, respectively. Fe-Ef refers to groundwater effluent samples collected from the bottom of the Fe filter (prior to Mn filtration). Backwash water samples from Fe and Mn filters are denoted as Fe-BW and Mn-BW, respectively. The 19 samples, including GW samples in triplicate and all other samples (BWS, Fe-Ef, Fe-An Mn-An, Fe-Sa, Mn-Sa, Fe-BW and Mn-BW) in duplicate, were analysed using microbial community and/or Mn-oxide characterization.

4.4.4. DNA extraction and high-throughput amplicon sequencing

Genomic DNA was extracted from the 19 samples using PowerWater® DNA Isolation Kits (MoBio Laboratories). The DNA concentrations of the samples were measured using the Qubit® dsDNA High Sensitivity Assay kit (Thermo Scientific Canada) and ranged between 0.1 and 20.8 ng/µL. DNA purity (A260/A280: 1.7±0.3 for the 19 samples) was determined using a NanoDrop 1000 (Thermo Scientific Canada).

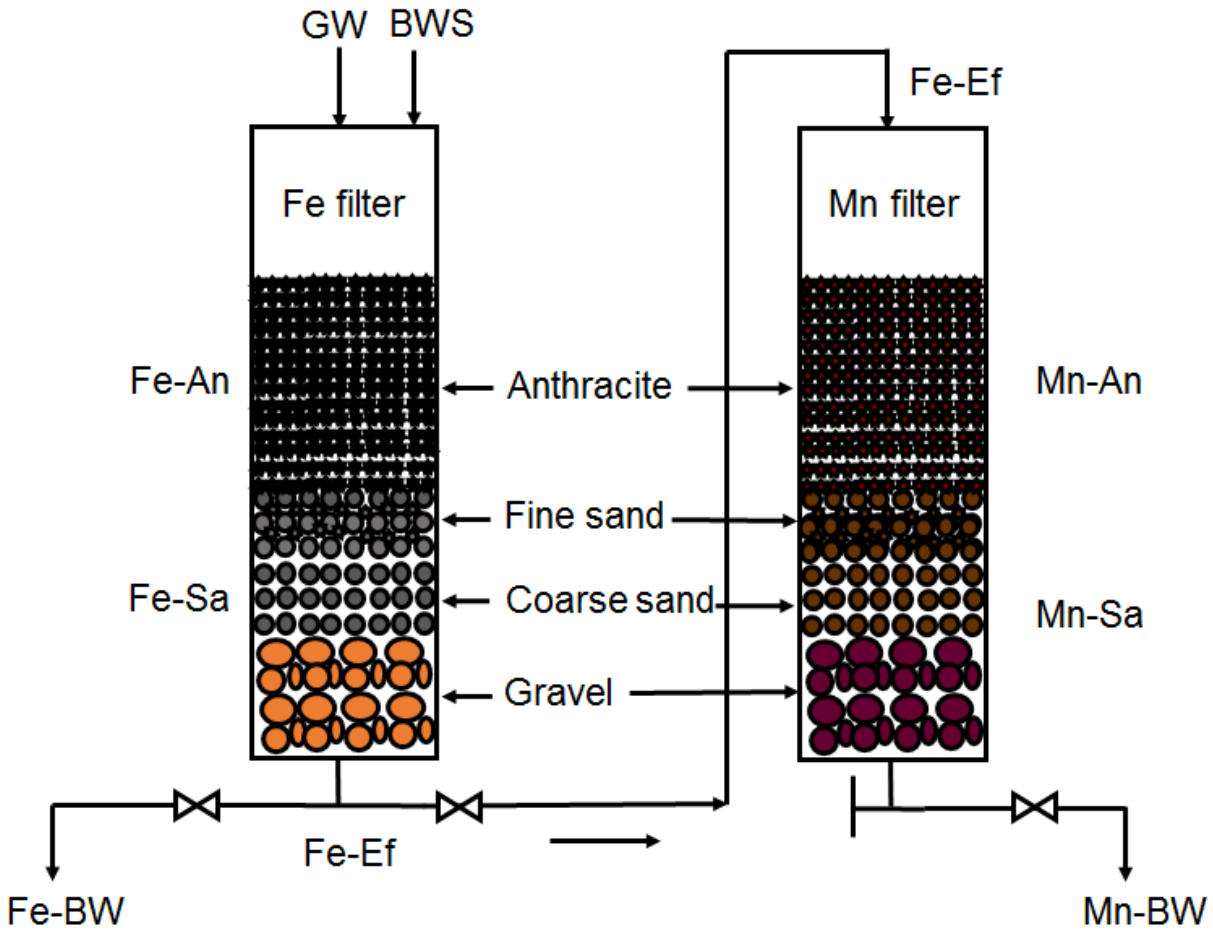

Fig. 4.1 A schematic representation of the two-stage flow-through pilot-scale biofiltration unit with anthracite, sand, and gravel as filter media, as well as the sampling locations and sample types. Sample abbreviations: GW: Influent groundwater; BWS: Initial backwash sludge used as an inoculum for the Fe filter; Fe-An: Fe-filter anthracite; Fe-Sa: Fe-filter sand; Fe-BW: Fe-filter backwash; Fe-Ef: Fe-filter effluent; Mn-An: Mn-filter anthracite; Mn-Sa: Mn-filter sand; and Mn-BW: Mn-filter backwash waste.

The extracted DNA samples were submitted to RTL Genomics, Lubbock, Texas, for Illumina MiSeq sequencing of the V4-region of the 16S rRNA Bacterial and Archaeal gene for amplicons. The Earth Microbiome Project universal primers 515F 5'-GTGCCAGCMGCCGCGGTAA-3' and 806R 5'-GGACTACHVGGGTWTCTAAT-3' were used for amplification (Caporaso et al., 2011). The pair-end sequences were processed using mothur,

version v.1.32 (Schloss et al., 2009). The mothur Illumina MiSeq standard operating procedure (SOP) was followed to align, filter, trim, remove chimeras, and classify and assign taxonomy to the reads. Read pairs were combined in to contigs and screened to remove short reads with degenerate bases or reads of 8+ homopolymers. The screened sequences were aligned using the SILVA rRNA database for bacterial and archaeal small-subunit rRNA reference alignments (v.119), and were pre-clustered with the single-linkage algorithm. Chimeras were removed using UCHIME, with the most abundant sequences used as references (Edgar et al., 2011, Schloss et al., 2011). Sequences were then classified using the Bayesian algorithm of the Ribosomal Database Project (RDP) classifier with a minimum bootstrap confidence cut-off of 80% (Wang et al., 2007). The lowest number of sequence reads obtained from the 19 samples was 8209, these number of sequences reads per sample were subsampled to 8,000. The subsampled sets of reads were clustered into operational taxonomic units (OTUs) by setting a 0.03 distance limit (equivalent to 97% similarity) using the average neighbor algorithm in mothur.

Rarefaction curves, Good's coverage values, and the Shannon diversity index (H′) were calculated by using the mothur community diversity calculators (Schloss and Handelsman, 2005). Shannon diversity index was used to calculate the Evenness (J′) based on Pielou's evenness index (J' = H'/ln(S); S=OTUs) and effective number of species ($e^{H'}$) ($e^{H'} = \exp(H')$) (Blackwood et al., 2007). To examine beta diversity, OTU-based distance matrices were created using Yue & Clayton theta values (Yue and Clayton, 2005) via the mothur "dist.shared" command. Principal coordinate analysis (PCoA) plots for the sequence reads were constructed to visualize sample clustering, and analysis of molecular variance (AMOVA) was used to determine significant differences between the microbial compositions of the samples. OTU-based Venn diagrams were constructed to compare the shared richness among samples. The raw sequence reads of the 19 samples were deposited into the European Nucleotide Archive (ENA) database of the European Molecular Biology Laboratory (http://www.ebi.ac.uk/ena) under project number PRJEB15260 (accession numbers ERS1310608 to ERS1310626) (http://www.ebi.ac.uk/ena/data/view/PRJEB15260).

4.4.5. MnOB isolation

MnOB were isolated from 10^{-2} and 10^{-3} dilutions of the GW, Fe-Ef, Fe-BW, and Mn-BW samples (diluted in phosphate buffer solutions) on J agar medium prepared using the groundwater samples (Nealson, 2006). The detailed composition of the J medium is described in Tebo et al.

(2007) and Nealson (2006). All cultures were incubated in the dark at 8 and 17 °C. Pure cultures were isolated by iterative plate streaking (at least five times) at room temperature. Mn(II)-oxidation activity was confirmed in these isolates by adding 0.04% leucoberbelin blue I (LBB I) to the brown precipitates that formed in the flasks (Cerrato et al., 2010). Genomic DNA from the cultured putative MnOB isolates was extracted using the PowerWater® DNA Isolation Kits (MoBio Laboratories). The extraction protocol was conducted as per the manufacturer's instructions. The extracted DNA was used as template to amplify partial 16S rRNA gene amplicons by polymerase chain reaction (PCR) on a Veriti™ Thermal Cycler (Applied Biosystems). Universal primers, 27F 5'-AGAGTTTGATCMTGGCTCAG-3' and 1492R 5'-GGWTACCTTGTTACGACTT-3' (obtained from Sigma-Aldrich), were used in the PCR amplifications. Each 50 μL of PCR reaction contained 1 μL of template DNA, 27.5 μL of Econotaq plus 2x mix (Lucigen), 10 μM of each primer, and PCR grade water. The amplification protocol was as follows: an initial denaturation of 94 °C for 2 min; 30 cycles of 94 °C for 30 sec, 54 °C for 30 sec, 72 °C for 90 s; and a final extension of 72 °C for 10 min. PCR amplification for each isolate was conducted in triplicate. The presence and the size of amplified 16S rRNA gene amplicons in the PCR products were confirmed using gel electrophoresis (Lonza- FlashGel™ DNA system, 1.2% agarose, 13 well). The amplified PCR products were sequenced with 27F and 1492R sequencing primers at the Genome Quebec Innovation Centre, McGill University. The forward and reverse 16S rRNA gene sequences were assembled into contigs and were manually curated using Sequencher software (Gene Codes Corporation). The curated 16S rRNA gene contig sequences were compared using the Basic Local Alignment Search Tool (BLAST) and Genbank database on the National Centre for Biotechnology Information (NCBI) website. RDP version 11.4 was used to determine the species similarity and to assign the taxonomic affiliation (Cole et al., 2014) (https://rdp.cme.msu.edu/seqmatch/seqmatch_intro.jsp). The curated amplicon sequences were deposited into the European Nucleotide Archive (ENA) database of the European Molecular Biology Laboratory (http://www.ebi.ac.uk/ena; accession numbers LT628526 to LT628536).

4.4.6. Synchrotron-based XANES analyses

XANES analyses were performed at the Mn K-edge (6539 eV) in fluorescence mode employing a single element Ketek AXAS-M (M5T1T0-H80-ML5BEV) silicon drift detector on the IDEAS beamline (08B2-1) at the Canadian Light Source (CLS), Saskatoon, SK. The beamline

was equipped with a Ge(220) crystal monochromator. Two to eight scans were collected for each sample, over the Mn K-edge region from -50 eV to -20 eV (step size 1eV, 3s dwell time), and -20 eV to +100 eV (step size 0.3 eV, dwell time 3 s). A Mn(0) metal mesh was used to calibrate the monochromator, based on the first derivative of the K-edge for Mn(0). The commercial standards for different Mn-oxidation states were $Mn(II)SO_4$ (Sigma-Aldrich, 99% pure), Mn(III) oxide (Sigma-Aldrich, 99% pure), Mn(IV) oxide (Sigma-Aldrich, 99% pure), and $KMn(VII)O_4$ (Sigma-Aldrich, 99% pure). The filter samples (Fe-BW, Fe-An, Fe-Sa, Mn-BW, Mn-An, and Mn-Sa) were air-dried in a desiccator and ground with boron nitride. The samples were loaded, fixed, and sealed onto the holders using Kapton tape. Manganite, birnessite, pyrolusite, and bixbyite were used as mineral standards; J. Dynes supplied the birnessite sample and the remainder of the samples were acquired from the USask Geological Sciences minerals collection.

ATHENA (Demeter© 2006-2016) (Ravel and Newville, 2005) was employed for data analysis. The K-edge absorption edges of Mn in the spectra of each filter sample (Fe-BW, Fe-An, Fe-Sa, Mn-BW, Mn-An, and Mn-Sa) were obtained based on the position of the first derivative of the K-edge in each spectrum. A linear regression model was applied to these values to determine the oxidation states (valences) of the Mn absorption edges (eV) in the XANES spectra of the standards and filter samples (Nam et al., 2007). Principal component analysis and linear combination fitting (LCF) were conducted in ATHENA to determine the proportions of each Mn phase in the Mn-filter samples (Mn-An, Mn-Sa, and Mn-BW). The R-factor and reduced chi-squared (χ^2) values were used to verify the goodness of fit and check for reliability and consistency.

4.4.7. XRF and SEM-EDS

The anthracite filter media samples (Fe-An and Mn-An) collected from both the Fe and Mn filters on Day 183 at the end of the biofiltration experiment were sent to the Saskatchewan Research Council (SRC) in Saskatoon for XRF and SEM-EDS analyses. Briefly, the elemental composition of the anthracite surface coatings was determined by Wavelength Dispersive (WD) XRF (S8-Tiger Bruker) with XS-55, PET, and Li200 analyzer crystals. Samples were prepared using the loose powder method and loaded onto Teflon containers with Mylar windows. Geochemical standards GSP2 and DC73301 were used to calibrate the instrument.

SEM-EDS was employed to characterize the morphology and elemental composition of the anthracite samples. The carbon-coated anthracite was analyzed using a QEMSCAN 650F

equipped with two energy dispersive X-ray detectors (Bruker 5030). EDS measurements were taken on the spots where crystal morphologies were consistent with the presence of Mn-oxides. The samples were observed in secondary electron mode at an acceleration potential of 10 to 15 keV and a working distance of ~10 mm.

4.4.8. EPR analyses

To identify the origins (biogenic or abiogenic) of Mn-oxides from air-dried, ground Mn-filter samples (Mn-BW, Mn-An, and Mn-Sa), EPR analysis was performed at 295 K, using an X-band Bruker EMX EPR spectrometer (9.8 GHz) in the Saskatchewan Structural Sciences Centre (SSSC) at the University of Saskatchewan. Chemically-synthesized birnessite mineral was provided by J. Dynes (CLS) as the reference standard (Hardie et al., 2007). The EPR spectral data was processed using Xenon (version 1.1b60, Bruker Organization). The line width (ΔH in gauss; distance between the highest and lowest points of the first-order signal wave) in the EPR spectra was used to clarify the results as either biogenic or abiotic Mn-oxides. Kim et al. (2011) report that biogenic, biomineral, and abiogenic origins of Mn-oxides exhibit ΔH values of < 600, 600 to 1200, and > 1200, respectively.

4.5. Results

4.5.1. Microbial diversity indices

With an average length of 275 bp, a total of 288,116 v4-region 16S rRNA gene sequences derived from the 19 samples (GW, BWS, Fe-Ef, Fe-An Mn-An, Fe-Sa, Mn-Sa, Fe-BW and Mn-BW) passed all quality filtering in mothur (Table 4.1). The number of sequence reads for the samples ranged from 8,209 to 28,265 and were subsampled to 8,000 sequences per sample for comparative statistical analyses. The rarefaction curves for the different sample types are presented in Fig. 4.10 (Supplementary Information).

Community metrices for the samples are presented in Table 4.1. Good's coverage estimator ranged from 0.95 to 0.99 (mean 0.98, SD 0.01). The OTUs defined at 97% sequence identity ranged from 182 to 966 OTUs per sample. The richness (equal to OTUs) of the incoming natural groundwater (GW) ranged from 467 to 966 (mean 726, SD 250), which was generally higher than the filter samples (Fe-An, Fe-Sa, Fe-BW, Mn-An, Mn-Sa, and Mn-BW) which had richness values

of 182 to 486 (mean 329, SD 85). The community in the continuously flowing effluent stream from the Fe filter (FeFf) had a relatively greater richness (640 and 714, n=2) than the filter samples.

The biofilter communities exhibited lower diversity indices (i.e., richness, Shannon index, effective diversity number, and evenness) than the GW community (Table 4.1). The mean effective diversity number ($e^{H'}$) for the GW community was 191±30, whereas the Fe- and Mn- filter inner solid sample communities exhibited lower mean $e^{H'}$ values of 30±4 (Fe-An 1, Fe-An 2, Fe-Sa 1, and Fe-Sa 2) and 50±10 (Mn-An 1, Mn-An 2, Mn-Sa 1, and Mn-Sa 2), respectively. The evenness (J') of the GW community was 0.8±0.03, which was closer to 1.0 than the Fe- and Mn- filter inner solid samples (0.58±0.03 and 0.69±0.03, respectively).

4.5.2. PCoA and AMOVA analyses

Fig. 4.2 presents the result of PCoA analysis for the comparisons of the influent groundwater and biofilter communities (similarity/dissimilarity). The PCoA plots indicate the GW, Fe-filter, and Mn-filter communities clustered differently based on Yue & Clayton's measure of community dissimilarity. The PCoA plots show the GW community was more similar to the Fe filter effluent community (Fe-Ef) community than to the biofilter communities. Multiple detailed comparisons of the PCoA plots for the samples are presented in Supplementary Fig. 4.11.

The GW community was statistically different from the Fe-filter communities, including the inner filter and effluent samples (Fe-An, Fe-Sa, Fe-BW, BWS, and Fe-Ef), based on the AMOVA analyses (p<0.0001; Table 4.S1). The Mn-filter communities (Mn-An, Mn-Sa, and Mn-BW) were also significantly different from the GW community (p=0.009), the inner Fe-filter communities (p<0.0001), and the Fe-filter effluent community (p=0.008), as presented in Table 4.S1 (Supplementary Information).

Table 4.1 Community coverage, richness, diversity, and evenness measured for high-throughput sequencing data from groundwater, initial backwash sludge, Fe-filter, and Mn-filter communities.

Filter	Sample	Number of Sequences	Good's coverage[a, b]	Richness[a, b]	Diversity estimate[a, b]		Evenness[a, b]	Accession number
				OTUs (S)	H'	$e^{H'}$ [c]	J'[c]	(Project number: PRJEB15260)
Groundwater	GW 1	11375	0.99	467	5.1	157	0.82	ERS1310618
	GW 2	19068	0.97	745	5.4	215	0.81	ERS1310619
	GW 3	12567	0.95	966	5.3	200	0.77	ERS1310620
Initial backwash sludge*	BWS 1	8209	0.98	360	2.6	13	0.43	ERS1310614
	BWS 2	25643	0.98	403	2.8	17	0.47	ERS1310615
Fe filter	Fe-BW 1	9161	0.98	301	1.9	6	0.33	ERS1310610
	Fe-BW 2	10492	0.99	283	2.2	9	0.38	ERS1310611
	Fe-An 1	8669	0.98	354	3.2	25	0.55	ERS1310608
	Fe-An 2	21085	0.98	392	3.4	29	0.57	ERS1310609
	Fe-Sa 1	20527	0.99	328	3.5	34	0.61	ERS1310616
	Fe-Sa 2	9507	0.98	350	3.5	32	0.59	ERS1310617
	Fe-Ef 1	11229	0.96	640	3.3	27	0.51	ERS1310612
	Fe-Ef 2	9540	0.96	714	3.7	40	0.56	ERS1310613
Mn filter	Mn-BW 1	9389	0.97	445	4.2	65	0.68	ERS1310623
	Mn-BW 2	22228	0.97	486	4.3	71	0.69	ERS1310624
	Mn-An 1	28265	0.99	223	3.6	38	0.67	ERS1310621
	Mn-An 2	22662	0.99	182	3.4	31	0.66	ERS1310622
	Mn-Sa 1	14824	0.99	307	4	57	0.71	ERS1310625
	Mn-Sa 2	13676	0.99	295	4.1	60	0.72	ERS1310626

Abbreviations: LWTP, Langham water treatment plant; OTU, operational taxonomic unit; H', Shannon diversity index; $e^{H'}$, effective number of species; J', Pielou's evenness; GW, groundwater; BWS, backwash sludge; Fe-BW, Fe filter backwash; Fe-An, Fe filter anthracite; Fe-Sa, Fe filter sand; Fe-Ef, Fe filter effluent; Mn-BW, Mn filter backwash; Mn-An, Mn filter anthracite; Mn-Sa, Mn filter sand.

GW, Fe-BW, Fe-Ef, and Mn-BW samples were collected after 110 days of operation; Fe-An, Fe-Sa, Mn-An, and Mn-Sa samples were collected after 183 days of operation; BWS samples were collected from trial experiment at LWTP.

* BWS was used as inoculum to Fe filter at start of experiment.

[#] OTUs calculations were carried out at 97% sequence similarity.

a: All samples are subsampled to 8000 sequences.

b: Sequences are clustered using the average neighbor method.

c: Diversity estimates and evenness were calculated based on Shannon index.

4.5.3. Venn diagram analysis

The influent groundwater and Fe-filter effluent communities shared 527 OTUs in the continuous flow-through biofiltration unit (Fig. 4.3). A considerable number of OTUs were shared between the Fe- and Mn-filter communities (Fig. 4.3). For example, the Fe-BW and Mn-BW samples obtained from the backwash water from the two filters shared 235 OTUs (Fig. 4.3). The Mn-filter communities had relatively lower numbers of shared OTUs with the GW community; for instance, Mn-BW shared only 123 OTUs with the GW community (Fig. 4.3).

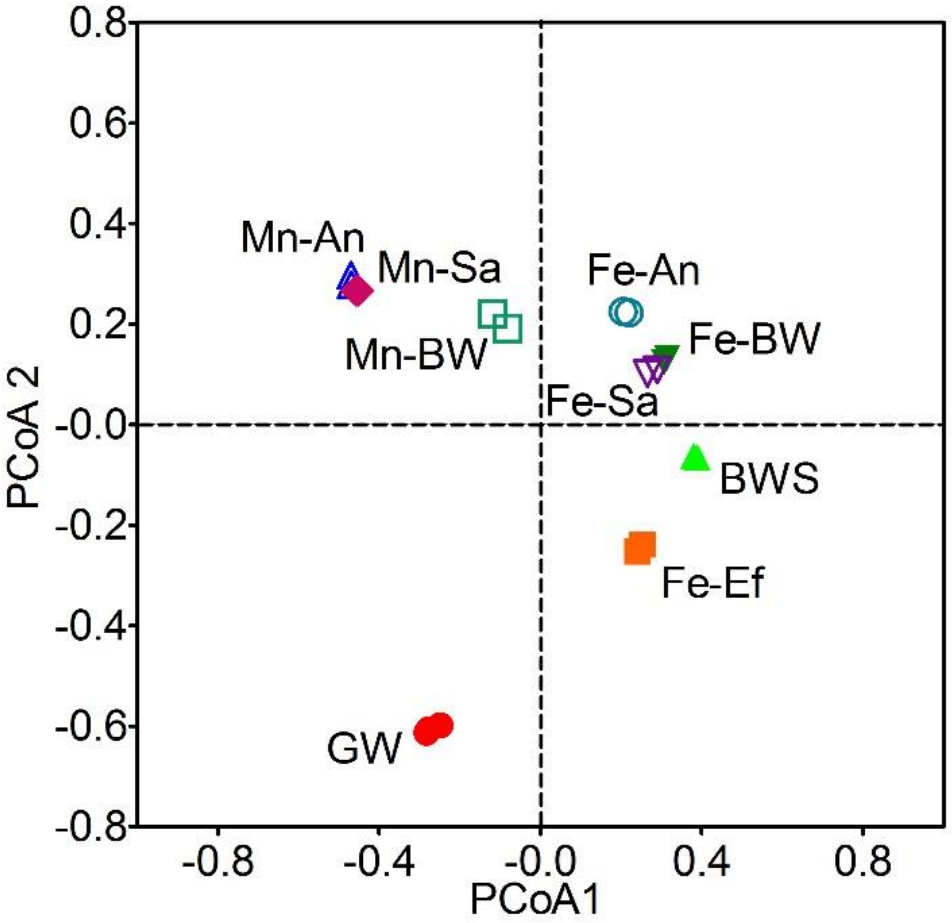

Fig. 4.2 The principle co-ordinate analysis (PCoA) plots for sequence reads from the GW, Fe- and Mn-filter-associated samples based on operational taxonomic unit (OTU) distance matrices created using Yue & Clayton theta values. The OTU clusters were defined using a 97% similarity threshold.

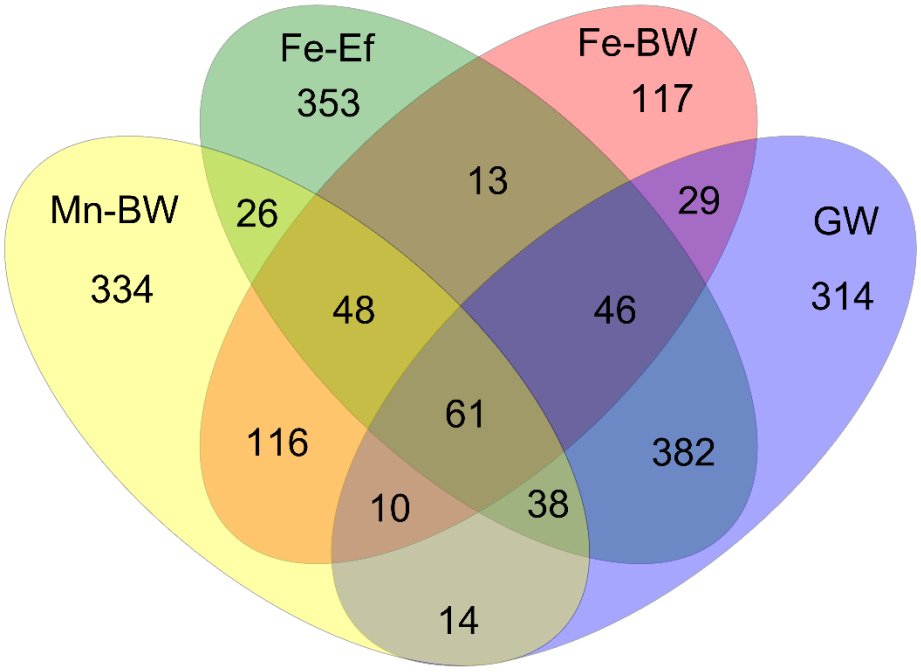

Fig. 4.3 A Venn diagram for illustrating the shared and non-shared OTUs within the GW, Fe-BW, Fe-Ef, and Mn-BW communities.

4.5.4. Community composition

For the 19 samples, 99.9% of the total subsampled sequence reads (151852/152000) could be taxonomically assigned using the SILVA v119 database at a minimum sequence identity cut-off of 80%. At the genus level, 487 taxa (473 bacteria and 14 archaea) were identified from the sequence reads. The GW and biofilter communities (both the Fe and Mn biofilters) were dominated by bacteria (92±2 and 99±2%, respectively). Archaea in the GW communities represented only 8±2% (1869/16000) of the total sequence reads.

At the phylum level, *Proteobacteria* predominated in the communities associated with the GW, Fe filter, and Mn filter. *Proteobacteria* represented 40±4, 79±7, and 67±9% of the sequence reads in the GW, Fe-filter, and Mn-filter communities, respectively (Fig. 4.4A). Bacteria belonging

to the *Nitrospirae* and *Verrucomicrobia* phyla were enriched in the Mn filter-associated communities, comprising 12±7 and 5±1 %, respectively. As shown in Fig. 4.4B, within

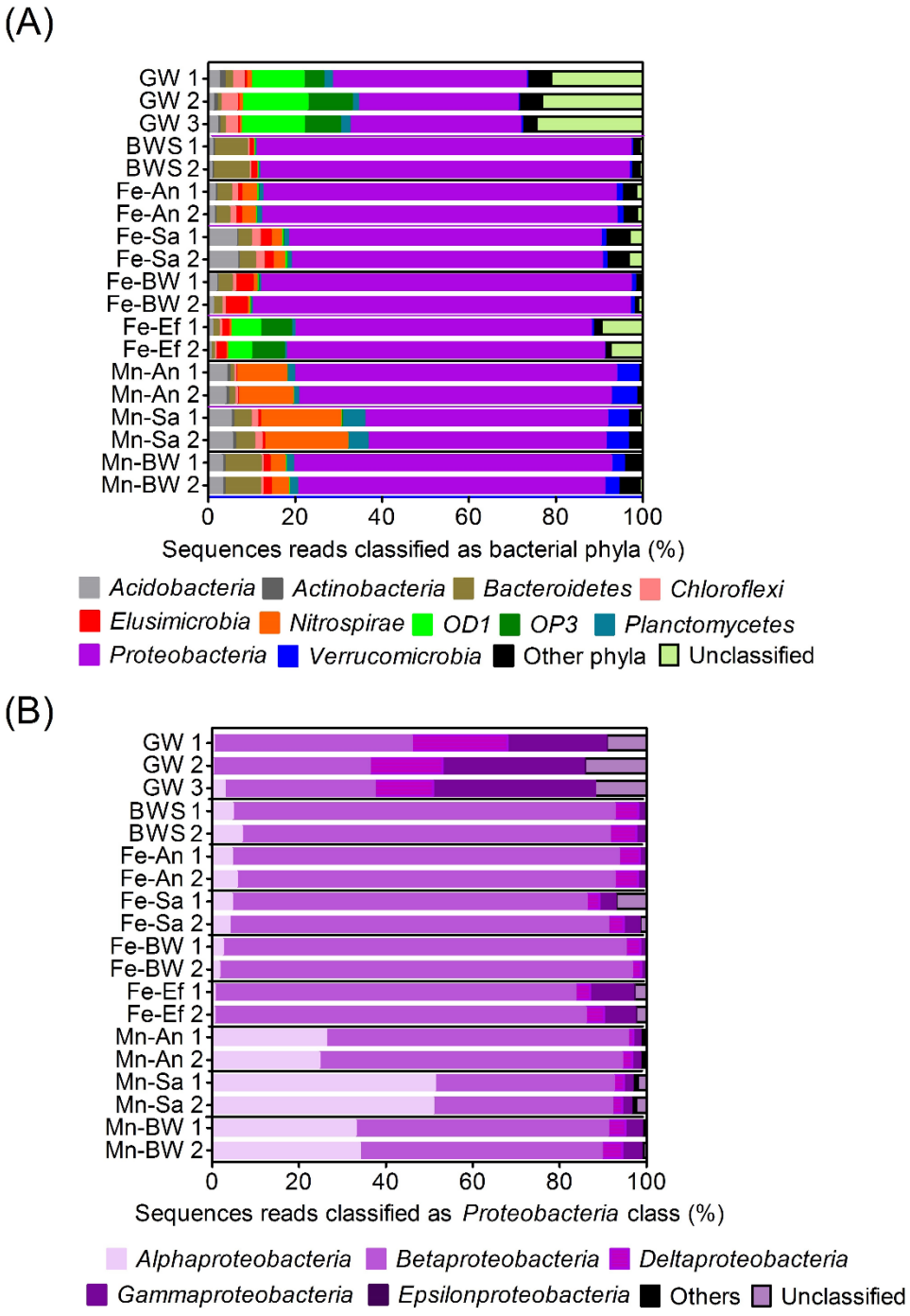

Fig. 4.4 The community compositions in the GW and Fe and Mn filters at (A) the phylum level and (B) *Proteobacteria* classes. Results show percent of total sequence reads for each sample type.

the *Proteobacteria* classes, the GW, Fe-filter and Mn-filter community compositions varied considerably. The GW community mainly consisted of *Betaproteobacteria* (39±6%), *Gammaproteobacteria* (31±8%), and *Deltaproteobacteria* (17±4%). However, *Betaproteobacteria* were dominant in the Fe-filter communities (87±4%). The abundance of *Alphaproteobacteria* communities in the Mn filter reached 40±10%. *Alphaproteobacteria* populations were low in the GW and Fe-filter communities, but notably abundant in the Mn-filter communities (Mn-An, Mn-Sa, and Mn-BW).

4.5.5. Genus-level heat map integrated with chemistry data and flow direction of biofiltration

To construct the heat map shown in Fig. 4.5, the top 30 genera based on the percentage of sequence reads, including unclassified genera, were considered for each of the four distinctive microbial habitats (GW, BWS, Fe filter, and Mn filter), representing 70 unique genera out of a total of 120. The heat map shows the percentages of sequence reads for the 70 most abundant genera, which are aligned with respect to the direction of flow through the biofiltration unit. Shifts in the representative genera from the influent groundwater to the Fe and Mn filters are easily visible (i.e., darker blue pixels refer to more abundant genera, and yellow pixels represent minor genera in the heat map). In addition, shared genera that appeared in both the Fe and Mn filter samples may be metabolically versatile members of the microbial communities, may include genera capable of both Fe and Mn oxidation, and can be easily identified in the heat map. Results for the functional genera are presented in further detail in the next section.

The concentrations of Fe, Mn, and NH_3-N in the influent groundwater collected on Day 106 of biofiltration operation were 2.8, 0.9, and 0.53 mg/L, respectively. The Fe concentration decreased to 0.018 mg/L (below the DWS) in the Fe filter effluent collected on the same day, while Mn and NH_3-N concentrations were unchanged. In the Mn filter effluent, the concentration of Mn decreased to 0.0036 mg/L (also below the DWS), the NH_3-N concentration decreased to 0.13 mg/L, and the NO_3^--N concentration increased to 0.49 mg/L (from <0.009 mg/L in GW). Furthermore, the XRF analyses of the Fe and Mn filters consistently confirmed the precipitation of Fe or Mn on the filter media (Table 4.S2; Supplementary Information). In the Fe-An sample, the XRF analyses showed a larger quantity of Fe precipitates (4.3%, w/w) than Mn precipitates

(0.03%, w/w), whereas Mn precipitates (2.9%, w/w) exceeded Fe precipitates (0.03%, w/w) in the Mn-An samples.

4.5.6. FeOB, MnOB, AOB, and NOB

A few known relatives of FeOB, MnOB, ammonia-oxidizing bacteria (AOB), and nitrite-oxidizing bacteria (NOB) were identified among the 70 screened genera in the heat map for GW, BWS, Fe-filter, and Mn-filter samples (Fig. 4.5). Relatives of known FeOB *Gallionella* (Hallbeck et al., 1993) and *Sideroxydans* (Liu et al., 2012) were a high proportion of reads in the Fe-filter communities (20±20 % and 30± 20 %, respectively). Relatives of the MnOB genera *Planctomyces* (Schmidt et al., 1981) and *Hydrogenophaga* (Marcus et al., 2017) are included in the core taxa presented in the heat map in both the Fe and Mn filters (Fig. 4.5). Relatives of other known MnOB belonging to the genera *Pseudomonas, Hyphomicrobium, Albidiferax, Athrobacter*, *Acinetobacter*, *Zoogloea*, *Ralstonia*, and *Pedomicrobium* (Tebo et al., 2005, Akob et al., 2014, Beukes and Schmidt, 2012) were detected in both the Fe- and Mn-filter communities. However, their abundances were very low or negligible in both filters (less than 1% of sequence reads each), and were thus not included in the heat map of the top 30 genera. Relatives of known AOB in genus *Nitrosomonas* (Arp et al., 2002) were identified in both biofilters, but were present in higher proportions in the Mn filter (20±10%) than in the Fe filter (6±3%). Similarly, relatives of known NOB of the *Nitrospira* (Lücker et al., 2010) genus were present in higher proportions in the Mn filter (15±4%) than in the Fe filter (2.8±0.4%).

The shift in microbial community composition from the GW to the Fe filter and the Mn filter involved enrichment of many unclassified genera (Fig. 4.5). Well-known FeOB relatives in the *Betaproteobacteria* (*Gallionella, Sideroxydans, Ferriphaselus, and Hydrogenophaga*) were identified in the Fe filter (Fig. 4.5). Interestingly, the known FeOB genera *Gallionella*, *Sideroxydans, Hydrogenophaga* (Chan, 2014), and *Ferriphaselus* (Kato et al., 2014), which were within the representative taxa (70 genera), appeared in both the Fe- and Mn-filter communities. In particular, *Hydrogenophaga*, also reported to be capable of iron oxidation (Chan, 2014), was recently recognized as an MnOB (Marcus et al., 2017). This genus was found in high read abundance in both Fe- and Mn-filter samples in this study. Furthermore, the *Hydrogenophaga* sp. strain CDMN isolated in this study was culturable as a MnOB at 8 °C; this has not been previously reported.

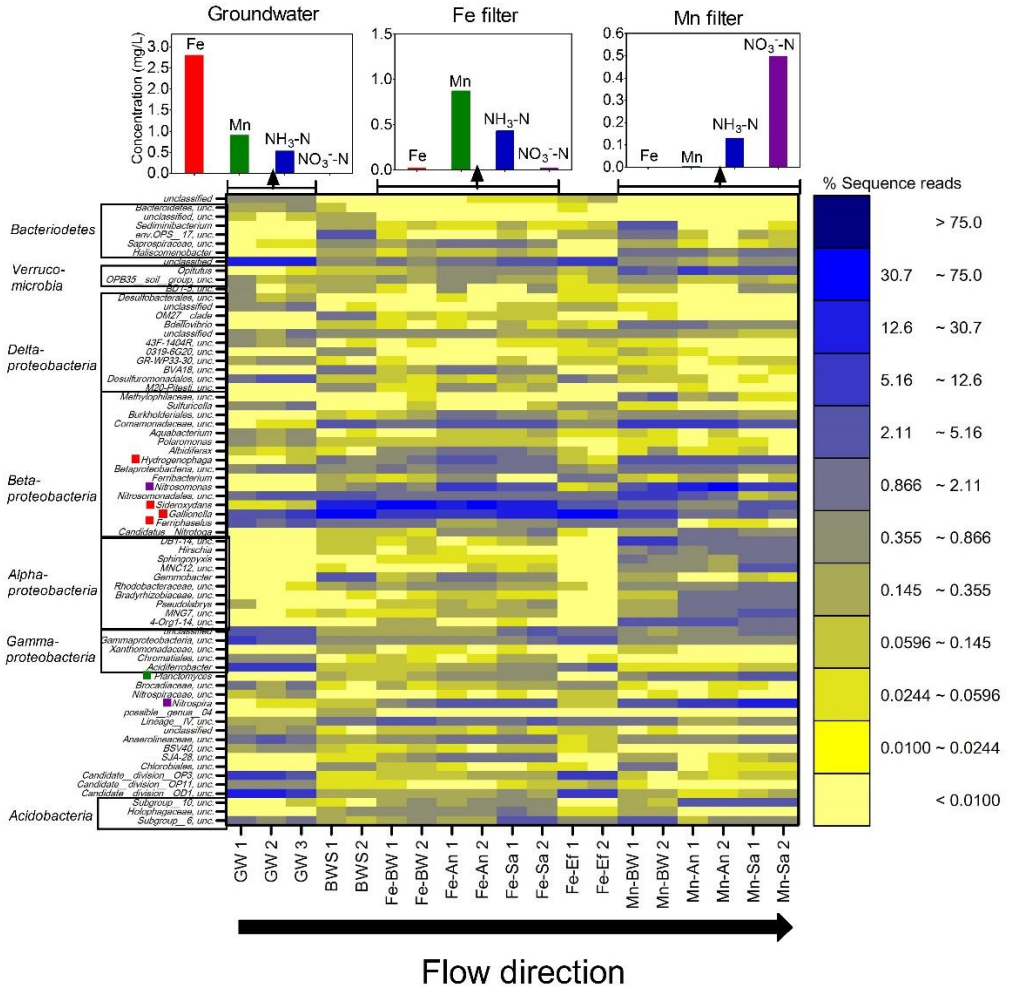

Fig. 4.5 A heat map for the 70 most abundant bacterial genera (including unclassified genera) classified from the sequence reads from the 19 samples (GW and Fe- and Mn-filter samples). In the heat map, red, green, and purple boxes indicate the relatives of known FeOB, MnOB, and AOB or NOB, respectively (unc.: unclassified genus). Note that the heat map is shown on a log scale. Water chemistry data graphs show ICP-MS results for groundwater and effluent water samples.

From the detailed survey of the 70 genera within the heat map, only 24 genera had been reported in the literature at the time of this study. The remaining 46 genera were unclassified or not previously reported in terms of their detailed characteristics. These unclassified genera comprised 66±3%, 21-23% (n=2), 25±8%, and 31±9% of the sequence reads in the GW, BWS, Fe filter, and Mn filter, respectively. Interestingly, as visualized in the heat map, the distinct emergence of *Alphaproteobacteria* in the Mn filter did not include previously known MnOB.

4.5.7. Putatively new MnOB isolates

A total of 11 isolates were cultured from the samples associated with the Fe and Mn filters (Table 4.2). Of these, *Azospirillum* sp. CDMB, *Solimonas soli* CDMK, *Paenibacillus* sp. CDME, and *Paenibacillus* sp. CDMG, which exhibited Mn(II) oxidative activity during the LBB I assays showing Mn(III/IV) oxide formation, have not been reported as MnOB. These are new putative MnOB identified in this study. The phylogenetic tree, which includes the genera with percent sequence reads greater than 1% as well as previously known functional species (FeOB, MnOB, AOB, and NOB), indicates the putative MnOB are clustered within five major phyla: *Actinobacteria, Firmicutes,* and *Proteobacteria* (*Alpha-, Beta-, and Gamma-*) (Fig. 4.12; Supplementary Information).

Table 4.2 MnOB isolates from this study

Isolate Name	Mn-oxides formation (LBB I assay)	Close relative	Identity (%)	Accession No.	Phyla/ Subphyla	Source
			Putatively new MnOB			
CDMB	+	*Azospirillum sp.*	99%	LT628527	*Alphaproteobacteria*	Mn filter
CDME	+	*Paenibacillus sp. MC5-1*	99%	LT628529	*Firmicutes*	Mn filter
CDMG	+	*Paenibacillus sp. MC5-1*	99%	LT628531	*Firmicutes*	Fe filter
CDMK	+	*Solimonas soli (T) DCY12*	96%	LT628533	*Gammaproteobacteria*	Fe filter
			Known MnOB			
CDMA	+	*Pseudomonas sp. LAB-21*	99%	LT628526	*Gammaproteobacteria*	Fe filter
CDMC	+	*Mycobacterium Frederiksbergense (T) DSM 44346*	99%	LT628528	*Actinobacteria*	Fe filter
CDMH	+	*Mycobacterium sp. 22-29*	99%	LT628532	*Actinobacteria*	Mn filter
CDML	+	*Pseudomonas sp. 12A 19*	99%	LT628534	*Gammaproteobacteria*	Mn filter
CDMM	+ (17 °C)	*Hydrogenophaga sp. Esa.33*	99%	LT628535	*Betaproteobacteria*	Mn filter
CDMN	+ (8 °C)	*Hydrogenophaga sp. Esa.33*	99%	LT628536	*Betaproteobacteria*	Mn filter
			Non-MnOB			
CDMF	-	*Rhodococcus sp. I7*	99%	LT628530	*Actinobacteria*	Mn filter backwash

4.5.8. XANES analyses

The XANES spectra of the Mn(0) to Mn(VII) standards covered K-edge energies from 6539 eV for Mn(0) to ~6557 eV for Mn(VII) (Fig. 4.13). The Mn K-edge XANES spectra of the Fe-filter samples (Fe-BW, Fe-An, and Fe-Sa) identified Mn phases dominated by the +3 oxidation state (Figs. 4.6 and 4.13). However, the Mn-filter inner samples (Mn-BW, Mn-An, and Mn-Sa) displayed distinctly higher Mn oxidation states of nearly +4 (Figs. 4.6 and 4.13).

The XANES-based LCF analysis for known Mn minerals (bixbyite, birnessite, and pyrolusite) and the Mn-filter inner samples revealed birnessite (with Mn oxidation states of +3.5 to +3.9) is the dominant Mn-oxide in the Mn-BW (93.1%), Mn-An (92.5%), and Mn-Sa (100%) samples (Fig. 4.7).

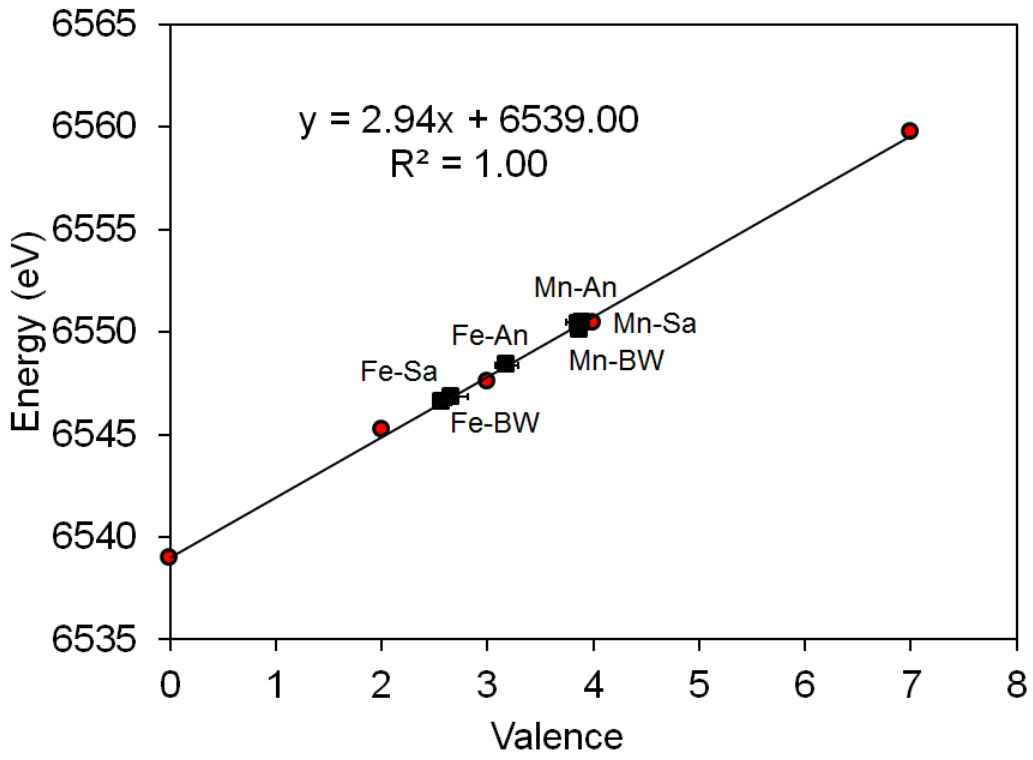

Fig. 4.6 The oxidation states of Mn in the Fe-filter (Fe-BW, Fe-An, and Fe-Sa) and Mn-filter (Mn-BW, Mn-An, and Mn-Sa) samples based on linear regression analysis for the Mn oxidation states and corresponding absorption edges (eV) of the XANES spectra of the standards: Mn (0) metal, Mn(II)SO_4, Mn(III) oxide, Mn(IV) oxide, and KMn(VII)O_4.

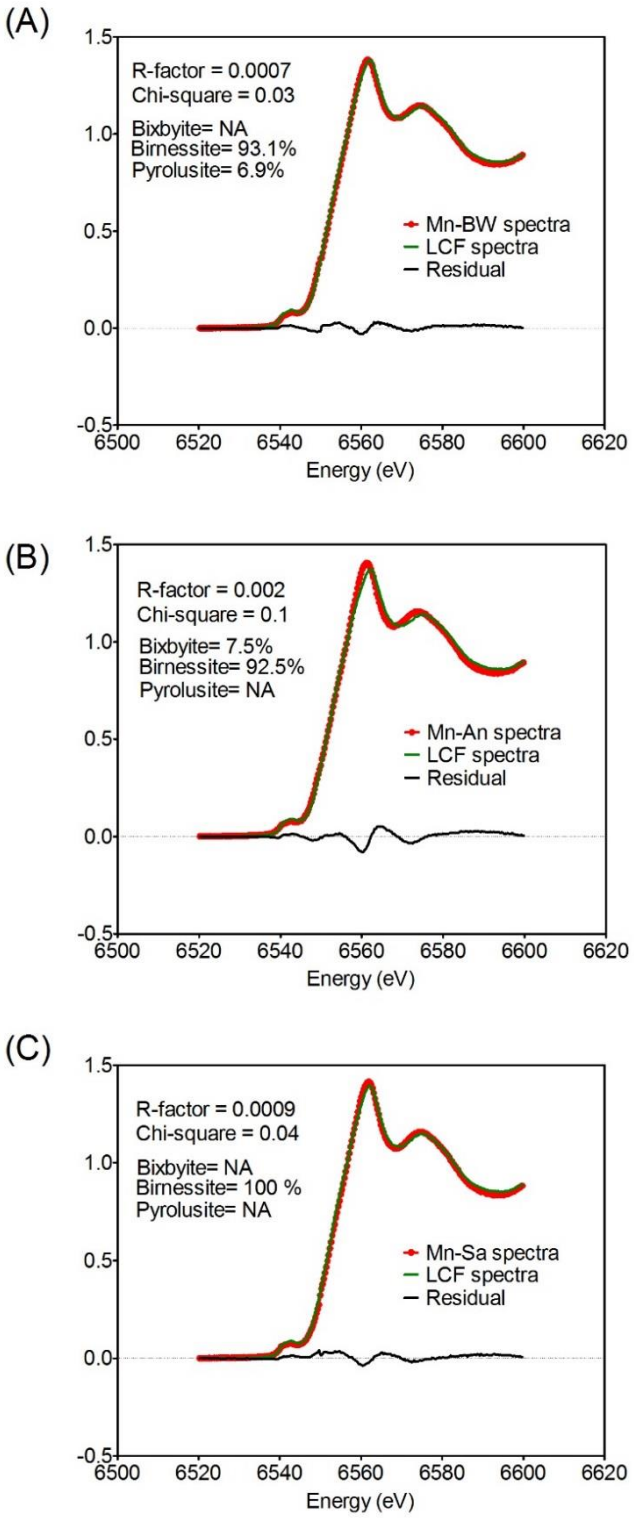

Fig. 4.7 The linear combination fitting (LCF) analysis of the mineral spectra (bixbyite, birnessite, and pyrolusite) for the Mn filter samples: (A) Mn-BW, (B) Mn-An, and (C) Mn-Sa.

4.5.9. SEM-EDS analyses

The typical features of FeOB—twisted stalks and filamentous sheaths (Emerson et al., 2010) — were observed in SEM images of the surfaces of the Fe-An samples (Figs. 4.8A and 4.8B). The correponding EDS analyses confirmed the high intensity of the Fe peak (Fig. 4.15A). For the surface coatings of the Mn-An samples, a visible coral-like morphology was consistently observed, reflecting the autocatalytic nature of the Mn-oxides (Bruins et al., 2015a) (Fig. 4.8D). However, an irregular amorphous surface morphology, which is relevant to biogenic Mn-oxide formation (Miller et al., 2012), was also consistently observed (Fig. 4.8C). The corresponding EDS analyses for the Mn-An samples showed high peak intensities for Mn and Fe (Fig. 4.15B).

4.5.10. EPR analysis

The EPR spectra of birnessite (control standard), and the Mn-BW, and Mn-Sa samples are presented in Fig. 4.9. The chemically synthesized birnessite mineral produced a signal centered at a g-factor of 2.0 and a ΔH of 2710 gauss in the EPR spectra, confirming its abiotic origin (Kim et al., 2011) (Fig. 4.9A). On the other hand, the EPR spectra of Mn-BW (centrifuged solids) and Mn-Sa centered at a g-factor of around 2.0 and had ΔH values of 504 and 487 gauss, respectively (Figs. 4.9B and 4.9D). The ΔH values observed in the Mn-BW and Mn-Sa spectra were less than 600 gauss, indicating a biogenic origin of Mn-oxides as similarly observed by Kim et al. (2011). The EPR spectra of Mn-BW (Fig. 4.9B) and Mn-Sa (Fig. 4.9D) samples showed a sextet of hyperfine lines of Mn. These spectral patterns around g-factor=2 are typical for Mn (III/IV) oxides possibly containing Mn(II) (Bruins et al., 2015b, Saisaha et al., 2013). In addition, a sharp signal at g-factor=2.0 with a narrow ΔH of 6 gauss appeared in the EPR spectrum of the Mn-Sa sample (Figs. 4.9C and 4.9D), where suggests the presence of biologically oriented organic radicals (protein) interacted with Mn(IV) (Nick et al., 1991, Chang et al., 2004).

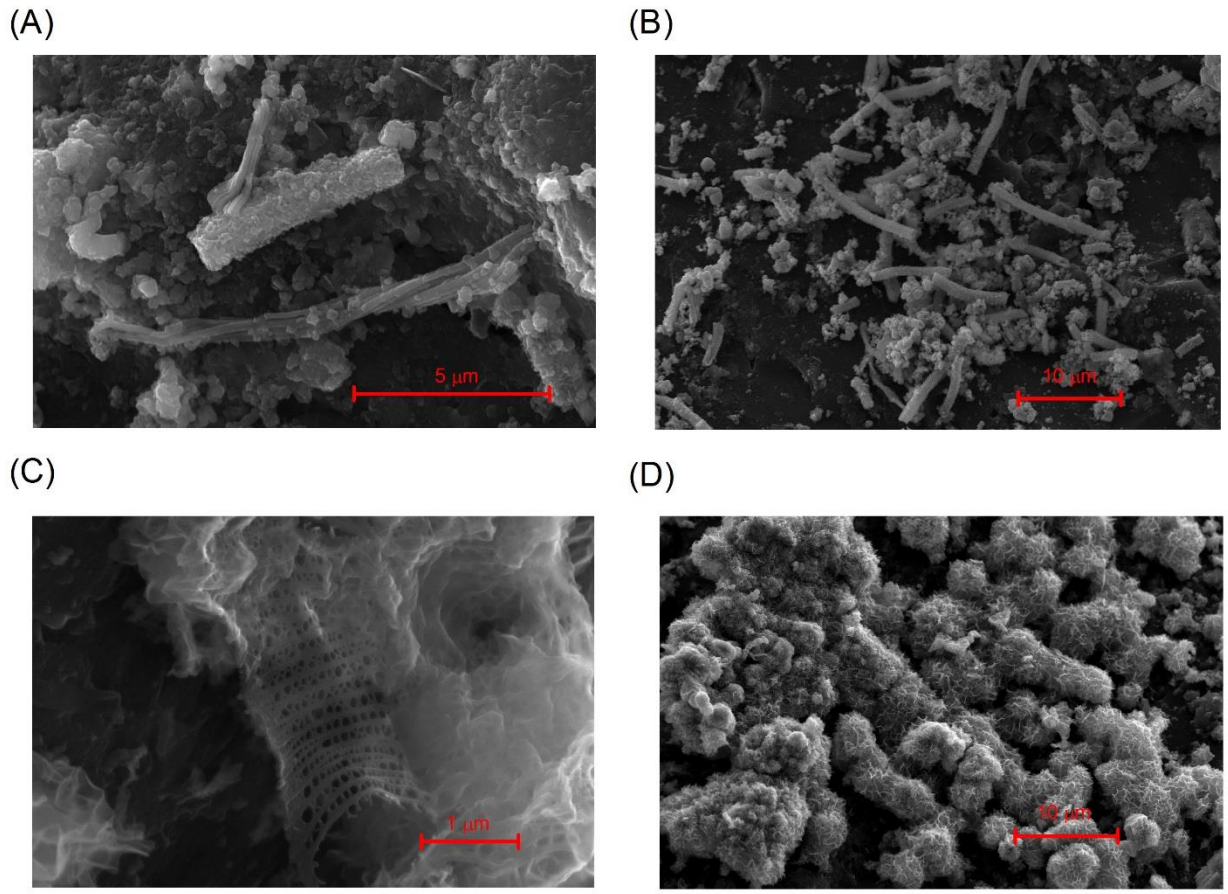

Fig. 4.8 The scanning electron microscopy (SEM) images of the surface morphologies of the anthracite filter media collected on Day 183 (at the end of the field experiment). The typical features of FeOB, twisted stalks (A) and filamentous sheaths (B), were observed in the SEM images of the surfaces of the Fe-An samples. An amorphous, unregularly reticulated, fluffy and filamentous surface morphology (C) was observed in the SEM images of the Mn-An sample, along with a repetitious, coral-like, crystallized surface morphology (D) on other surfaces in the same Mn-An sample.

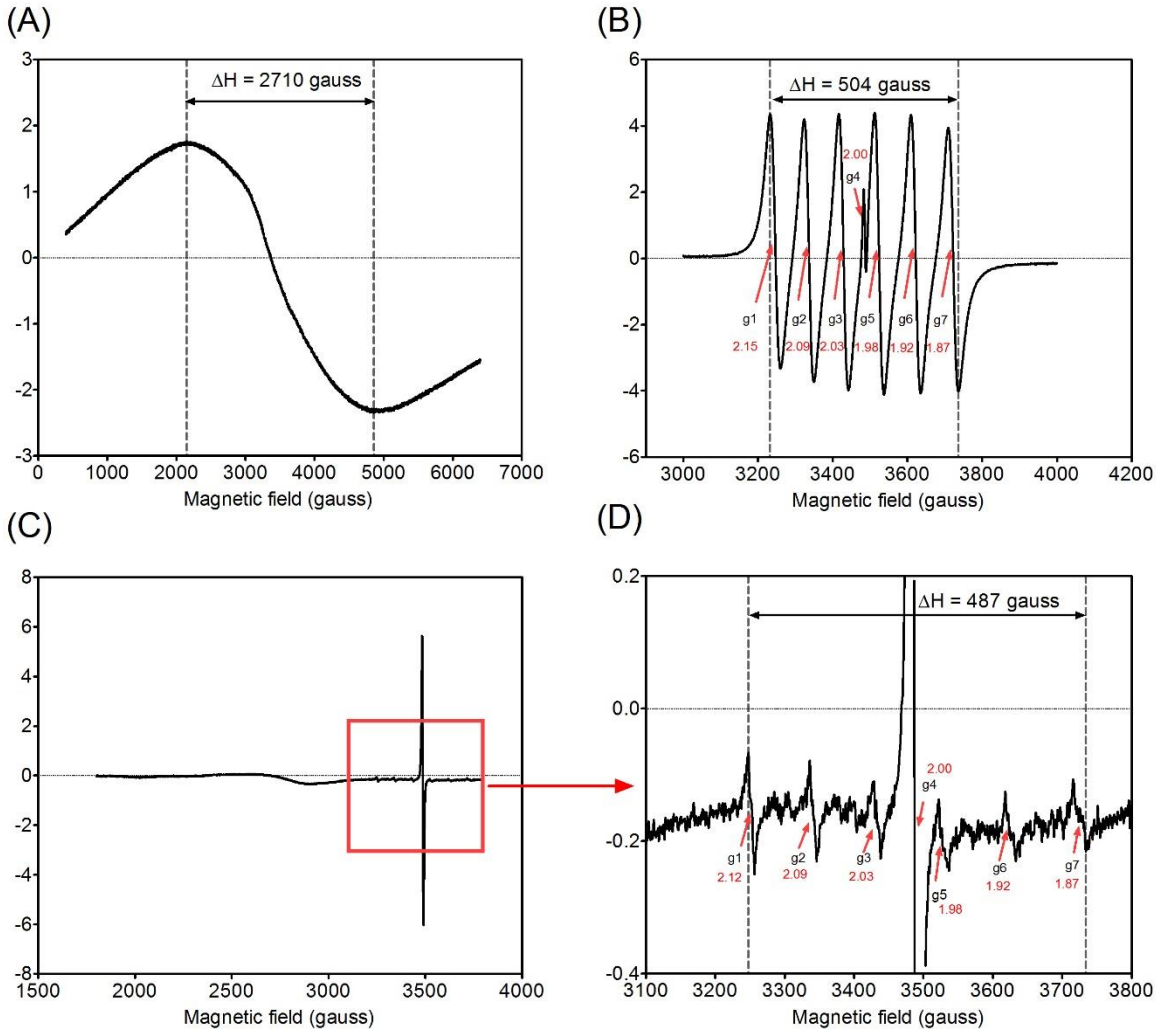

Fig. 4.9 The EPR spectra recorded at room temperature for the (A) birnessite reference standard, (B) Mn-BW, and (C) Mn-Sa, and a zoomed-in EPR spectrum for the Mn-Sa sample (D) (g1-g7 refer to the g-factor).

4.6. Discussion

4.6.1. Distinctive functional enrichment in the Fe and Mn filters

Differences in the microbial community diversity metrics, along with the similarity-dissimilarity analysis between the communities, indicated there is less diversity in both biofilter communities compared to the microbial community of the influent natural groundwater. The biofilter communities were significantly different from the groundwater community. In addition, Fe and Mn biofilter communities significantly differed from each other, although they shared a considerable number of OTUs. These results reflect the enrichment of microbial populations specifically adapted to the inner environments of the Fe and Mn biofiltration columns.

Based on the heat map of the representative genera (Fig. 4.5), genus-level shifts in microbial communities were confirmed to occur sequentially from the influent natural groundwater to the Fe-filter community, and further to the Mn-filter community. The compiled evidence from the microbial community heat map, key chemistry data throughout the biofiltration system, and the XRF analyses, which confirmed the precipitation of Fe and Mn as oxides on the biofilter media, supports the conclusion that microbial enrichment has occurred for functional microorganisms that enhance Fe(II) and Mn(II) oxidation, and nitrification, in the biofiltration unit that continuously received cold groundwater during operation in the field (4 to 8 °C).

However, the enrichment characteristics of the FeOB- and MnOB-related populations were considerably different at the genus level. Two distinctive microbial enrichments occurred in the *in situ* biofilter in the field; (1) the Fe filter was mainly enriched with easily culturable, well-known FeOB, and (2) the microbial community in the controlled environment of the Mn filter has enriched in populations that are not previously recognized as MnOB. Specifically, the Fe filter was predominantly enriched in members of the *Betaproteobacteria* (Fig. 4.5). This is mainly due to the high sequence read proportion (50±10%) of well-known FeOB relatives, which include the genera *Gallionella, Sideroxydans, Ferriphaselus,* and *Hydrogenophaga*. However, the previously known MnOB (*Pseudomonas, Hyphomicrobium, Albidiferax, Athrobacter, Acinetobacter, Zoogloea, Ralstonia,* and *Pedomicrobium*) identified in the Mn filter comprised less than 1% of the total sequence reads when combined. Furthermore, members of the *Leptothrix* genus, which are widely studied as representative MnOB (Burger et al., 2008a) were not identified in the Mn filter. The

only genus of previously known MnOB of note in the Mn filter was *Planctomyces* (2±2% of sequence reads) (Fig. 4.5).

The distinctive shift in microbial community compositions from the Fe filter (including Fe-Ef) to the Mn filter is due to the substantially increased abundance of *Alphaproteobacteria* (40±10%), which included the genera *Hirschia, Sphingopyxis, Gemmobacter, Pseudolabrys*, and 6 other unclassified genera. These genera are not known for Mn oxidation. In addition, the genera *Haliscomenobacter, Sediminibacterium, Terrimonas, Opitutus, Bdellovibrio, Thiobacillus, Hirschia, Woodsholea,* and *Sphingopyxis*, which are not known as MnOB, were also abundant in the Mn filter. Whether these populations act as MnOB, or are indirectly involved in Mn oxidation (e.g., through co-metabolism), or are active using other substrates available in the biofilter or incoming groundwater is not known.

The MnOB isolated from the Fe- and Mn-filter samples (confirmed by the formation of Mn(III/IV) precipitates) broadly belong to the class *Alphaproteobacteria, Betaproteobacteria, Gammaproteobacteria, Firmicutes,* and *Actinobacteria.* As stated earlier, *Azospirillum* sp. CDMB, *Solimonas soli* CDMK, *Paenibacillus* sp. CDME, and *Paenibacillus* sp. CDMG have not been reported previously as MnOB. *Mycobacterium* sp. (strain CDMC) and *Hydrogenophaga* sp. (strains CDMM and CDMN) have only recently been reported as MnOB (Marcus et al., 2017).

4.6.2. Potential microbial versatility for Fe and Mn oxidation

Betaproteobacteria, including common FeOB, appeared in both the Fe and Mn filters. The common known FeOB genera *Gallionella, Sideroxydans,* and *Hydrogenophaga* were abundant in the Mn filter (totalling 8±3% of the sequence reads). Based on the heat map showing microbial community shifts across the biofiltration system (Fig. 4.5), members of the *Betaproteobacteria* including *Gallionella, Sideroxydans,* and *Hydrogenophaga*, were also abundant in the effluent stream (Fe-Ef) of the Fe filter. The Fe filter effluent is the influent to the Mn filter and therefore a source of FeOB populations for the Mn filter. Likely as a result of this transfer, a considerable number of OTUs were shared between the Fe- and Mn-filter communities (Figs. 4.3 and 4.12).

This interpretation of an enrichment of FeOB in the Mn filter communities is supported by the changes in Fe concentration in the effluent water. The Fe concentration in the Mn-filter influent was one-fold magnitude lower after flowing through the Mn filter i.e., from 0.018 mg/L in Mn filter influent (Fe-Ef) to 0.001 mg/L in Mn filter effluent. In addition, the Mn filter backwash

sludge (Mn-BW) also contained a considerable amount Fe precipitates. The FeOB in the Mn-filter likely caused Fe(II) oxidation in the Mn filter, and thus a decrease in Fe concentrations in the effluent. In addition, known MnOB were observed in the Mn filter, and were likely responsible for Mn(II) oxidation. The microbial communities in the Mn filter can thus support both Fe and Mn removal. This is consistent with previous single-columned biofiltration studies where Fe and Mn removal can be successfully achieved in a single column (Li et al., 2013, Yang et al., 2014).

In the Mn filter microbial communities, the relatives of known FeOB (*Gallionella, Sideroxydans,* and *Hydrogenophaga)* and MnOB (*Planctomyces,* and *Hydrogenophaga)* co-existed. The co-existence of FeOB and MnOB also occurs commonly in natural environments (e.g., ferromanganese deposits) (Northup et al., 2003, Sujith et al., 2017) and engineered environments (Fe and Mn biofilters) (Thapa Chhetri et al., 2013, Cai et al., 2015, Yang et al., 2014). However, the identity of microbes that are able to oxidize both iron and manganese are still an area of investigation.

Hydrogenophaga sp. have been reported to oxidize both Fe(II) and Mn(II) (Chan, 2014, Marcus et al., 2017). This genus was present in the Mn filter (2.7±0.3% of the sequence reads) and can oxidize Fe(II) and Mn(II), which suggests it has a potential dual function in this biofiltration system, oxidizing both Fe and Mn (Chan, 2014, Marcus et al., 2017). The adaptation of *Hydrogenophaga* sp. strain CDMN, to the low temperatures and redox conditions present in the Mn filter (7 to 14.5 °C, >300 mV) could make this strain functionally important for biofiltration in cold climates. Biogenic Mn(III/IV) production, resulting from Mn(II) oxidation in the early stages of biofiltration, can promote autocatalytic Mn(II) oxidation and potentially shorten the typically long start-up period required for Mn biofiltration at low temperatures (below 15 °C).

4.6.3. Biogenic birnessite as a signature of microbially mediated Mn(II) oxidation

Based on the synchrotron-based XANES analysis, the precipitates on the Mn-filter materials exhibited Mn oxidation states between +3.7 and +4.0. Semi-quantitative LCF analyses of the XANES spectra of the Mn filter indicated that birnessite was the primary Mn-oxide (>90% in Fig. 4.7). In addition, the EPR analyses for these precipitates confirmed the biogenic origin (vs. abiotic origin) of the birnessite-dominant precipitates in all samples associated with the Mn filter (Mn-BW and Mn-Sa). Linking the microbial community data for the Mn filter to the biogenic

birnessite formation conclusively indicated the Mn-filter community (most members of which have not been previously recognized as MnOB) was promoting biological Mn(II) oxidation in the Mn-biofilters.

Bruins et al. (2015a) observed shifts in the origins of birnessite from biogenic to abiogenic in an aged pilot-scale RSF system for Mn removal from groundwater (pretreated to remove Fe(II)) using EPR analyses of the aged filter media. Bruins et al. (2015b) also report that birnessite formed by abiotic Mn(II) oxidation on the surfaces on the ripened filter media in full-scale RSF systems. These findings suggest physico-chemical Mn(II) oxidation is the dominant mechanism in RSF systems. RSF treatment technology has generally higher flow velocities (e.g., 4-21 m/h) than biofiltration systems (e.g., 2-10 m/h), and often requires chemical oxidizing agents. MnOB might have initiated and/or enhanced Mn(II) oxidation, resulting in the formation of Mn(III/IV) oxides that acted as adsorbents and autocatalysts for further physico-chemical Mn(II) oxidation on the Mn-oxide surface coatings during the course of the RSF treatment (Bruins et al., 2015a, Bruins et al., 2015b). However, the role of MnOB in field-aged filter media enriched with abiotic Mn-oxides (birnessite) is not known (Bruins et al., 2015a).

In this study, the formation of biogenic birnessite in the nearly fully-aged Mn biofilter materials (183 days) is observed to progress vertically along with Mn(II) oxidation in the field (Chapter 3; accepted to Water Quality Research Journal, July 2017). Based on the EPR analyses for the filter media, no notable conversion of the Mn(II)-oxidation mechanism from biological to physico-chemical Mn(II) oxidation is associated with the surface-catalytic reaction on the aged filter media. The characteristics of the EPR spectra for the inner Mn-filter solids (with $\Delta H<600$ gauss), along with the results of the XANES analyses (+3.86 to +3.88 oxidation states in the Mn-filter samples), provide additional insight into the biogenic nature of the Mn (III/IV) oxides, which potentially contain organic radicals associated with enzymatic reactions and biological derivatives (Nick et al., 1991, Chang et al., 2004). This further supports the notion that Mn filter solids were biologically aged in the field. Furthermore, an amorphous, unregularly reticulated, fluffy, and filamentous surface morphology, which is characteristic of biogenic Mn-oxides (Miller et al., 2012), was easily observed in the SEM images for the Mn filter media (Mn-An; Fig. 4.8C). Biological Mn(II) oxidation, indicated by the characteristic EPR signal for biogenic Mn-oxide formation, may be responsible not only for the initiation but also the maintenance of biological Mn(II) oxidation in biofiltration systems.

Interestingly, autocatalytic Mn(II) oxidation on the surface coatings was also observed. A repetitious, coral-like, crystallized surface morphology on other surfaces in the same Mn-filter media (Mn-An) was concurrently observed in the SEM images (Fig. 4.8D). This surface morphology reflects the autocatalytic nature of some Mn-oxide surface coatings, as reported by Jiang et al. (2010) and Bruins et al. (2015a). Such variations in the surface morphology of the aged filter media in this study imply both biogenic and abiotic Mn(II) oxidation occurred in the on-site Mn filter, rather than a complete conversion from one dominant oxidation mechanism to another (biological to physico-chemical) as observed in the RSF study by Bruins et al. (2015a).

Biogenic Mn-oxides act as strong oxidizing agents with high surface areas that potentially accelerate Mn(II) oxidation (Learman et al., 2011). The formation of biogenic birnessite is therefore advantageous for initiating, enhancing, and maintaining biological Mn(II) oxidation. Birnessite is an intermediate product of the Mn oxidation pathway and pyrolusite (Mn(IV) oxide) is thermodynamically favored as the final oxidation product (Stumm and Morgan, 1996, Bruins et al., 2015b). In our study, pyrolusite is a minor mineral and birnessite is the dominant Mn-oxide in the filter media. This implies that, in biofiltration systems, the continuous supply of biogenic birnessite by metabolically-active MnOB adapted to low on-site temperatures may play a critical role in shortening the start-up period, maintaining Mn(II) oxidative activity, and further increasing the rate of Mn(II) removal in cold climates. As a result, this study suggests the formation of biogenic birnessite can be a key indicator, and even a prerequisite, for successful biofiltration systems that combine biological and autocatalytic Mn(II) oxidation at low temperatures.

4.7. Conclusions

High-throughput sequencing of the microbial community, coupled with extensive instrumentation analyses of the field-aged filter media, confirmed the enrichment of microbial communities that microbially mediate oxidation of Fe(II) and Mn(II) in a continuous, flow-through, on-site biofiltration system for cold groundwater. The heat map (genus level) integrated with sequential changes in the chemistry of the groundwater throughout the biofiltration system confirmed the occurrence of shifts in microbial community compositions and their functions from the influent groundwater, to the Fe filter, to the Mn filter. The members of the microbial biofilter communities in the Fe and Mn filters were unique for Fe(II) and Mn(II) oxidation; however, significant numbers of new putative MnOB appeared in both biofilters (class *Betaproteobacteria*).

More specifically, this study revealed that *Hydrogenophaga* sp. can oxidize manganese and generate Mn(III/IV) oxides even at low temperatures (8 °C).

The enrichment characteristics differed in the Fe and Mn filters. Well-known, readily culturable FeOB were abundant in the Fe filter whereas MnOB relatives were enriched in the Mn filter. The notable emergence of several genera in the Mn filter (belonging to the class *Alphaproteobacteria*) not traditionally known as MnOB was observed. This study indicated putatively new MnOB belonging to the *Alphaproteobacteria*, *Firmicutes,* and *Gammaproteobacteria* (isolates *Azospirillum* sp. CDMB, *Solimonas soli* CDMK, *Paenibacillus* sp. CDME, and *Paenibacillus* sp. CDMG).

The lines of evidence obtained from multiple instrumental analyses for the characterization of the aged filter media revealed the formation of biogenic birnessite, which can promote further autocatalysis for Mn(II) oxidation activity. Biogenic birnessite can be a robust indicator for the occurrence of biological Mn(II) oxidation and a crucial driver for the potential subsequent autocatalytic oxidation of Mn(II).

4.8. Acknowledgements

This research was funded by the Natural Sciences and Engineering Research Council of Canada (NSERC CRD #CRDPJ 487008-15) and Delco Water, Inc. We thank L. Sawatzky, operator at Langham Water Treatment, for support in pilot-scale biofilter operation. XANES analyses were performed at the Canadian Light Source, which is supported by NSERC, the National Research Council of Canada, the Canadian Institutes of Health Research, the Province of Saskatchewan, Western Economic Diversification Canada, and the University of Saskatchewan. We thank J. Dynes for provision of Mn-oxide standards; D. Muir for assistance with beamtime at the CLS; J. Stobbs for assistance with lab activities at CLS; S. Samaila, J. Essilfie-Dughan, and V. Bondici for assistance with XANES data interpretation; R. Sammynaiken for assistance at the Saskatchewan Structural Sciences Centre; and H. Yin for assistance in the Environmental Engineering Laboratory, University of Saskatchewan.

4.9. Supplementary information

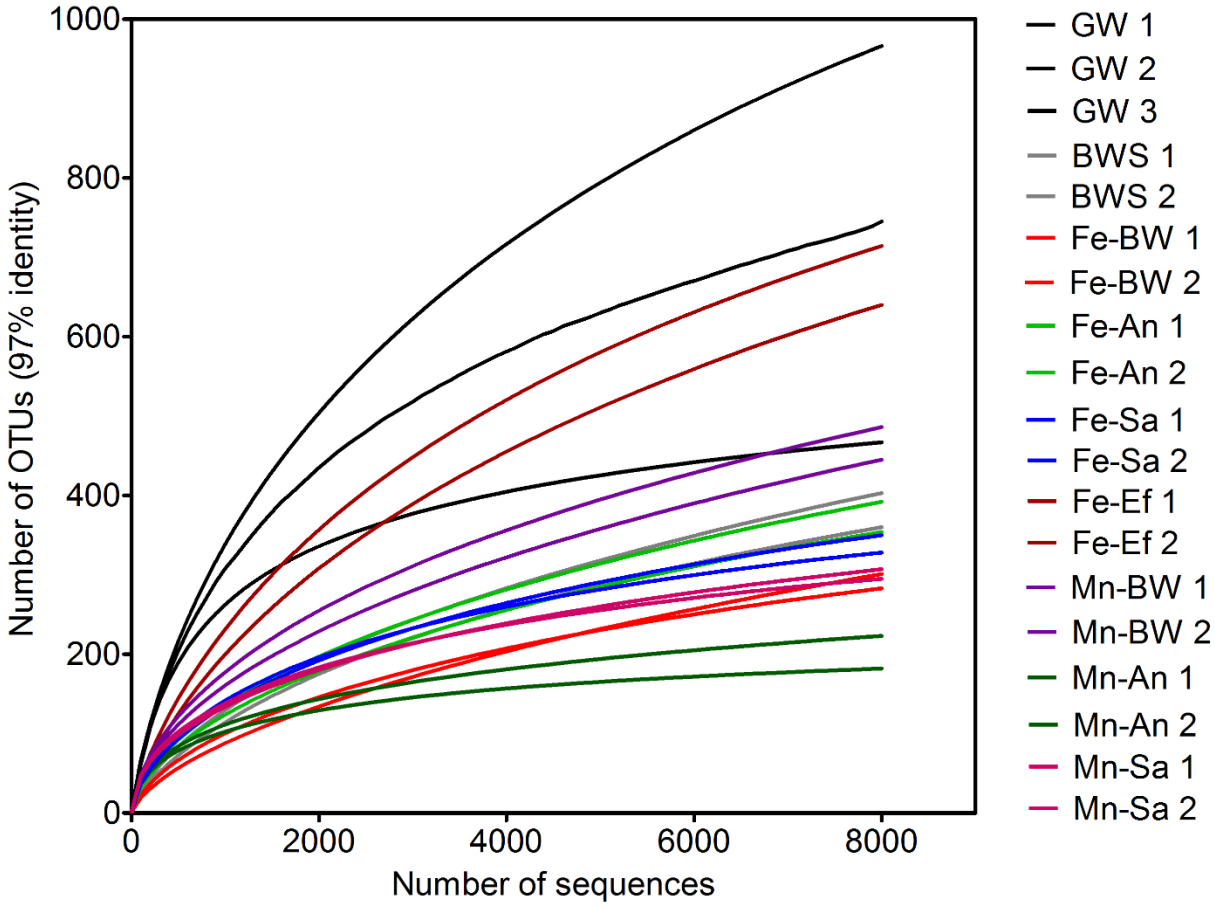

Fig. 4.10 Rarefaction curves for sequence reads from the biofilter samples.

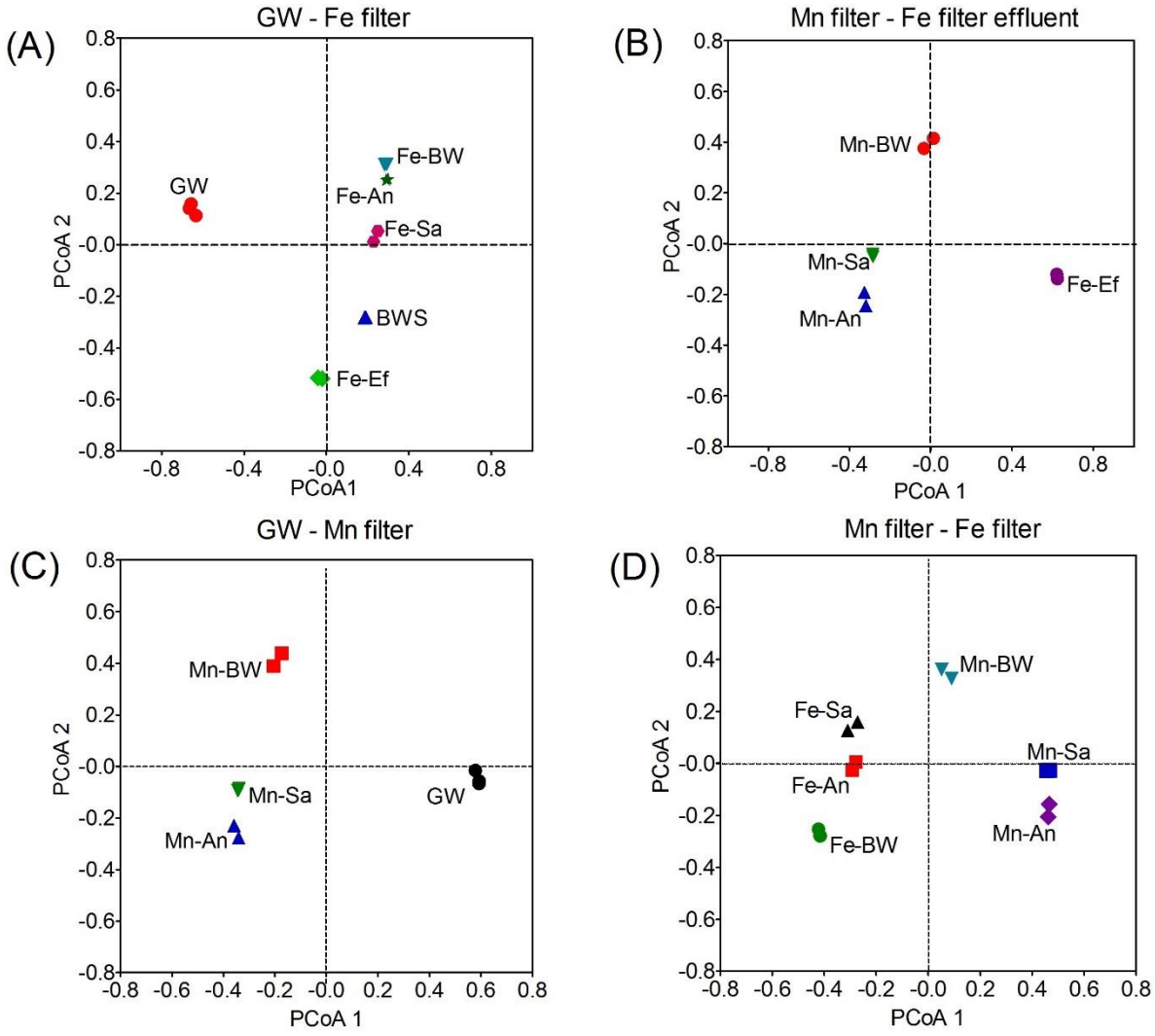

Fig. 4.11 Principal coordinate analysis (PCoA) plots of microbial communities for (A) GW and Fe-filter communities (Fe-BW, Fe-An, Fe-Sa, Fe-Ef, and BWS), (B) Fe-Ef and Mn-filter communities (Mn-BW, Mn-An, and Mn-Sa), (C) GW and Mn-filter communities (Mn-BW, Mn-An, and Mn-Sa), and (D) Fe-filter (Fe-BW, Fe-An, and Fe-Sa) and Mn-filter communities (Mn-BW, Mn-An, and Mn-Sa).

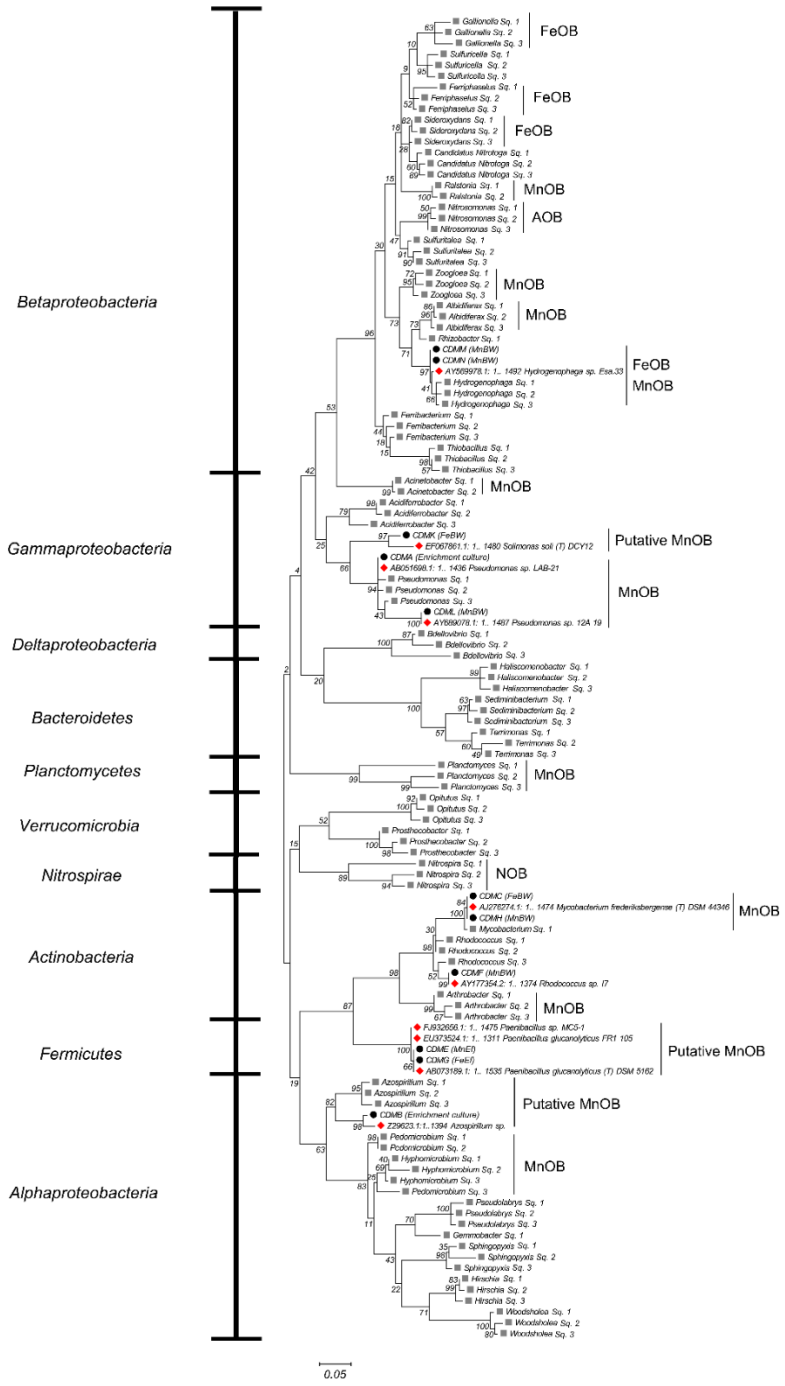

Fig. 4.12 A dendrogram representing the phylogenetic relationship between culture-dependent and -independent approaches. This tree was generated using partial 16S rRNA gene sequences from the culture-dependent (isolation) and -independent (Illumina Miseq, labelled "Sq.") methods used in this study. The dendogram was generated using the maximum likelihood method of the Jukes and Cantor model. Bootstrap values were generated from 1000 sampling replicates.

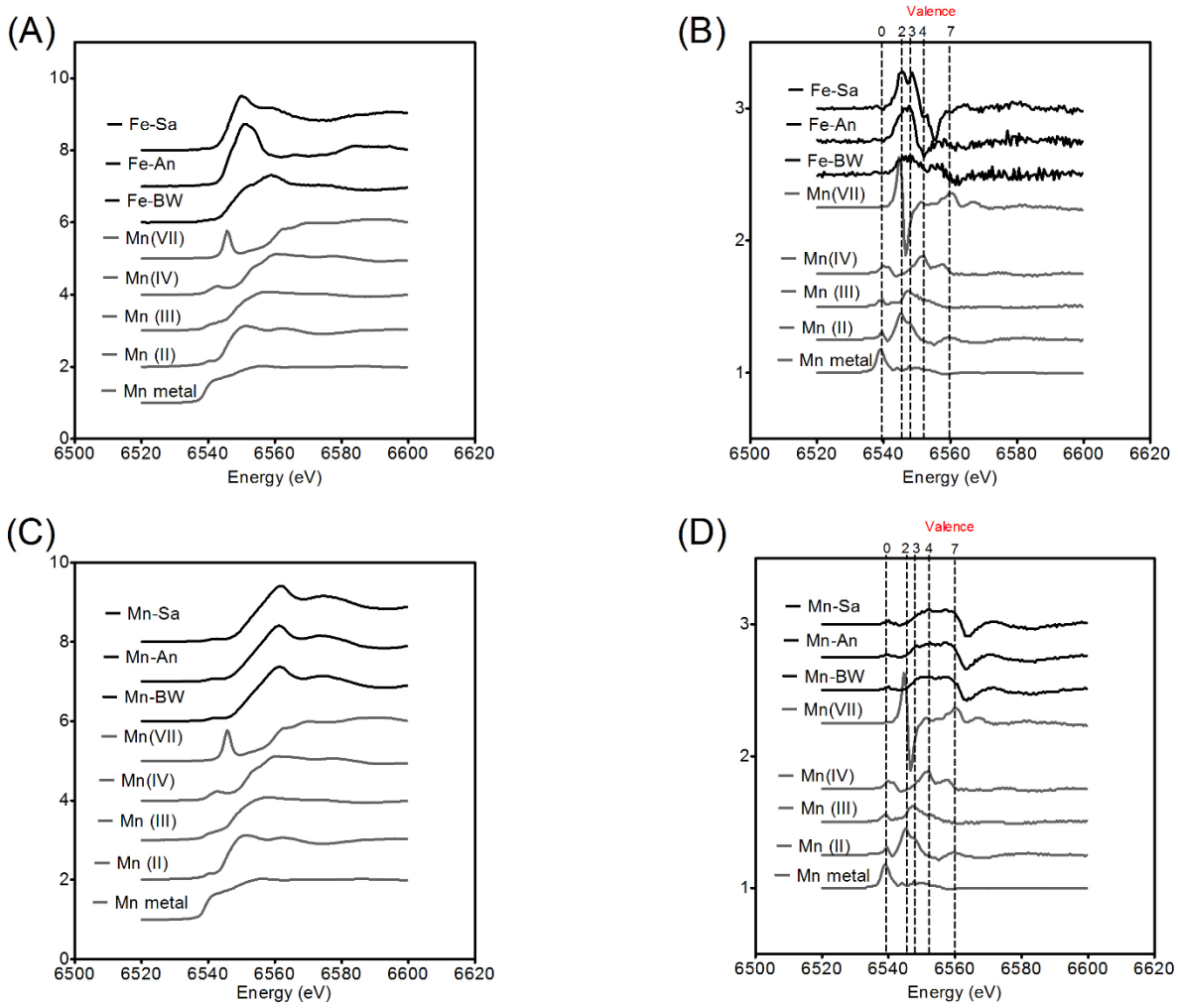

Fig. 4.13 The Mn K-edge XANES spectra for Fe-filter (Fe-BW, Fe-An, and Fe-Sa) and Mn-filter (Mn-BW, Mn-An, and Mn-Sa) samples: (A) the XANES spectra plotted for standards and Fe-filter samples, (B) the first derivatives of XANES spectra plotted for standards and Fe-filter samples, (C) the XANES spectra plotted for standards and Mn-filter samples, and (D) the first derivatives of XANES spectra plotted for standards and Mn-filter samples. The vertical lines indicate the absorption edge energies of Mn (0), Mn (II), Mn (III), Mn (IV), and Mn(VII) species.

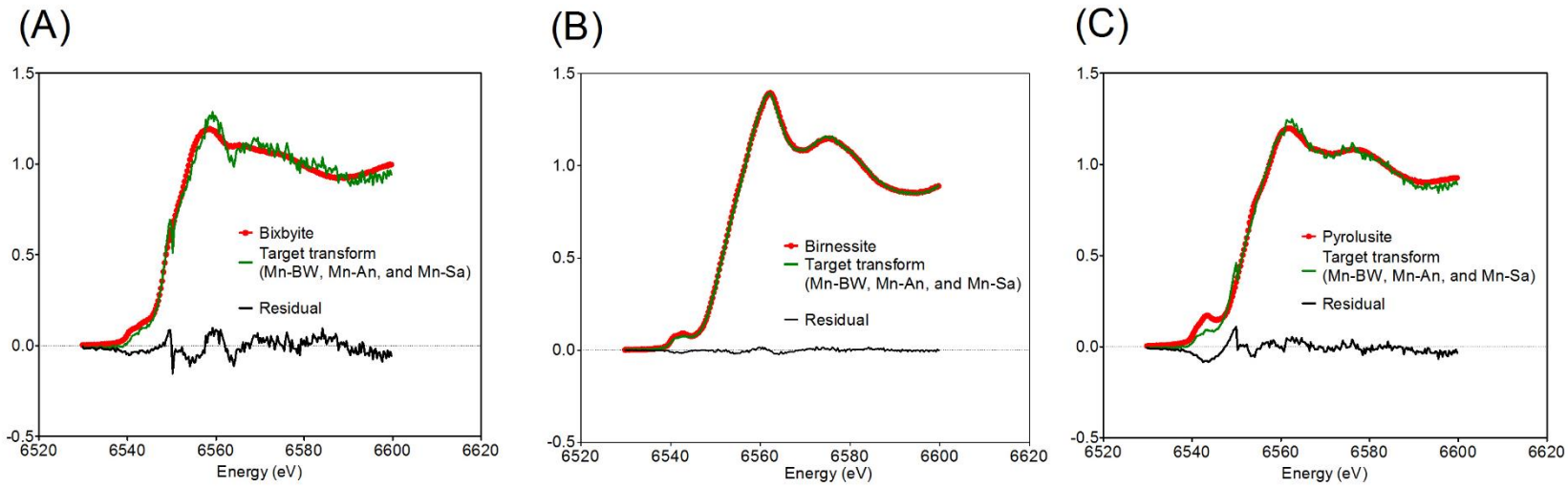

Fig. 4.14 Principal component analyses (PCA) of Mn-BW, Mn-An, and Mn-Sa samples. Target transformation was used to assess whether the standard spectra was consistent with the presence of (A) bixbyite, (B) birnessite, and (C) pyrolusite in the samples.

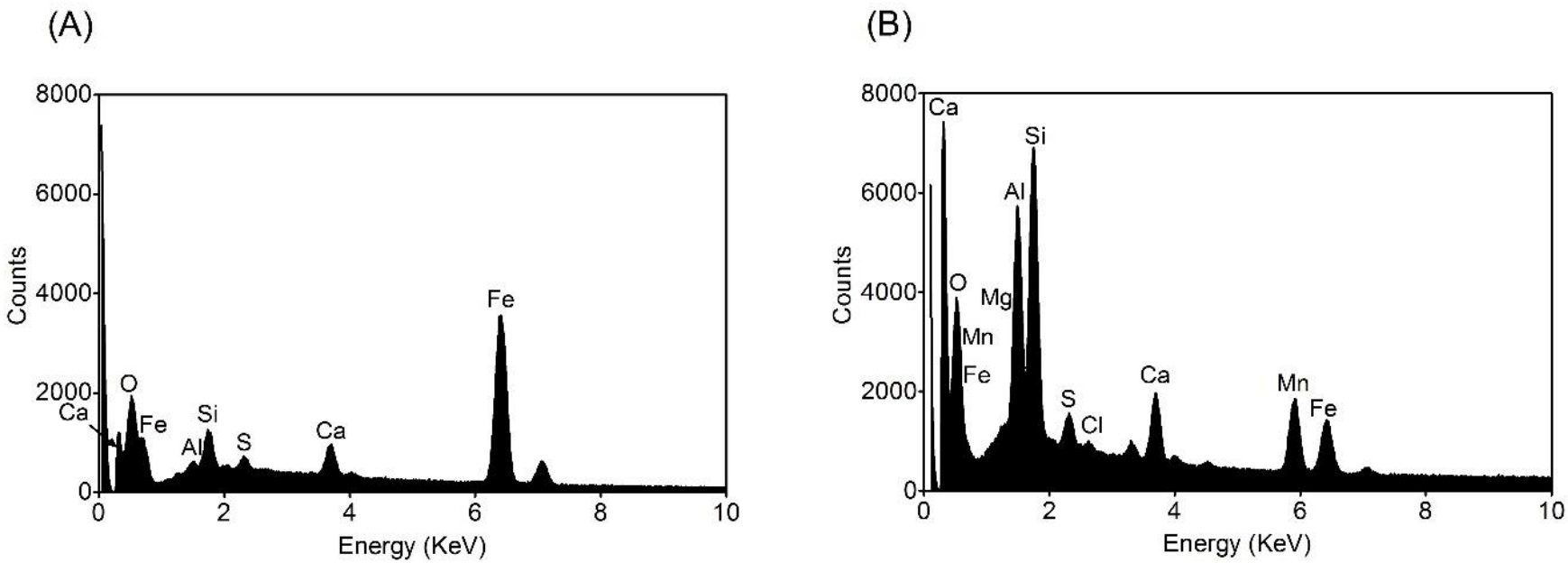

Fig. 4.15 EDS plots for (A) Fe-An in Fig. 4.8A and (B) Mn-An in Fig. 4.8C.

Table 4.S1 Statistical comparison of microbial communities between GW and Fe- and Mn-filter-associated samples based on the OTU distance matrix calculated by Yue & Clayton's measure of community dissimilarity

Sample comparison	*p*-value
GW vs. Fe filter-associated samples (Fe-An, Fe-Sa, Fe-BW, Fe-Ef, and BWS)	< 0.0001*
GW vs. Mn filter-associated samples (Mn-An, Mn-Sa, and Mn-BW)	0.009*
Fe-Ef vs. Mn filter-associated samples (Mn-An, Mn-Sa, and Mn-BW)	0.008*
Fe filter-associated (Fe-An, Fe-Sa, and Fe-BW) vs. Mn filter-associated samples (Mn-An, Mn-Sa, and Mn-BW)	< 0.0001*

* for $p < 0.05$ (mothur)

Table 4.S2 Elemental composition of Fe-An, Mn-An, and virgin anthracite (control) in weight percent determined using XRF analyses.

Sample	Ca	Si	Fe	Al	S	P	K	Cl	Mg	Mn
Virgin anthracite	2.97	5.3	1.56	2.62	1.04	0.035	0.091	0.19	0.054	0.023
Fe-An (day 183)	2.2	5.61	4.29	1.816	1.12	0.079	0.12	0.11	0.04	0.023
Mn-An (day 183)	1.34	3.92	0.03	1.9	1.73	0.061	0.13	0.13	0.05	2.91

Unit: wt. %

5. CONCLUSIONS

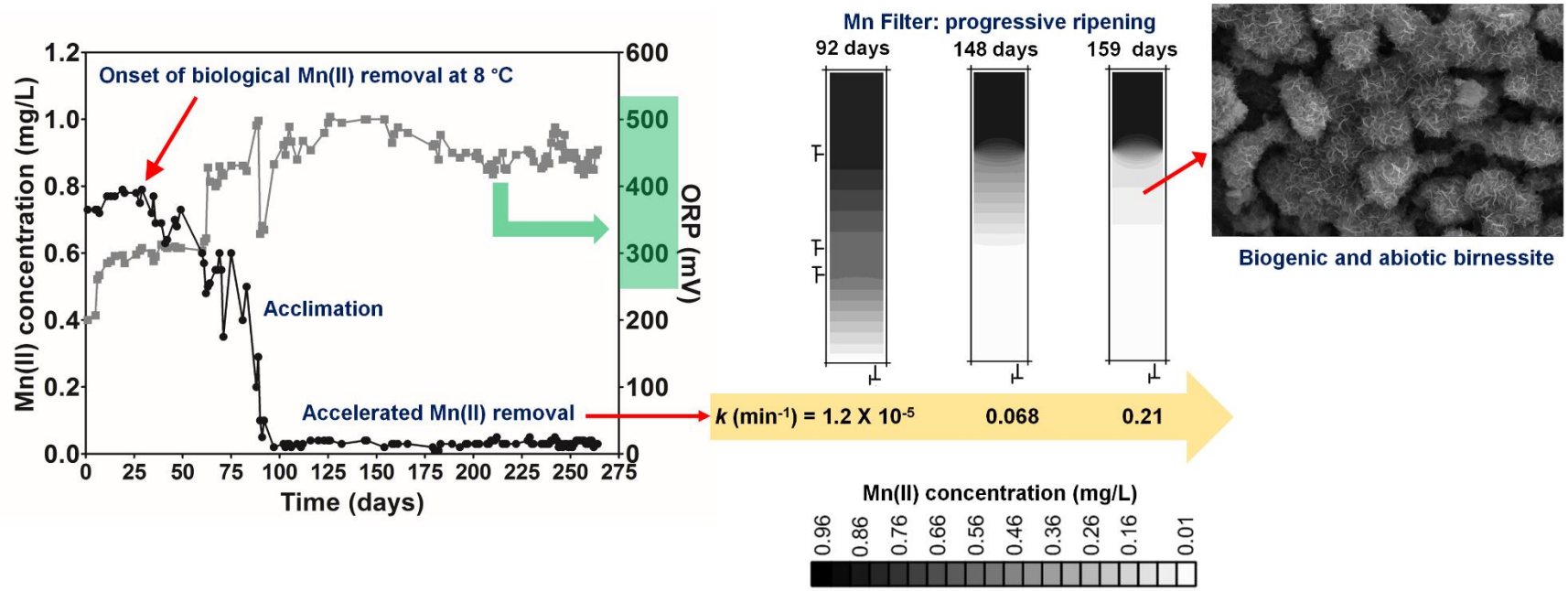

5.1. Key findings and conclusions

Understanding the roles of Mn(II)-oxidizing bacteria (MnOB) and Mn(III/IV) oxides during the start-up, acclimation, acceleration and successful maintenance of Mn(II) removal by biofiltration is a prerequisite for improving Mn biofiltration functionalization. Furthermore, this information can be applied in the development of innovative strategies and technologies to shorten the long start-up periods, especially when Mn biofiltration technology is implemented in cold regions.

To meet the proposed objectives of this thesis, we studied a continuous pilot-scale biofiltration unit comprised of two flow-through columns (Fe filter and Mn filter) installed at the Langham water treatment plant. This pilot-scale biofiltration unit is operated to treat dissolved Fe(II) and Mn(II) from a local, low-temperature groundwater source (4–8 °C).

Dissolved Fe(II) concentrations in the Mn filter effluent rapidly decreased below the DWS within 5 days of operation. The biofiltration system operated at steady-state thereafter in terms of Fe(II) concentrations. Mn(II) removal in the pilot-scale biofilters commenced at 8 °C after 29 days of operation, and dissolved Mn(II) concentrations in the Mn filter effluent started decreasing as ORP values rose over +300 mV. After 97 days of operation, the pilot-scale biofiltration unit consistently exhibited a high Mn(II) removal efficiency of 97.0±0.9%, which corresponded to a mean effluent temperature of 12.1±0.6 °C during the period of steady-state functioning. Between Days 92 and 127, the Mn filter still exhibited lower first-order Mn(II) removal rate constants (*k* values) ranging from 10^{-6} to 10^{-5} min^{-1}. However, immediately after multiple backwashes and the inoculation of the biofilter with biologically-acclimated backwash sludge (Days 127 to 132), *k* values markedly increased to 0.21 min^{-1} at 11.0±0.6 °C, which is comparable to *k* values obtained at higher temperatures in previous studies. The vertical progression of Mn filter media ripening was related to the drastic increase in the *k* values. This study indicated that the biofilter inoculation with biologically-aged backwash sludge is important for promoting the acceleration of Mn(II)-removal, as evidenced by high ORP values (> +400 mV) and the presence of acclimated MnOB and solid precipitates containing biogenic Mn-oxides.

Based on the research results presented in this thesis, we conclude that biological Mn(II)-oxidation activity was significantly enhanced in the biofiltration unit at low temperatures. Evidence for this includes: (a) the growth of viable MnOB populations active at the low start-up

temperature (8 °C), (b) a shift in redox conditions in favor of biological Mn(II) oxidation, and (c) higher ATP concentrations in the biofilter effluent relative to the influent groundwater.

Illumina MiSeq high-throughput amplicon sequencing for the microbial community, coupled with extensive characterization of the backwash sludge and field-aged filter media, confirmed the enrichment of microbial communities that can actively mediate Fe(II) and Mn(II) oxidation. The heat map (Fig. 4.5, genus level) integrated with changes in the chemistry of the groundwater throughout the biofiltration system confirmed the occurrence of shifts in microbial community composition and their functions from the influent groundwater to inside the biofilters. The members of the microbial biofilter communities in the Fe and Mn filters were unique for Fe(II) and Mn(II) oxidation; however, significant numbers of FeOB and MnOB appeared in both biofilters (class *Betaproteobacteria*). The enrichment characteristics differed in the Fe and Mn filters. Well known FeOB were abundant in the Fe filter, and a number of relatives of known MnOB were present in the Mn filter. The sequencing results also showed several genera were present in the Mn filter that belong to the subphylum *Alphaproteobacteria* that are not traditionally known as MnOB. This study identified several putative MnOB belonging to the subphyla *Alphaproteobacteria*, *Firmicutes,* and *Gammaproteobacteria*: *Azospirillum* sp. CDMB, *Solimonas soli* CDMK, *Paenibacillus* sp. CDME, and *Paenibacillus* sp. CDMG.

The surface morphologies of Mn-oxides on the aged filter media exhibited both biological and autocatalytic origins. Evidence obtained from SEM, PXRD, and XANES analyses of the aged filter media revealed the presence of biogenic birnessite, which can further promote autocatalysis and Mn(II)-oxidation. The detection of biogenic birnessite in the fully ripened filter media, largely coated by birnessite-type minerals, may be connected to the acceleration of Mn(II) removal kinetics observed in this pilot-scale biofiltration study. Biogenic birnessite may therefore be a robust indicator of the occurrence of biological Mn(II) oxidation and a crucial driver for potential subsequent autocatalytic Mn(II) oxidation.

Finally, this study indicated the feasibility of triggering the rapid formation of biogenic Mn-oxides using a cold-adapted MnOB consortium derived from the aged Mn biofilter materials. In particular, the rapid formation of biogenic Mn-oxides at 8 °C, within 5 days from the start of microbial culturing, was confirmed. The *Illumina*-MiSeq 16S rRNA gene sequencing analysis for the microbial consortium cultured at 8 °C identified relatives of known MnOB, including the genera *Pseudomonas, Leptothrix, Flavobacterium, Hydrogenophaga,* and *Zoogloea.* More

specifically, culture-dependent and -independent approaches in this study revealed that *Hydrogenophaga* sp., can produce Mn(III/IV) oxides, even at the low on-site temperature of 8 °C. The findings of this study have important implications for improving biofiltration functionalization in cold regions, and represent a potential breakthrough for accelerating the onset and kinetics of Mn(II) oxidation in challenging conditions.

5.2. Recommendations

The outcomes and conclusions drawn from this research have important implications for improving our understanding of the role of MnOB and Mn(III/IV) oxides in biofiltration systems and facilitating biofiltration functionalization for cold Fe(II)- and Mn(II)-rich groundwater. This study has described the acceleration of Mn(II) removal kinetics and addressed the relationships between the microbial community, groundwater chemistry, and field ripening of filter media in a pilot-scale biofiltration system operating at varying low on-site temperatures (8–14.8 °C). The research outcomes can therefore offer important insight into a potential breakthrough for developing innovative strategies to improve Mn-biofilter functionalization and shorten start-up periods for Mn(II) removal in groundwater below 15 °C. The following recommendations can be made for improving Mn-biofilter function:

- Track the changes in the EBCT-based first-order rate constant for Mn(II) removal. This is a simple indicator for filter ripening. In the field, especially in the initial phases of biofilter operation, changes in the EBCT-based first-order rate constant can provide a meaningful understanding for filter ripening and biofilter performance. This information could be helpful in the process optimization especially when biofilters are operated below 15 °C.
- Inoculate the biofilters with field-aged backwash sludge containing acclimated MnOB and biogenic Mn-oxides. This is an important way to trigger the acceleration of Mn(II) removal kinetics.
- Mn removal in biofilters can be accelerated by creating favorable conditions for MnOB to rapidly produce biogenic birnessite on the filter media or by replacing the virgin filter materials by media coated with biogenic birnessite.
- *Hydrogenophaga* sp. have dual function to mediate both Fe(II) and Mn(II) oxidation at 8 °C. Inoculate the biofilters treating Fe and Mn-rich groundwater with *Hydrogenophaga* sp.

to reduce the start-up time at low temperatures. Use *Hydrogenophaga* sp. as a genus-specific marker to identify bacterial mediated Fe(II) and Mn(II) oxidation in biofilters.

- Inoculate biofilters with virgin filter media with cold-adapted MnOB consortia derived from field-aged biofilters. This may be a feasible approach for triggering the rapid formation of biogenic Mn-oxides, shortening the onset of Mn(II) oxidation, and accelerating overall Mn(II) oxidation kinetics at low temperatures.

In addition to the recommendations made for practical application to Mn biofiltration systems, following future research directions are recommended to expand the current knowledge:

- Biological and physico-chemical Mn(II) oxidation mechanisms govern the Mn removal in biofilters. However, further research is still needed to understand the synergy between these mechanisms in filter ripening. This knowledge will help the water treatment industry to develop technologies to reduce or eliminate the filter ripening time completely.
- Inoculating biofilters with MnOB or using pre-coated (or pre-aged) Mn-oxide filter media to shorten the start-up period in Mn biofiltration systems are currently in use. However, the combined effects of MnOB bioaugmentation and pre-coated Mn-oxide filter media on Mn(II) oxidation in cold groundwater remain to be characterized.
- Cold-adapted MnOB enriched in the biofilters play a key role in initiating, accelerating and maintaining Mn(II) oxidation. It is thus important to assess how conventional operation and design parameters for biofiltration units improve or inhibit the growth kinetics of cold-adapted MnOB at low temperatures.
- As an alternative to the field aged Mn-oxide coated filet media, fresh birnessite coated filter can be used to reduce the start-up time in Mn biofilters. However, when fresh birnessite coated filter media and MnOB are used in the biofilters, further understanding is needed in the (a). Optimization the filter media ripening, and (b). MnOB biofilm formations and their interactions with birnessite coated filter media.

REFERENCES

ABU HASAN, H., SHEIKH ABDULLAH, S. R., KAMARUDIN, S. K. & TAN KOFLI, N. 2015. Effective curves of completing simultaneous ammonium and manganese removal in polluted water using a biological aerated filter. *Journal of Industrial and Engineering Chemistry,* 30**,** 153-159.

ABU HASAN, H., SHEIKH ABDULLAH, S. R., KAMARUDIN, S. K., TAN KOFLI, N. & ANUAR, N. 2014. Kinetic evaluation of simultaneous COD, ammonia and manganese removal from drinking water using a biological aerated filter system. *Separation and Purification Technology,* 130**,** 56-64.

AKOB, D. M., BOHU, T., BEYER, A., SCHÄFFNER, F., HÄNDEL, M., JOHNSON, C. A., MERTEN, D., BÜCHEL, G., TOTSCHE, K. U. & KÜSEL, K. 2014. Identification of Mn(II)-oxidizing bacteria from a low-pH contaminated former uranium mine. *Applied and Environmental Microbiology,* 80**,** 5086-5097.

ARP, D. J., SAYAVEDRA-SOTO, L. A. & HOMMES, N. G. 2002. Molecular biology and biochemistry of ammonia oxidation by *Nitrosomonas europaea*. *Archives of Microbiology,* 178**,** 250-255.

BEAN, E. L. 1974. Potable water-quality goals. *Journal-American Water Works Association,* 66**,** 221-230.

BERBENNI, P., POLLICE, A., CANZIANI, R., STABILE, L. & NOBILI, F. 2000. Removal of iron and manganese from hydrocarbon-contaminated groundwaters. *Bioresource Technology,* 74**,** 109-114.

BEUKES, L. S. & SCHMIDT, S. 2012. Isolation and characterization of a manganese-oxidizing bacterium from a biofiltration system for the treatment of borehole water in KwaZulu-Natal (South Africa). *Engineering in Life Sciences,* 12**,** 544-552.

BLACKWOOD, C. B., HUDLESTON, D., ZAK, D. R. & BUYER, J. S. 2007. Interpreting ecological diversity indices applied to terminal restriction fragment length polymorphism data: insights from simulated microbial communities. *Applied and Environmental Microbiology,* 73**,** 5276-5283.

BOOGERD, F. C. & DE VRIND, J. P. 1987. Manganese oxidation by *Leptothrix discophora*. *Journal of Bacteriology,* 169**,** 489-94.

BOUCHARD, M. F., SAUVÉ, S., BARBEAU, B., LEGRAND, M., BRODEUR, M.-È., BOUFFARD, T., LIMOGES, E., BELLINGER, D. C. & MERGLER, D. 2011. Intellectual impairment in school-age children exposed to manganese from drinking water. *Environmental Health Perspectives,* 119**,** 138-143.

BOURGINE, F. P., GENNERY, M., CHAPMAN, J. I., KERAI, H., GREEN, J. G., RAP, R. J., ELLIS, S. & GAUMARD, C. 1994. Biological processes at Saints Hill Water-Treatment Plant, Kent. *Water and Environment Journal,* 8**,** 379-391.

BRUINS, J. H., PETRUSEVSKI, B., SLOKAR, Y. M., HUYSMAN, K., JORIS, K., KRUITHOF, J. C. & KENNEDY, M. D. 2015a. Biological and physico-chemical formation of birnessite during the ripening of manganese removal filters. *Water Research,* 69**,** 154-161.

BRUINS, J. H., PETRUSEVSKI, B., SLOKAR, Y. M., KRUITHOF, J. C. & KENNEDY, M. D. 2015b. Manganese removal from groundwater: characterization of filter media coating. *Desalination and Water Treatment,* 55**,** 1851-1863.

BURGER, M. S., KRENTZ, C. A., MERCER, S. S. & GAGNON, G. A. 2008a. Manganese removal and occurrence of manganese oxidizing bacteria in full-scale biofilters. *Journal of Water Supply: Research and Technology - Aqua,* 57**,** 351-359.

BURGER, M. S., MERCER, S. S., SHUPE, G. D. & GAGNON, G. A. 2008b. Manganese removal during bench-scale biofiltration. *Water Research,* 42**,** 4733-42.

CAI, Y. A., LI, D., LIANG, Y., LUO, Y., ZENG, H. & ZHANG, J. 2015. Effective start-up biofiltration method for Fe, Mn, and ammonia removal and bacterial community analysis. *Bioresource Technology,* 176**,** 149-155.

CAI, Y. A., LI, D., LIANG, Y., ZENG, H. & ZHANG, J. 2014. Operational parameters required for the start-up process of a biofilter to remove Fe, Mn, and NH_3-N from low-temperature groundwater. *Desalination and Water Treatment,* 57**,** 3588-3596.

CAPORASO, J. G., LAUBER, C. L., WALTERS, W. A., BERG-LYONS, D., HUNTLEY, J., FIERER, N., OWENS, S. M., BETLEY, J., FRASER, L., BAUER, M., GORMLEY, N., GILBERT, J. A., SMITH, G. & KNIGHT, R. 2012. Ultra-high-throughput microbial community analysis on the Illumina HiSeq and MiSeq platforms. *ISME J,* 6**,** 1621-1624.

CAPORASO, J. G., LAUBER, C. L., WALTERS, W. A., BERG-LYONS, D., LOZUPONE, C. A., TURNBAUGH, P. J., FIERER, N. & KNIGHT, R. 2011. Global patterns of 16S rRNA

diversity at a depth of millions of sequences per sample. *Proceedings of the National Academy of Sciences,* 108**,** 4516-4522.

CERRATO, J. M., FALKINHAM III, J. O., DIETRICH, A. M., KNOCKE, W. R., MCKINNEY, C. W. & PRUDEN, A. 2010. Manganese-oxidizing and -reducing microorganisms isolated from biofilms in chlorinated drinking water systems. *Water Research,* 44**,** 3935-3945.

CERRATO, J. M., KNOCKE, W. R., HOCHELLA, M. F., DIETRICH, A. M., JONES, A. & CROMER, T. F. 2011. Application of XPS and solution chemistry analyses to investigate soluble manganese removal by MnOx(s)-coated media. *Environmental Science & Technology,* 45**,** 10068-10074.

CHAN, C., CABANISS, K., WILLIAMS, K., MOORE, M., MICHAEL, H., CAPLAN, J., LIN, C. 2014. Fe-oxidizing microorganisms in microscopic model aquifer systems: feedbacks between flow and biomineralization. Proceedings of the *9th International Symposium on Subsurface Microbiology ISSM, Pacific Grove, California USA.*

CHANG, C. H., SVEDRUŽIĆ, D., OZAROWSKI, A., WALKER, L., YEAGLE, G., BRITT, R. D., ANGERHOFER, A. & RICHARDS, N. G. 2004. EPR spectroscopic characterization of the manganese center and a free radical in the oxalate decarboxylase reaction: identification of a tyrosyl radical during turnover. *Journal of Biological Chemistry,* 279**,** 52840-52849.

CHAUDHARY, D. S., VIGNESWARAN, S., NGO, H. H., SHIM, W. G. & MOON, H. 2003. Biofilter in water and wastewater treatment. *Korean Journal of Chemical Engineering,* 20**,** 1054-1065.

CHENG, Q., NENGZI, L., XU, D., GUO, J. & YU, J. 2016. Influence of nitrite on the removal of Mn(II) using pilot-scale biofilters. *Journal of Water Reuse and Desalination*. DOI: 10.2166/wrd.2016.210

COLE, J. R., WANG, Q., FISH, J. A., CHAI, B., MCGARRELL, D. M., SUN, Y., BROWN, C. T., PORRAS-ALFARO, A., KUSKE, C. R. & TIEDJE, J. M. 2014. Ribosomal Database Project: data and tools for high throughput rRNA analysis. *Nucleic Acids Research,* 42**,** D633-D642.

COOLEY, R. & KNOCKE, W. R. 2016. Low-temperature effects on the removal of soluble manganese in MnOx(s)-coated media systems. *Journal of Water Supply: Research and Technology - AQUA,* 65**,** 626-634.

DANGETI, S., ROSHANI, B., RINDALL, B., MCBETH, J. M. & CHANG, W. 2017. Biofiltration field study for cold Fe(II)- and Mn(II)-rich groundwater: accelerated Mn(II) removal kinetics and cold-adapted Mn(II)-oxidizing microbial populations. *Water Quality Research Journal,* 52**,** 229-242.

DE VET, W. W. J. M., DINKLA, I. J. T., MUYZER, G., RIETVELD, L. C. & VAN LOOSDRECHT, M. C. M. 2009. Molecular characterization of microbial populations in groundwater sources and sand filters for drinking water production. *Water Research,* 43**,** 182-194.

DEGEN, T., SADKI, M., BRON, E., KÖNIG, U. & NÉNERT, G. 2014. The HighScore suite. *Powder Diffraction,* 29**,** S13-S18.

DICK, G. J., LEE, Y. E. & TEBO, B. M. 2006. Manganese (II)-oxidizing *Bacillus* spores in Guaymas Basin hydrothermal sediments and plumes. *Applied and Environmental Microbiology,* 72**,** 3184-3190.

EDGAR, R. C., HAAS, B. J., CLEMENTE, J. C., QUINCE, C. & KNIGHT, R. 2011. UCHIME improves sensitivity and speed of chimera detection. *Bioinformatics,* 27**,** 2194-2200.

EMERSON, D., FLEMING, E. J. & MCBETH, J. M. 2010. Iron-oxidizing bacteria: an environmental and genomic perspective. *Annual review of microbiology,* 64**,** 561-583.

ENVIRONMENT AND CLIMATE CHANGE CANADA. 2013. *Water Sources- Groundwater*. Government of Canada.

FODJE, M., GROCHULSKI, P., JANZEN, K., LABIUK, S., GORIN, J. & BERG, R. 2014. 08B1-1: an automated beamline for macromolecular crystallography experiments at the Canadian Light Source. *Journal of Synchrotron Radiation,* 21**,** 633-637.

FORTIN, G., VAN DER KAMP, G. & CHERRY, J. A. 1991. Hydrogeology and hydrochemistry of an aquifer-aquitard system within glacial deposits, Saskatchewan, Canada. *Journal of Hydrology,* 126**,** 265-292.

FRANCIS, C. A., CO, E. M. & TEBO, B. M. 2001. Enzymatic manganese(II) oxidation by a marine *alpha-proteobacterium. Applied and Environmental Microbiology* 67**,** 4024-9.

GAGE, B., O'DOWD, D. & WILLIAMS, P. 2001. Biological iron and manganese removal, pilot plant and full scale application. *Proceedings of the Ontario Water Works Association Conference, Ontario*.

GOUZINIS, A., KOSMIDIS, N., VAYENAS, D. & LYBERATOS, G. 1998. Removal of Mn and simultaneous removal of NH_3, Fe and Mn from potable water using a trickling filter. *Water research,* 32**,** 2442-2450.

GRANGER, H. 2013. *Manganese removal from surface water using bench-scale biofiltration.* Dalhousie University

GRANGER, H. C., STODDART, A. K. & GAGNON, G. A. 2014. Direct biofiltration for manganese removal from surface water. *Journal of Environmental Engineering, ASCE,* 140**,** 04014006.

GRIFFIN, A. E. 1960. Significance and removal of manganese in water supplies. *Journal (American Water Works Association),* 52**,** 1326-1334.

GULAY, A., MUSOVIC, S., ALBRECHTSEN, H.-J., AL-SOUD, W. A., SORENSEN, S. J. & SMETS, B. F. 2016. Ecological patterns, diversity and core taxa of microbial communities in groundwater-fed rapid gravity filters. *ISME J,* 10**,** 2209-2222.

HACKBARTH, D. A. 1978. Groundwater temperatures in the Athabasca Oil Sands area, Alberta. *Canadian Journal of Earth Sciences,* 15**,** 1689-1700.

HALLBECK, L., STÅHL, F. & PEDERSEN, K. 1993. Phytogeny and phenotypic characterization of the stalk-forming and iron-oxidizing bacterium *Gallionella ferruginea*. *Microbiology,* 139**,** 1531-1535.

HARDIE, A., DYNES, J., KOZAK, L. & HUANG, P. 2007. Influence of polyphenols on the integrated polyphenol-maillard reaction humification pathway as catalyzed by birnessite. *Annals of Environmental Science*, 1, 91-110

HEALTH CANADA 1995. Guidelines for Canadian Drinking Water Quality: Guideline Technical Document – Temperature. Government of Canada.

INDUSTRY CANADA 2008. The Canadian Water Industry. Environmental Business International Inc.

ISLAND, P. E. 2016. Manganese in Drinking Water. *In:* Federal-Provincial-Territorial Committee on Drinking Water (ed.). Government of Canada.

JIA, H., LIU, J., ZHONG, S., ZHANG, F., XU, Z., GONG, X. & LU, C. 2015. Manganese oxide coated river sand for Mn(II) removal from groundwater. *Journal of Chemical Technology & Biotechnology,* 90**,** 1727-1734.

JIANG, S., KIM, D. G., KIM, J. & KO, S. O. 2010. Characterization of the biogenic manganese oxides produced by *Pseudomonas putida* strain MnB1. *Environmental Engineering Research,* 4**,** 183-190.

KATO, S., KREPSKI, S., CHAN, C., ITOH, T. & OHKUMA, M. 2014. *Ferriphaselus amnicola* gen. nov., sp. nov., a neutrophilic, stalk-forming, iron-oxidizing bacterium isolated from an iron-rich groundwater seep. *International Journal of Systematic and Evolutionary Microbiology,* 64**,** 921-925.

KATSOYIANNIS, I. A. & ZOUBOULIS, A. I. 2004. Biological treatment of Mn(II) and Fe(II) containing groundwater: Kinetic considerations and product characterization. *Water Research,* 38**,** 1922-1932.

KIM, S. S., BARGAR, J. R., NEALSON, K. H., FLOOD, B. E., KIRSCHVINK, J. L., RAUB, T. D., TEBO, B. M. & VILLALOBOS, M. 2011. Searching for biosignatures using electron paramagnetic resonance (EPR) analysis of manganese oxides. *Astrobiology,* 11**,** 775-786.

KNOCKE, W. R., OCCIANO, S. C. & HUNGATE, R. 1991. Removal of soluble manganese by oxide-coated filter media: sorption rate and removal mechanism issues. *Journal (American Water Works Association)***,** 64-69.

KOHL, P. M. & DIXON, D. 2012. *Occurrence, impacts, and removal of manganese in biofiltration processes,* Water Research Foundation.

KOHL, P. M. & MEDLAR, S. J. 2006. *Occurrence of manganese in drinking water and manganese control,* American Water Works Association.

KONDAKIS, X. G., MAKRIS, N., LEOTSINIDIS, M., PRINOU, M. & PAPAPETROPOULOS, T. 1989. Possible health effects of high manganese concentration in drinking water. *Archives of Environmental Health: An International Journal,* 44**,** 175-178.

KRISHNAN, K. P., SINHA, R. K., KRISHNA, K., NAIR, S. & SINGH, S. M. 2009. Microbially mediated redox transformations of manganese (II) along with some other trace elements: a study from Antarctic lakes. *Polar biology,* 32**,** 1765-1778.

LEARMAN, D. R., WANKEL, S. D., WEBB, S. M., MARTINEZ, N., MADDEN, A. S. & HANSEL, C. M. 2011. Coupled biotic–abiotic Mn(II) oxidation pathway mediates the formation and structural evolution of biogenic Mn oxides. *Geochimica et Cosmochimica Acta,* 75**,** 6048-6063.

LI, D., ZHANG, J., WANG, H., YANG, H. & WANG, B. 2005. Operational performance of biological treatment plant for iron and manganese removal. *Journal of Water Supply: Research and Technology - Aqua,* 54**,** 15-24.

LI, X.-K., CHU, Z.-R., LIU, Y.-J., ZHU, M.-T., YANG, L. & ZHANG, J. 2013. Molecular characterization of microbial populations in full-scale biofilters treating iron, manganese and ammonia containing groundwater in Harbin, China. *Bioresource Technology,* 147**,** 234-239.

LIU, J., WANG, Z., BELCHIK, S. M., EDWARDS, M. J., LIU, C., KENNEDY, D. W., MERKLEY, E. D., LIPTON, M. S., BUTT, J. N. & RICHARDSON, D. J. 2012. Identification and characterization of MtoA: a decaheme c-type cytochrome of the neutrophilic Fe (II)-oxidizing bacterium *Sideroxydans lithotrophicus ES-1*. *Frontiers in Microbiology***,** 3, 37.

LÜCKER, S., WAGNER, M., MAIXNER, F., PELLETIER, E., KOCH, H., VACHERIE, B., RATTEI, T., DAMSTÉ, J. S. S., SPIECK, E., LE PASLIER, D. & DAIMS, H. 2010. A *Nitrospira* metagenome illuminates the physiology and evolution of globally important nitrite-oxidizing bacteria. *Proceedings of the National Academy of Sciences,* 107**,** 13479-13484.

MARCUS, D. N., PINTO, A., ANANTHARAMAN, K., RUBERG, S. A., KRAMER, E. L., RASKIN, L. & DICK, G. J. 2017. Diverse manganese (II)-oxidizing bacteria are prevalent in drinking water systems. *Environmental Microbiology Reports,* 9**,** 120-128.

MILLER, A. Z., DIONÍSIO, A., BRAGA, M. A. S., HERNÁNDEZ-MARINÉ, M., AFONSO, M. J., MURALHA, V. S. F., HERRERA, L. K., RAABE, J., FERNANDEZ-CORTES, A. & CUEZVA, S. 2012. Biogenic Mn oxide minerals coating in a subsurface granite environment. *Chemical Geology,* 322**,** 181-191.

MOUCHET, P. 1992. From conventional to biological removal of Fe and Mn in France. *Journal of the American Water Works Association (AWWA),* 84**,** 158–166.

NAM, K. W., KIM, M. G. & KIM, K. B. 2007. In situ Mn K-edge X-ray absorption spectroscopy studies of electrodeposited manganese oxide films for electrochemical capacitors. *The Journal of Physical Chemistry C,* 111**,** 749-758.

NEALSON, K. H. 2006. The manganese-oxidizing bacteria. *Prokaryotes,* 5**,** 222–231.

NICK, R. J., RAY, G. B., FISH, K. M., SPIRO, T. G. & GROVES, J. T. 1991. Evidence for a weak Mn: O bond and a non-porphyrin radical in manganese-substituted horseradish peroxidase compound I. *Journal of the American Chemical Society,* 113**,** 1838-1840.

NORTHUP, D. E., BARNS, S. M., YU, L. E., SPILDE, M. N., SCHELBLE, R. T., DANO, K. E., CROSSEY, L. J., CONNOLLY, C. A., BOSTON, P. J., NATVIG, D. O. & DAHM, C. N. 2003. Diverse microbial communities inhabiting ferromanganese deposits in Lechuguilla and Spider Caves. *Environmental Microbiology,* 5**,** 1071-1086.

PACINI, V. A., INGALLINELLA, A. M. & SANGUINETTI, G. 2005. Removal of iron and manganese using biological roughing up flow filtration technology. *Water Research,* 39**,** 4463-4475.

POST, J. E. 1999. Manganese oxide minerals: Crystal structures and economic and environmental significance. *Proceedings of the National Academy of Sciences,* 96**,** 3447-3454.

RAVEL, B. & NEWVILLE, M. 2005. ATHENA, ARTEMIS, HEPHAESTUS: data analysis for X-ray absorption spectroscopy using IFEFFIT. *Journal of synchrotron radiation,* 12**,** 537-541.

SAHABI, D. M., TAKEDA, M., SUZUKI, I. & KOIZUMI, J. 2009. Removal of Mn^{2+} from water by "aged" biofilter media: the role of catalytic oxides layers. *Journal of Bioscience and Bioengineering,* 107**,** 151-7.

SAISAHA, P., DE BOER, J. W. & BROWNE, W. R. 2013. Mechanisms in manganese catalysed oxidation of alkenes with H_2O_2. *Chemical Society Reviews,* 42**,** 2059-2074.

SCHLOSS, P. D., GEVERS, D. & WESTCOTT, S. L. 2011. Reducing the effects of PCR amplification and sequencing artifacts on 16S rRNA-based studies. *PloS one,* 6**,** e27310.

SCHLOSS, P. D. & HANDELSMAN, J. 2005. Introducing DOTUR, a computer program for defining operational taxonomic units and estimating species richness. *Applied and environmental microbiology,* 71**,** 1501-1506.

SCHLOSS, P. D., WESTCOTT, S. L., RYABIN, T., HALL, J. R., HARTMANN, M., HOLLISTER, E. B., LESNIEWSKI, R. A., OAKLEY, B. B., PARKS, D. H. & ROBINSON, C. J. 2009. Introducing mothur: open-source, platform-independent, community-supported software for describing and comparing microbial communities. *Applied and environmental microbiology,* 75**,** 7537-7541.

SCHMIDT, J. M., SHARP, W. P. & STARR, M. P. 1981. Manganese and iron encrustations and other features of *Planctomyces crassus* Hortobágyi 1965, morphotype Ib of the *Blastocaulis-Planctomyces* group of budding and appendaged bacteria, examined by electron microscopy and X-ray micro-analysis. *Current Microbiology,* 5**,** 241-246.

SINGER, P. C. 1999. *Formation and control of disinfection by-products in drinking water*, American Water Works Association.

SLY, L., HODGKINSON, M. & ARUNPAIROJANA, V. 1989. The importance of high aesthetic quality potable water in tourist and recreational areas. *Water Science and Technology,* 21**,** 183-187.

ŠTEMBAL, T., MARKIĆ, M., RIBIČIĆ, N., BRIŠKI, F. & SIPOS, L. 2005. Removal of ammonia, iron and manganese from groundwaters of northern Croatia—pilot plant studies. *Process Biochemistry,* 40**,** 327-335.

STOKES, P. M. 1988. *Manganese in the Canadian environment*, National Research Council Canada, Associate Committee on Scientific Criteria for Environmental Quality.

STUMM, W. & MORGAN, J. J. 1996. Chemical equilibria and rates in natural waters. *Aquatic chemistry***,** 3rd ed, John Wiley & Sons, Inc.

SUJITH, P. P., GONSALVES, M. J. B. D., BHONSLE, S., SHAIKH, S. & LOKABHARATHI, P. A. 2017. Bacterial activity in hydrogenetic ferromanganese crust from the Indian Ocean: a combined geochemical, experimental and pyrosequencing study. *Environmental Earth Sciences,* 76**,** 191.

SUSANNE, A. B., PETER, B. & PHILIPP, B. 2017. Global patterns of shallow groundwater temperatures. *Environmental Research Letters,* 12**,** 034005.

TANI, Y., MIYATA, N., IWAHORI, K., SOMA, M., TOKUDA, S.-I., SEYAMA, H. & THENG, B. K. G. 2003. Biogeochemistry of manganese oxide coatings on pebble surfaces in the Kikukawa River System, Shizuoka, Japan. *Applied Geochemistry,* 18**,** 1541-1554.

TEBO, B. M., CLEMENT, B. G. & DICK, G. J. 2007. Biotransformations of manganese, 1223-1238. *In:* CHRISTON J. H,, RONALD L. C., JAY L. G., DAVID A.L., AARON L. M., & LINDA D. S. (ed), *Manual of Environmental Microbiology*, 3rd ed. ASM Press, Washington, DC.

TEBO, B. M. & EMERSON, S. 1985. Effect of oxygen tension, Mn(II) concentration, and temperature on the microbially catalyzed Mn(II) oxidation rate in a Marine Fjord. *Applied and Environmental Microbiology* 50**,** 1268-1273.

TEBO, B. M., JOHNSON, H. A., MCCARTHY, J. K. & TEMPLETON, A. S. 2005. Geomicrobiology of manganese(II) oxidation. *Trends in Microbiology,* 13**,** 421-428.

TEKERLEKOPOULOU, A. G., PAVLOU, S. & VAYENAS, D. V. 2013. Removal of ammonium, iron and manganese from potable water in biofiltration units: A review. *Journal of Chemical Technology and Biotechnology,* 88**,** 751-773.

THAPA CHHETRI, R., SUZUKI, I., TAKEZAKI, J., TABUSA, H., TAKEDA, M. & KOIZUMI, J.-I. 2013. Bacterial diversity in biological filtration plant for the removal of iron and manganese from groundwater. *Journal of Water and Environment Technology,* 11**,** 33-47.

TIPPING, E. 1984. Temperature dependence of Mn(II) oxidation in lakewaters: a test of biological involvement. *Geochimica et Cosmochimica Acta,* 48**,** 1353-1356.

TOBY, B. H. & VON DREELE, R. B. 2013. GSAS-II: the genesis of a modern open-source all purpose crystallography software package. *Journal of Applied Crystallography,* 46**,** 544-549.

TUREKIAN, K. K. & WEDEPOHL, K. H. 1961. Distribution of the elements in some major units of the earth's crust. *Geological Society of America Bulletin,* 72**,** 175-192.

VANDENABEELE, J., DE BEER, D., GERMONPRE, R. & VERSTRAETE, W. 1992. Manganese oxidation by microbial consortia from sand filters. *Microbial Ecology,* 24**,** 91-108.

VOEGELIN, A., KAEGI, R., BERG, M., NITZSCHE, K. S., KAPPLER, A., LAN, V. M., TRANG, P. T. K., GÖTTLICHER, J. & STEININGER, R. 2014. Solid-phase characterisation of an effective household sand filter for As, Fe and Mn removal from groundwater in Vietnam. *Environmental Chemistry,* 11**,** 566-578.

WANG, Q., GARRITY, G. M., TIEDJE, J. M. & COLE, J. R. 2007. Naive Bayesian classifier for rapid assignment of rRNA sequences into the new bacterial taxonomy. *Applied and environmental microbiology,* 73**,** 5261-5267.

WATER SECURITY AGENCY 2012. 25 Year Saskatchewan Water Security Plan. Government of Saskatchewan.

WEBB, S. M., DICK, G. J., BARGAR, J. R. & TEBO, B. M. 2005. Evidence for the presence of Mn (III) intermediates in the bacterial oxidation of Mn (II). *Proceedings of the National Academy of Sciences of the United States of America*, 102**,** 5558-5563.

YANG, H., SUN, W., GE, H. & YAO, R. 2015. The oxidation of As (III) in groundwater using biological manganese removal filtration columns. *Environmental technology,* 36**,** 2732-2739.

YANG, L., LI, X., CHU, Z., REN, Y. & ZHANG, J. 2014. Distribution and genetic diversity of the microorganisms in the biofilter for the simultaneous removal of arsenic, iron and manganese from simulated groundwater. *Bioresource Technology,* 156**,** 384-8.

YUE, J. C. & CLAYTON, M. K. 2005. A Similarity Measure Based on Species Proportions. *Communications in Statistics - Theory and Methods,* 34**,** 2123-2131.

ZENG, X., XIA, J., WANG, Z. & LI, W. 2015. Removal of iron and manganese in steel industry drainage by biological activated carbon. *Desalination and Water Treatment,* 56**,** 2543-2550.